THE EFFECTS OF PERMAFROST DEGRADATION ON SOIL CARBON

DYNAMICS IN ALASKA'S BOREAL REGION

By

Jonathan A. O'Donnell
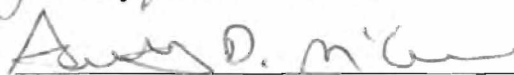

RECOMMENDED:

E. Hood

V. Romanosly

Jenny Harden
Advisory Committee Co-Chair

_A. D. M'C_
Advisory Committee Co-Chair
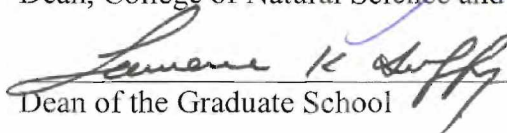
_____
Chair, Biology and Wildlife Department

APPROVED:

Paul W. Layer
Dean, College of Natural Science and Mathematics

Lawrence K Duffy
Dean of the Graduate School

Dec 6, 2010
Date

THE EFFECTS OF PERMAFROST DEGRADATION ON SOIL CARBON

DYNAMICS IN ALASKA'S BOREAL REGION

A

THESIS

Presented to the Faculty

of the University of Alaska Fairbanks

in Partial Fulfillment of the Requirements

For the Degree of

DOCTOR OF PHILOSOPHY

By

Jonathan A. O'Donnell, M.S., B.S.

Fairbanks, Alaska

December 2010

Abstract

High-latitude regions store large quantities of organic carbon (C) in permafrost

soils and peatlands, accounting for nearly half of the global belowground C pool.

Projected climate warming over the next century will likely drive widespread thawing of

near-surface permafrost and mobilization of soil C from deep soil horizons. However,

the processes controlling soil C accumulation and loss following permafrost thaw are not

well understood. To improve our understanding of these processes, I examined the

effects of permafrost thaw on soil C dynamics in forested upland and peatland

ecosystems of Alaska's boreal region. In upland forests, soil C accumulation and loss

was governed by the complex interaction of wildfire and permafrost. Fluctuations in

active layer depth across stand age and fire cycles determined the proportion of soil C in

frozen or unfrozen soil, and in turn, the vulnerability of soil C to decomposition. Under

present-day climate conditions, the presence of near-surface permafrost aids C

stabilization through the upward movement of the permafrost table with post-fire

ecosystem recovery. However, sensitivity analyses suggest that projected increases in air

temperature and fire severity will accelerate permafrost thaw and soil C loss from deep

mineral horizons. In the lowlands, permafrost thaw and collapse-scar bog formation

resulted in the dramatic redistribution of soil water, modifying soil thermal and C

dynamics. Water impoundment in collapse-scar bogs enhanced soil C accumulation in

shallow peat horizons, while allowing for high rates of soil C loss from deep inundated

peat horizons. Accumulation rates at the surface were not sufficient to balance deep C

losses, resulting in a net loss of 26 g C m^{-2} y^{-1} from the entire peat column during the

3000 years following thaw. Findings from these studies highlight the vulnerability of soil

C in Alaska's boreal region to future climate warming and permafrost thaw. As a result,

permafrost thaw and soil C release from boreal soils to the atmosphere should function as

a positive feedback to the climate system.

Table of Contents

List of Figures

List of Tables

Preface

This dissertation is in manuscript format, and has been divided into 6 chapters. Chapter 1 provides an introduction to soil carbon cycling in relation to permafrost thaw and an overview of each thesis chapter. Chapter 2 has been formatted for submission to *Global Change Biology*, and is currently *in press*. Chapter 3 has been formatted for submission to *Soil Science*, where it was accepted and published in 2009. Chapter 4 has been formatted for submission to *Biogeosciences*, where it is currently *in review*. Chapter 5 is currently *in preparation* for submittal to *Ecosystems*. Finally, Chapter 6 summarizes and synthesizes findings from this work.

Co-authors made important contributions to each dissertation chapter. For Chapter 2, Jennifer Harden assisted with field work, data analysis and editing, Dave McGuire assisted with data analysis and editing, Mikhail Kanevskiy helped with field and laboratory work, Torre Jorgenson assisted with field work, and Xiaomei Xu help with radiocarbon sample analysis and data interpretation. For Chapter 3, Vladimir Romanovsky, J. Harden and D. McGuire assisted with data analysis and editing. For Chapter 4, J. Harden, D. McGuire and V. Romanovsky assisted with model development, data analysis and editing. For Chapter 5, T. Jorgenson and J. Harden assisted with field work, data analysis, and editing, D. McGuire assisted with data analysis and editing, M. Kanevskiy and Kimberly Wickland assisted with field work.

Chapter 1: Introduction

Background and overview

High-latitude regions have experienced rapid warming in recent decades, with surface temperature increases of nearly 0.35 °C decade^{-1} between 1970 and 2000 (Serreze and Francis 2006; Euskirchen et al. 2007). This recent warming has stimulated dramatic change in the physical and ecological systems of the arctic and boreal region (Hinzman et al. 2005; Post et al. 2009). Recent evidence suggests that permafrost, which is a product of cold climates, has warmed and thawed in high-latitude regions in response to surface warming (Osterkamp and Romanovsky 1999; Jorgenson et al. 2006; Romanovsky et al. 2010). Soils of the northern permafrost region harbor large quantities of organic carbon (OC; 1672 Pg C), of which a large proportion is preserved in frozen ground (Tarnocai et al. 2009). Upon thaw, some of this OC will likely be released to the atmosphere upon thaw as carbon dioxide or methane (Walter et al. 2006; Schuur et al. 2009). Given the size of the OC pool, post-thaw release of soil OC to the atmosphere has the potential to function as a positive feedback, amplifying rates of atmospheric warming.

This dissertation has been divided into six chapters, including the introduction and conclusion chapters. Chapter 2 focuses on the interactive effects of fire and permafrost on soil C dynamics in upland black spruce ecosystems. Chapter 3 examines the effects of soil moisture on thermal conductivity of organic horizons in black spruce ecosystems. In Chapter 4, I assess the sensitivity of permafrost and soil C dynamics to a suite of future climatic and disturbance scenarios. In Chapter 5, I report findings from a study where I

examine the effects of permafrost degradation on soil C dynamics in Alaskan peatlands. And finally, in Chapter 6, I synthesize findings from the four main data chapters, discuss implications of these findings, and suggest future directions for research in this field.

Fire and permafrost effects on soil carbon dynamics

Permafrost is particularly vulnerable to thaw in the boreal region, where ground temperatures are relatively warm (Osterkamp and Romanovsky 1999) and frequent wildfire can exacerbate rates of thaw (Yoshikawa et al. 2003). Recent analyses suggest that the magnitude and intensity of wildfires will likely increase over the next century in response to continued warming (Balshi et al. 2009; Flannigan et al. 2009). Climate models have also predicted widespread thawing of near-surface permafrost over the next century (Euskirchen et al. 2006; Lawrence et al. 2008), but these analyses do not include the compounding effects of fire. While it is clear that wildfire and permafrost both are dominant controls on carbon dynamics of the boreal region (Harden et al. 2000; Bond-Lamberty et al. 2007; Schuur et al. 2009), less is known about the interactive effects of fire and permafrost on soil carbon dynamics (Harden et al. 2006).

To address the interactive effects of fire and permafrost on soil carbon dynamics, I examined rates of soil carbon accumulation and loss across an upland fire chronosequence near Hess Creek, Alaska. Findings from this study are reported in Chapter 2 ("The effect of fire and permafrost interactions on soil carbon accumulation in an upland black spruce ecosystem of interior Alaska: Implications for post-thaw carbon loss") and O'Donnell et al. (2010). Using field observations, radiocarbon techniques, and

a simple process-based model (modified from Harden et al. 2000), I quantify the

sensitivity of deep soil carbon (i.e. organic carbon in mineral soil in the top one meter) to

changes in active layer depth across fire regimes. Findings from this chapter provide

insight into the role of permafrost as a carbon sink and the vulnerability of soil carbon

storage to permafrost thaw.

Improving model simulations of permafrost and active layer dynamics

Chapter 2 also highlights the importance of active layer depth as a control on the

decomposition of soil organic matter and carbon loss from soil. However, simulation of

active layer depth in Chapter 2 was relatively simplistic and did not incorporate the

effects of future climate variability or changes in soil thermal properties. To improve

active layer simulations, I first conducted a study to evaluate the effects of soil moisture

on thermal conductivity of soil organic horizons in black spruce ecosystems. Findings

from this study helped to refine model parameterizations of soil thermal dynamics, and

are reported in Chapter 3 ("The effect of moisture content on the thermal conductivity of

moss and organic soil horizons from black spruce ecosystems in Interior Alaska") and in

O'Donnell et al. (2009). This chapter illustrates the importance of moisture, moss type

(feather moss vs. *Sphagnum* spp.) and decomposition extent on unfrozen thermal

conductivity values of organic soil horizons, which strongly govern active layer depth in

the boreal region (Yoshikawa et al. 2003).

The next step for improved active layer depth simulations was to calibrate a soil

thermal model that would incorporate the effects of climatic fluctuations and soil

properties on ground temperatures and active layer depth. In Chapter 4 ("Exploring the sensitivity of soil carbon dynamics to climate change, fire disturbance and permafrost thaw in a black spruce ecosystem"), I use the Geophysical Institute Permafrost Laboratory (GIPL) model in conjunction with field measurements of temperature and moisture to simulate active layer dynamics across the Hess Creek chronosequence. The GIPL model uses a numerical modeling approach to simulate soil temperature fields and active layer depth. I used thermal conductivity-moisture relationships (as established in Chapter 3) to parameterize organic horizon properties. By using the GIPL model to simulate active layer depth, I was now able to predict the effects of future climate scenarios and disturbance on active layer depth with more confidence.

Active layer depth and soil climate effects on soil carbon dynamics

In addition to the effects of active layer depth on decomposition (O'Donnell et al. 2010), soil climate also plays a critical role in governing microbial activity and rates of decomposition in the boreal region (Wickland and Neff 2007; Fan et al. 2008). To incorporate soil climate controls on decomposition, I modified rates of decomposition (as reported in Chapter 2) so that they were sensitive to temperature fluctuations and moisture. The modifications to the soil carbon model reflect both physical (i.e. active layer depth) and biological (i.e. soil climate) controls on soil carbon accumulation and loss, and are discussed in detail in Chapter 4.

Using this modified modeling framework, I address three primary research questions in Chapter 4: 1) what is the sensitivity of ALD and soil climate to air

temperature, soil moisture, snow depth, and fire severity?, 2) what is the sensitivity of

soil carbon storage to air temperature, soil moisture, snow depth, and fire severity?, and

3) what are the relative effects of ALD, soil climate, and ALD x soil climate on soil OC

losses across climate and fire scenarios? Through these analyses, I was able to assess the

impact of various climatic factors and fire severity on both permafrost and soil carbon

dynamics.

Permafrost thaw and soil carbon dynamics in Alaska peatlands

Permafrost degradation has accelerated in northern peatlands in recent decades

(Jorgenson et al. 2001; Camill 2005). Peatlands harbor large quantities of soil organic

carbon (Tarnocai et al. 2009), and the response of soil carbon dynamics to permafrost

thaw is of critical interest (Dorrepaal et al. 2009). Permafrost thaw in peatlands typically

results in dramatic changes in soil drainage (Jorgenson and Osterkamp 2005), which is a

dominant control on peatland carbon cycling (Clymo 1984; Ise et al. 2008). Despite this,

considerable uncertainty exists regarding the fate of soil C stocks and accumulation

following permafrost thaw in northern peatlands (Limpens et al. 2008).

In Chapter 5 ("The effects of permafrost thaw on soil carbon dynamics and soil

thermal conditions in Alaska peatlands"), I examine soil thermal and carbon dynamics

across a collapse-scar bog chronosequence at Koyukuk National Wildlife Refuge, Alaska.

Collapse-scar bogs form in lowland areas following thawing of ice-rich sediments

(Jorgenson and Osterkamp 2005), and typically expand laterally over time. In this

chapter, I use chronosequence and radiocarbon methodologies to estimate carbon

accumulation rates before and after permafrost thaw. I also measure soil temperature, moisture and thaw depth in order to evaluate the effects of ground subsidence on spatial variability in soil thermal dynamics. Findings from this study help to reduce the uncertainties with respect to soil carbon dynamics following permafrost thaw in northern peatlands.

In Chapter 6 ("Conclusions"), I synthesize the findings from Chapters 2 through 5 by highlighting the overarching themes and trends drawn from these studies. I also discuss some gaps that have been identified as a result of this research, and point towards future research that will reduce the uncertainties related to permafrost controls on soil carbon dynamics and carbon cycle feedbacks to the climate system.

References

Balshi MS, McGuire AD, Duffy P, Flannigan M, Walsh J, Melillo J. 2009. Assessing the response of area burned to changing climate in western boreal North America using a Multivariate Adaptive Regression Splines (MARS) approach. Global Change Biology 15: 578-600, doi:10.1111/j.1365-2486.2008.01679.x.

Bond-Lamberty B, SD Peckham, DE Ahl, and ST Gower. 2007. Fire as the dominant driver of central Canadian boreal forest carbon balance. Nature 450: doi:10.1038/nature06272.

Camill P. 2005. Permafrost thaw accelerates in boreal peatlands during late-20th century climate warming. Climatic Change 68: 135-152.

Clymo RS. 1984. The limits to peat bog growth. Proceedings of the Royal Society of
London B: 303: 605-654.

Dorrepaal E, S Toet, RSP van Logtestijn, E Swart, MJ van de Weg, TV Callahan, and R
Aerts. 2009. Carbon respiration from subsurface peat accelerated by climate
warming in the subarctic. Nature 460, doi:10.1038/nature08216.

Euskirchen, E. S., A. D. McGuire, D. W. Kicklighter, Q. Zhuang, J. S. Clein, R. J.
Dargaville, D. G. Dye, J. S. Kimball, K. C. McDonald, J. M. Melillo, V. E.
Romanovsky, and N. V. Smith. 2006. Importance of recent shifts in soil thermal
dynamics on growing season length, productivity and carbon sequestration in
terrestrial high-latitude ecosystems. Global Change Biology 12: 731-750.

Euskirchen ES, AD McGuire, and FS Chapin III. 2007. Energy feedbacks of northern
high-latitude ecosystems to the climate system due to reduced snow cover during
20th century warming. Global Change Biology 13: 2425-2438.

Fan Z, JC Neff, JW Harden, and KP Wickland. 2008. Boreal soil carbon dynamics under
a changing climate: A model inversion approach. Journal of Geophysical
Research 113, doi:10.1029/2008JG000723.

Flannigan M, Stocks B, Turetsky M, Wotton M. 2009. Impacts of climate change on fire
activity and fire management in the circumboreal forest. Global Change Biology
15: 549-560, doi:10.1111/j.1365-2486.

Harden JW, SE Trumbore, BJ Stocks, A Hirsch, ST Gower, KP O'Neill, ES Kasischke. 2000. The role of fire in the boreal carbon budget. Global Change Biology 6 (Suppl. 1): 174-184.

Harden JW, KL Manies, MR Turetsky, and JC Neff. 2006. Effects of wildfire and permafrost on soil organic matter and soil climate in interior Alaska. Global Change Biology 12: 2391-2402, doi:10.1111/j.1365-2486.2006.01255.x.

Hinzman LD, ND Bettez, WR Bolton, FS Chapin, MB Duyrgerov, CL Fastie, B Griffith, RD Hollister, A Hope, HP Huntington, AM Jensen, GJ Jia, T Jorgenson, DL Kane, DR Klein, G Kofinas, AH Lynch, AH Lloyd, AD McGuire, FE Nelson, WC Oechel, TE Osterkamp, CH Racine, VE Romanovsky, RS Stone, DA Stow, M Sturm, CE Tweedie, GL Vourlitis, MD Walker, DA Walker, PJ Webber, JM Welker, KS Winker, and K Yoshikawa. 2005. Evidence and implications of recent climate change in northern Alaska and other arctic regions. Climatic Change 72: 251-298.

Ise T, AL Dunn, SC Wofsy, and PR Moorcroft. 2008. High sensitivity of peat decomposition to climate change through water-table feedback. Nature Geoscience 1: 763-766.

Jorgenson MT, CH Racine, JC Walters, and TE Osterkamp. 2001. Permafrost degradation and ecological changes associated with a warming climate in central Alaska. Climatic Change 48: 551-579.

Jorgenson MT, and TE Osterkamp. 2005. Response of boreal ecosystems to varying modes of permafrost degradation. Canadian Journal of Forest Research 35: 2100-2111.

Jorgenson MT, YL Shur, and ER Pullman. 2006. Abrupt increase in permafrost degradation in Arctic Alaska. Geophysical Research Letters 33, L02503, doi:10.1029/2005GL024960.

Lawrence, D. M., A. G. Slater, V. E. Romanovsky, and D. J. Nicolsky. 2008. Sensitivity of a model projection of near-surface permafrost degradation to soil column depth and representation of soil organic matter. Journal of Geophysical Research 113: F02011, doi:10.1029/2007JF000883.

Limpens J, F Berendse, C Blodau, JG Canadell, C Freeman, J Holden, N Roulet, H Rydin, and G Schaepman-Strub. 2008. Peatlands and the carbon cycle: from local processes to global implications – a synthesis. Biogeosciences 5: 1475-1491.

O'Donnell JA, VE Romanovsky, JW Harden, AD McGuire. 2009. The effect of moisture content on the thermal conductivity of moss and organic soil horizons from black spruce ecosystems in interior Alaska. Soil Science 174: 646-651.

O'Donnell JA, JW Harden, AD McGuire, MZ Kanevskiy, MT Jorgenson, and X Xu. 2010. The effect of fire and permafrost interactions on soil carbon accumulation in an upland black spruce ecosystem of interior Alaska: implications for post-thaw carbon loss. Global Change Biology. In press.

Osterkamp TE, and VE Romanovsky. 1999. Evidence for warming and thawing of

   discontinuous permafrost in Alaska. Permafrost and Periglacial Processes 10: 17-

   37.

Post E, MC Forchhammer, MS Bret-Harte, TB Callaghan, TR Christensen, B Elberling,

   AD Fox, O Gilg, DS Hik, TT Hoye, RA Ims, E Jeppesen, DR Klein, J Madsen,

   AD McGuire, S Rysgaard, DE Schindler, I Stirling, MP Tamstorf, NJC Tyler, R

   van der Wal, J Welker, PA Wookey, NM Schmidt, and P Aastrup. 2009.

   Ecological dynamics across the Arctic associated with recent climate change.

   Science 325: 1355-1358.

Romanovsky VE, SL Smith, and HH Christiansen. 2010. Permafrost thermal state in the

   polar northern hemisphere during the International Polar Year 2007-2009: a

   Synthesis. Permafrost and Periglacial Processes 21: 106-116.

Schuur EAG, JG Vogel, KG Crummer, H Lee, JO Sickman, and TE Osterkamp. 2009.

   The effect of permafrost thaw on old carbon release and net carbon exchange

   from tundra. Nature 459: 556-559.

Serreze MC, and JA Francis. 2006. The Arctic amplification debate. Climatic Change 76:

   241-64.

Tarnocai C, JG Canadell, EAG Schuur, P Kuhry, G Mazhitova, and S Zimov. 2009. Soil

   organic carbon pools in the northern circumpolar permafrost region. Global

   Biogeochemical Cycles 23, doi:10.1029/2008GB003327.

Walter KM, Zimov SA, Chanton JP, Verbyla D, and Chapin FS III. 2006. Methane
bubbling from Siberian thaw lakes as a positive feedback to climate warming.
Nature 443: doi:10.1038/nature05040.

Wickland KP, and JC Neff. 2007. Decomposition of soil organic matter from boreal
black spruce forest: environmental and chemical controls. Biogeochemistry,
doi:10.1007/s10533-007-9166-3.

Yoshikawa K, WR Bolton, VE Romanovsky, M Fukuda, and LD Hinzman. 2003.
Impacts of wildfire on the permafrost in the boreal forests of interior Alaska.
Journal of Geophysical Research 108: doi:10.1029/2001JD000438.

Chapter 2: The effect of fire and permafrost interactions on soil carbon accumulation in an upland black spruce ecosystem of interior Alaska: Implications for post-thaw carbon loss[1]

Abstract

High-latitude regions store large amounts of organic carbon (OC) in active-layer soils and permafrost, accounting for nearly half of the global belowground OC pool. In the boreal region, recent warming has promoted changes in the fire regime, which may exacerbate rates of permafrost thaw and alter soil OC dynamics in both organic and mineral soil. We examined how interactions between fire and permafrost govern rates of soil OC accumulation in organic horizons, mineral soil of the active layer and near-surface permafrost in a black spruce ecosystem of interior Alaska. To estimate OC accumulation rates, we used chronosequence, radiocarbon and modeling approaches. We also developed a simple model to track long-term changes in soil OC stocks over past fire cycles and to evaluate the response of OC stocks to future changes in the fire regime. Our chronosequence and radiocarbon data indicate that OC turnover varies with soil depth, with fastest turnover occurring in shallow organic horizons (~60 years) and slowest turnover in near-surface permafrost (> 3000 years). Modeling analysis indicates that OC accumulation in organic horizons was strongly governed by carbon losses via

---

combustion and burial of charred remains in deep organic horizons. OC accumulation in mineral soil was influenced by active layer depth, which determined the proportion of mineral OC in a thawed or frozen state and thus, determined loss rates via decomposition. Our model results suggest that future changes in fire regime will result in substantial reductions in OC stocks, largely from the deep organic horizon. Additional OC losses will result from fire-induced thawing of near-surface permafrost. From these findings, we conclude that the vulnerability of deep OC stocks to future warming, and thus the magnitude of terrestrial carbon cycle feedbacks to the climate system from permafrost-dominated regions, are closely linked to the sensitivity of permafrost to wildfire disturbance.

Introduction

High-latitude regions harbor large amounts of organic carbon (OC) in soil (Ping *et al.*, 2008a; Schuur *et al.*, 2008; Tarnocai *et al.*, 2009; Kuhry *et al.*, 2009). Some permafrost soils in particular began accumulating OC prior to the Last Glacial Maximum (Schirrmeister *et al.*, 2002). Recent climate warming at northern latitudes has resulted in warming and thawing of permafrost in many regions (Osterkamp & Romanovsky, 1999; Jorgenson *et al.*, 2001, 2006), which may mobilize OC stocks from deep soil reservoirs via decomposition, leaching or erosion. Future warming will likely increase the frequency and severity of wildfires in the boreal region (Flannigan *et al.*, 2009; Balshi *et al.*, 2009a) and consequently, may increase rates of permafrost degradation (Shur & Jorgenson 2007). Release of OC stocks from permafrost as carbon dioxide or methane

may function as a strong positive feedback to atmospheric warming (Walter *et al.*, 2006; Schuur *et al.*, 2009).

A recent analysis suggests that the terrestrial carbon (C) sink of the boreal region may be in weakening, partly in response to changes in the wildfire regime and widespread permafrost thaw (McGuire *et al.*, 2010). Previous modeling studies have quantified the influence of fire on soil carbon dynamics in surface organic horizons of black spruce ecosystems (Harden *et al.*, 2000; Carrasco *et al.*, 2006; Fan *et al.*, 2008), but considerable uncertainty still exists regarding the fate of deeper C pools in unfrozen mineral soil and permafrost (Trumbore & Czimczik, 2008). Given the sensitivity of organic matter decomposition to temperature (Cox *et al.*, 2000; Davidson & Janssens, 2006), active layer depth (ALD; defined as the depth of soil above permafrost that thaws and refreezes annually) should influence decomposition rates of organic matter in mineral soil, if only by determining the proportion of organic carbon in a thawed or frozen state. Immediately following fire, ALD typically increases due to the combustion of surface organic horizons, which insulate permafrost from warm summer air temperatures (Yi *et al.*, 2009a, 2009b; Jorgenson *et al.*, 2010). However, recovery of surface organic horizons and the forest canopy between fire cycles can help attenuate long-term degradation of near-surface permafrost and allow recovery of the active layer to pre-fire depths (Yi *et al.*, 2009a, 2009b). In this way, the sensitivity of permafrost to fire disturbance is intimately coupled to deep soil C dynamics, and in turn, to terrestrial carbon feedbacks to the climate system (Chapin *et al.*, 2008).

Here, we quantify soil C stocks and model long-term patterns of C storage in an upland black spruce ecosystem in interior Alaska developed on Pleistocene loess deposits that contain high-ice permafrost (yedoma; Tomirdiaro *et al.*, 1984; Schirrmeister *et al.*, 2002). Our primary objectives were to 1) measure C storage in active-layer soils and deep permafrost (~20 meters), 2) quantify rates of OC accumulation using both chronosequence and radiocarbon methodologies, and 3) develop a fire-carbon interaction model to evaluate the effects of different fire regimes on soil C storage. By integrating field observations and radiocarbon estimates of C turnover into a modeling framework, we are able to assess the interactive effects of fire and permafrost on long-term soil C storage. We also discuss the potential of permafrost thaw on post-thaw C loss from mineral soil horizons.

Materials and Methods

Description of sites along fire/thaw chronosequence

Using aerial photography, satellite imagery, and maps of historical fire perimeters, we selected fire chronosequence sites near Hess Creek, approximately 150 km north of Fairbanks, Alaska (see Supplementary Figure 1). All study sites were located in north-facing forests underlain by permafrost and were somewhat poorly drained, and are generally representative of black spruce ecosystems in the discontinuous permafrost zone of Alaska (e.g. Kane et al. 2005) and Canada (Harden et al. 1997). Study sites were located within the 2003 Erickson Creek Burn (n = 3 stands), a 1993

Burn (n = 1), a 1990 Burn (n = 1), a 1967 Burn (n = 1), and mature unburned stands (n = 3; age = 148 ± 28 years).

The regional climate of interior Alaska is characterized by a continental climate, with temperature extremes ranging from -50 to 35 °C. At the Hess Creek study region, the average daily air temperature ranges from -25 °C in January to 15 °C in July. Annual precipitation averages 270 mm, 65% of which falls during the summer growing season (mid-May to early September). The cold snow period in interior Alaska is typically greater than 210 days long and at our sites, maximum snow accumulation (average = 44 cm; J. O'Donnell *unpublished data*) occurred in late March.

Vegetation at each stand was described according to the Alaska Vegetation Classification System (Viereck *et al.*, 1992). The dominant forest type on north-facing slopes of the Hess Creek region is open black spruce (*Picea mariana* (Mill.) B.S.P.). In mature black spruce stands, the forest understory was composed of small woody shrubs, such as *Vaccinium vitis-idaea* and *Ledum groenlandicum*. Feather mosses (*Pleurozium schreberi* and *Hylocomium splendens*), Sphagnum (*S. fuscum*) and reindeer lichens (*Cladina stellaris* and *C. arbuscula*) dominated ground cover in the mature black spruce stands. In the recently burned black spruce stands (2003 Erickson Creek fire), vegetation was dominated by standing dead *P. mariana*, and *V. vitis-idaea*, *V. uliginosum*, *L. groenlandicum*, and *Equisetum spp*. Burned organic soil surfaces were quickly colonized by *Ceratodon purpureus* in the recently burned stands. The intermediate stand age (i.e. 1990 Burn, 1993 Burn) was dominated by the shrubs *Salix pulchra*, *L. groenlandicum*, and *V. vitis-idaea*. The 1990 Burn was also colonized by paper birch (*Betula*

neoalaskana) and bluejoint (*Calamagrostis canadensis*). In the stands that burned in 1967, *P mariana* and *B. neoalaskana* were the dominant tree species, *V. vitis-idaea* and *L. groenlandicum* were the dominant understory shrubs, and the feather moss *H. splendens* dominated ground cover.

Soils at Hess Creek were classified as Gelisols, due to the presence of permafrost within 100 cm of the soil surface (USDA NRCS). Organic soil horizons overlying mineral soil were composed of live moss, fibrous and amorphous (Oi and Oe or Oa) organic matter, and varied in thickness with stand age. Parent material across the chronosequence was composed primarily of loess silt deposited during the Late Pleistocene. Permafrost development at Hess Creek occurred in conjunction with loess sedimentation (i.e. syngenetic permafrost formation) and is commonly referred to as "yedoma" in the literature (e.g. Tomirdiaro *et al.*, 1984). We observed numerous buried organic horizons and undecomposed moss parts and rootlets in the frozen loess deposits. The thickness of frozen loess at Hess Creek varied spatially, and ranged from 1 to 26 meters (based on the drilling of 62 boreholes). Volumetric ice content of permafrost at Hess Creek was high, ranging from 60 to 90%. Furthermore, massive ice wedges at some locations account for up to 30-50% of permafrost soil volume. High ice content of permafrost contributed to thaw settlement following fire at Hess Creek, and numerous thermokarst depressions have been observed.

Soil sampling and chemical analyses

In September 2007, we dug pits and described soil horizons at each site along the chronosequence following USDA-NRCS (Staff, 1998) and Canadian (Committee, 1998) methodologies. Common terms used for describing organic horizons included lichen, live moss, dead moss (more moss than roots), fibric (slightly decomposed, often dominated by fine roots), mesic (moderately decomposed), and humic (highly decomposed organics). Mineral soil horizons were characterized for texture and the presence of buried organic material. We sampled organic and mineral soil horizons to a minimum of two meters from one intensive profile at each replicate stand along the chronosequence. For the 2003 Burn and Unburned Mature stands, we sampled and analyzed soil chemistry from five profiles across three stands. For the 1967, 1990 and 1993 Burn stands, we only sampled one profile because most easily-accessible stands of intermediate age re-burned during the massive 2004 and 2005 fire years. In addition to the intensive profiles, we dug ten shallow pits at each stand for each age class to describe and note the depths of horizons within the soil profile as well as note the depth of the active layer. These field soil descriptions were used to estimate OC stocks in organic horizons using simple linear equations between OC concentration and organic horizon thickness for each horizon type. These equations were based on data from two sites within Interior Alaska (Manies *et al.*, 2004, Kristen Manies, *personal communication*) and one site within Canada (Manies *et al.*, 2006). For more information on these equations, see Supplementary Table 1.

We used a range of tools to sample different soil horizons for chemistry, bulk density, and moisture content. Organic soil horizons were sampled by hand using a variety of soil knives, scissors and saws to ensure good volume measurements. Surface organic samples were taken in small increments (2-5 cm), depending on the horizon thickness and homogeneity of material. Mineral samples in the active layer were taken in 5 to 10 cm increments using small soil augers or soil knives. Near-surface permafrost (< 3 meters) cores were obtained using a SIPRE (Snow, Ice, and Permafrost Research Establishment) corer (7.5 cm inside diameter) with Tanaka power head. We collected a minimum of one near-surface permafrost core from each stand. Deep permafrost samples (up to 21.5 m) were collected in May 2008 in association with the State of Alaska Department of Transportation and Public Facilities (AKDOT&PF). Samples were obtained along a transect spanning both Unburned Mature and 2003 Burn stands. Hollow stem drilling was performed by AKDOT&PF with a drill rig equipped with a modified CME sampler (Central Mine Equipment, Inc, St. Louis, MO, USA). Subsamples of frozen soil were collected from deep permafrost cores based on differences in visible ice content, soil texture, and the presence or absence of organic matter.

We analyzed soil samples (organic horizons, mineral soil of the active layer, near-surface and deep permafrost) for total C and nitrogen (N) using a Carlo Erba NA1500 elemental analyzer. For organic horizon samples, where inorganic carbon (IC) is largely absent, total carbon represents total OC. For all mineral soil horizons, we first removed carbonates using the acid fumigation technique (Hedges & Stern, 1984; Komada *et al.*, 2008) prior to running samples to determine total organic carbon concentration. Briefly,

we pre-weighed samples in silver capsules and transferred them to a small desiccator. Samples were wet with 50 μL of deionized water and then exposed to vaporous hydrochloric acid (1 N) for 6 hours, during which carbonates degassed from samples as carbon dioxide. We also ran mineral samples without acid fumigation to determine total carbon concentration. Total IC was calculated as the difference between total C and total OC. OC stocks were calculated by horizon type by multiplying OC concentration (% by mass), bulk density (oven-dry) and horizon thickness. We then calculated total OC stocks to 1 m and estimated the range of OC stocks in yedoma deposits.

Organic matter and mineral soil samples from three profiles (Unburned Mature, 2003 Burn, 1967 Burn) were analyzed for radiocarbon (^{14}C) to evaluate accumulation rates and turnover times of organic carbon throughout the soil profile. Samples were sent to the W.M. Keck C Cycle AMS Laboratory at the University of California Irvine for analysis as described in Southon *et al.* (2004). To evaluate the effect of acid fumigation on carbonate removal, a subset of bulk mineral samples received an acid-base-acid (ABA) pre-treatment, consisting of an acid wash (HCl), repeated base washes (NaOH), and one final HCl treatment followed by a rinse with deionized water. A sample of ^{14}C-free coal was also ABA treated to ensure no ^{14}C contamination during the pre-treatment process. Organic matter from soil was then combusted at 900 °C in evacuated, sealed quartz tubes in the presence of cupric acid (CuO) and silver (Ag) wire. Following cryogenic purification, carbon dioxide was reduced to graphite in a reaction at 500-550 °C using the sealed tube Zn reduction method (Xu *et al.*, 2007). Radiocarbon data are reported as $\Delta^{14}C$, or the per mil deviation of the $^{14}C/^{12}C$ ratio in the sample from that of

an oxalic standard that has been decay corrected to 1950 (Stuiver & Polach, 1977). The $\Delta^{14}C$ values we report have been corrected for mass-dependent fractionation using the *in situ* simultaneous AMS $\delta^{13}C$ measurement.

Soil C accumulation rates in organic, mineral and permafrost soils

We used a fire chronosequence approach to quantify rates of C accumulation in surface organic layers (Harden *et al.*, 1997) and a radiocarbon model (e.g., Trumbore & Harden, 1997) to quantify rates of C accumulation in thawed mineral soil and near-surface permafrost. For both methods, the net change in C storage (dC/dt) is governed by annual C inputs (modeled as constant I; kg C m^{-2} y^{-1}), decomposition (modeled as first order loss constant, k; y^{-1}), and OC stocks in a given year ($C(t)$). The carbon balance for any given year is reflected in the equation

$$dC/dt = I - kC(t) \qquad (1)$$

Solving this equation yields the following equation

$$C(t) = (I/k)*(1 - exp^{(-kt)}) \qquad (2)$$

To determine the net rate of C accumulation in surface organic horizons, we plotted recent C ($C(t)$) stocks (i.e. C recovery, or C stocks above char layer in organic horizon) versus t (as determined by chronosequence fire scars). This plot was then fit with equation (2) to derive estimates of I and k for shallow organic horizons between fire events. For thawed mineral soil and permafrost, we used radiocarbon data to determine the age of OC at a given depth. We then plotted cumulative OC stocks ($C(t)$) versus t (as determined by radiocarbon) and fit equation (2) to the data to determine I and k.

Trumbore and Harden (1997) used this radiocarbon method for sites dominated by moss

(e.g., *Sphagnum spp.*), where vertical mixing of layers is minimal. Here, we also assume

that mixing of organic matter in mineral soil is minimal. This assumption is supported by

the occurrence of syngenetic permafrost, which formed in conjunction with the

accumulation of sediment. However, in some soil horizons, we observed the effects of

cryoturbation, which is an important mechanism of soil mixing and carbon burial

(Bockheim, 2007; Ping *et al.*, 2008b). Our estimates of soil C accumulation in mineral

soil incorporate both syngenetic aggradation and cryoturbation processes.

Model description and development

Harden *et al.* (2000) developed a long-term C accumulation model to examine the

role of wildfire on C dynamics in shallow and deep organic horizons. We modified the

model to include both unfrozen and frozen mineral soil horizons (see Supplemental

Material for model details). To incorporate C dynamics of mineral soil into the model,

we first simulated permafrost dynamics over time using the simple empirical relationship

between ALD and organic horizon thickness (OHT), as measured across the fire

chronosequence at Hess Creek. OHT at a given time-step was calculated from OC stocks

in each organic horizon ($C_{shallow}$ and C_{deep} at time t), following the equations of Yi *et al.*

(2009a) and modified to fit our observations at Hess Creek:

$$C_{sum} = ax_{sum}^{b} \qquad (3)$$

where C_{sum} are the cumulative C stocks for a given horizon type, x_{sum} is the summed

thickness of the horizon, and a and b are regression parameters. Summed thickness refers

to the addition of multiple sample thicknesses taken from a given horizon (e.g. fibric horizon) for carbon analysis. For our study, we divided organic soils in three distinct horizons following the approach of Yi *et al.* (2009a): live/dead moss, fibrous organic matter, and amorphous organic matter. In our model simulations, ALD averaged between 40-50 cm in a mature black spruce stand and between 75-85 cm in a recently burned stand.

Inputs ($I_{mineral}$) of C to mineral soil ($C_{mineral}$) were based on equation (2) for thawed mineral soil at a recently burned stand (2003 Burn). $C_{mineral}$ consists primarily of roots, char, and buried wood. Initial $C_{mineral}$ values were determined from the simple linear relationship between cumulative C stocks and cumulative thawed mineral thickness as measured at Hess Creek (equation 4). ALD governs the proportion of $C_{mineral}$ that is either in the seasonally-thawed ($C_{active-layer}$) or perennially-frozen ($C_{permafrost}$) state, and thus determines the rate at which $C_{mineral}$ will decompose. $C_{active-layer}$ decomposes at first order decay constant $k_{active-layer}$ (as determined from equation 2), while $C_{permafrost}$ decomposes at first order decay constant $k_{permafrost}$ (as determined from equation 2). Maximum ALD measured at Hess Creek was 84 cm from 2007-2009, which suggests that burn severity of recent fires was not sufficient to cause deeper thaw in this ice-rich silt. For each soil horizon, our estimates of I and k represent average input rates and turnover, respectively, and thus integrate past climatic, nutrient and successional controls on C inputs to soil.

Forecasting changes in deep soil

To evaluate the potential effect of future changes in the fire regime on soil C dynamics, we conducted a full factorial experiment varying fire return interval (FRI) and burn severity (SEV) and evaluated C storage in organic and mineral soil horizons. This approach allowed us to evaluate both the effects of individual factors on soil C dynamics, and also to evaluate the interaction between these two factors. For FRI, we prescribed two frequencies (120 and 80 years), based on the range of FRIs reported for other black spruce ecosystems in the boreal region (Kasischke *et al.*, 1995). We also prescribed burn severities of 64 and 77%, which reflect average modern burn severities for north (i.e. intermediate severity) and south-facing slopes (i.e. high severity), respectively, in interior Alaska (Kane *et al.*, 2007). FRI and SEV parameters were prescribed to reflect potential changes in the fire regime of black spruce ecosystems in response to future warming (e.g. Flannigan *et al.*, 2009). Since active-layer dynamics in the model were governed by our field measurements across the chronosequence, the model did not cause deep thawing of near-surface permafrost in any of the four future scenarios. To evaluate the effect of deep thawing on soil C dynamics, we ran a fifth scenario where all of the near-surface permafrost thawed with a FRI of 80 years and SEV of 77%. For each fire scenario, we ran the calibrated model up to the year 6500, at which point we shifted the fire regime and tracked OC stocks under these different fire treatments. We assume in the model that I and k values remain constant. While we recognize that this is unlikely due to sensitivity of I and k parameters to the changes in fire regime, air and soil temperature, and soil

moisture, this assumption allows us to isolate the interactions among fire regime,

permafrost, and deep C storage.

Results

Field characterization of soil properties

We observed a negative exponential relationship between ALD and OHT (R^2 =

0.79; P = 0.0029; Fig. 1), characterized by the equation

$$ALD = 103.7537 * e^{(-0.0349 * OHT)} \qquad (4)$$

OHT varied across the fire chronosequence, averaging 24 ± 1 cm (± SE) in unburned

mature stands, 16 ± 1 in the 1967 burn, and 14 ± 1 in the 2003 Burn. ALD also varied

across the fire chronosequence, averaging 45 ± 1 cm in unburned mature stands, 53 ± 2 in

the 1967 Burn, and 65 ± 2 cm in the 2003 Burn.

In general, bulk density (oven-dry) pooled for all chronosequence sites varied

with soil horizon type (Table 1). Organic soil horizons had low bulk density values,

averaging 0.05 ± 0.01 g cm^{-3} in both live moss and fibrous horizons and 0.23 ± 0.05 g

cm^{-3} in amorphous organic horizons (Table 1). Mineral soil of the active layer (A, B, and

C horizons) generally had higher mean bulk density values (1.23 ± 0.06 g cm^{-3}) than

frozen mineral soil (0.93 ± 0.02 g cm^{-3}). This difference in bulk density between frozen

and thawed mineral soil can be attributed to the high volumetric ice content of syngenetic

permafrost, which averaged between 66 and 78 % in the top 10 m of permafrost (Table

1).

Soil chemistry

OC concentration averaged between 38.17 ± 1.00 % in the organic soil horizons,

3.37 ± 0.68 % in mineral soil of the active layer, and 1.70 ± 0.11 % in permafrost when

data were pooled for all sites (Table 1). Similarly, organic N averaged between 1.02 ±

0.03 % in the organic horizons, and 0.15 ± 0.02 % in mineral soil (active layer and

permafrost). IC averaged 0.10 ± 0.07 % in mineral soil of the active layer and 0.43 ±

0.03 % in permafrost. In the mineral soils of the active layer, IC only accounted for 3%

of total C. However, in permafrost, IC accounted for between 14 and 25% of total C.

OC stocks in the Unburned Mature stand averaged 6.59 ± 2.46, 6.11 ± 3.15, and 4.43 ±

1.95 kg C m^{-2} in the organic horizon, mineral soil of the active layer, and near-surface

permafrost, respectively (Fig. 2a). In the 2003 Burn, OC stocks averaged 4.26 ± 0.65,

9.79 ± 0.80, and 4.66 ± 0.62 kg C m^{-2} in the organic horizon, mineral soil of the active

layer, and near-surface permafrost, respectively (Fig. 2a). The relationships between C_{sum}

and x_{sum} for each organic horizon type are illustrated in Fig. 3a. For mineral soil in the

active layer, we observed a positive linear relationship between cumulative OC stocks

and the summed thickness of mineral soil horizons in the active layer (Fig. 3b), and is

described by the equation

$$mineral\ soil\ (active\ layer) \qquad C_{sum} = 0.1843x_{sum} + 0.1503 \qquad (5)$$

where x_{sum} is thickness in cm and C_{sum} is OC in gC cm^{-2} summed to that depth. OC

density in deep permafrost (i.e. yedoma deposits) from all sites was relatively consistent

with depth (in top 20 m), averaging 15.48 ± 1.02 kg m^{-3} (Fig. 2b). IC density in yedoma

was considerably lower than OC density, averaging less than 5 kg m^{-3} throughout the

entire profile. To estimate total OC stocks, we stratified our study region into ice-rich yedoma (gravimetric moisture content = 94.9%; wedge ice volume = 34.7%; frozen loess thickness = 16-30 m) and ice-poor yedoma (gravimetric moisture content = 76.0%; wedge ice volume = 2.4%; frozen loess thickness = 9.5-12 m). Based on our estimates, OC stocks in the ice-rich region ranged between 117-333 kg C m^{-2}, whereas OC stocks in the ice-poor region varied between 162-205 kg C m^{-2}.

In general, $\Delta^{14}C$ values of organic matter decreased with depth in three soil profiles along the fire chronosequence (Fig. 4), reflecting the shift from young (i.e. modern) C in shallow organic horizons, to intermediate age C in deep organic horizons and mineral soil of the active layer, to old C stabilized in permafrost. In shallow organic horizons, we observed the incorporation of bomb-spike ^{14}C into re-growing moss layers (note positive $\Delta^{14}C$ values in Fig. 4a, b), which reflects the recent balance between C inputs from NPP and decomposition rates. We also measured $\Delta^{14}C$ of bulk mineral samples and pieces of charred wood buried in mineral soil; however, we did not measure substantial differences in $\Delta^{14}C$ values between them. In one soil profile, we observed a zig-zag pattern between $\Delta^{14}C$ values and depth (Fig. 4a), which likely reflects burial of younger organic matter below older sediments through the process of cryoturbation. We used two acid fumigation treatments (ABA and acid fumigation) to remove carbonates from mineral soil samples prior $\Delta^{14}C$ analysis. The effect of these treatments on $\Delta^{14}C$ values of mineral soil was small, as reflected by the similarity in values across ABA, acid fumigation, and untreated samples (Figure 4a and 4c). This similarity suggests that the

precipitation of carbonate and incorporation of organic matter were synchronous during

the formation of syngenetic permafrost.

Rates of organic C accumulation

The rate of net C accumulation and the inputs and decomposition rates varied

considerably among shallow organic horizons, mineral soil in the active layer, and

mineral soil in the permafrost. In shallow organic horizons, we estimated net

accumulation rate to be 0.015 kg C m^{-2} y^{-1}, where $I_{shallow}$ averaged 0.050 ± 0.011 kg C m^{-2}

y^{-1} and $k_{shallow}$ averaged 0.017 ± 0.006 y^{-1} (Fig. 5a; Table 2). To estimate $I_{mineral}$ and $k_{active-layer}$, we used OC and radiocarbon inventories from the 2003 Burn, because mineral soil

dominated over organic soil in the recent burn stands. Net C accumulation in thawed

mineral soil was considerably lower (0.002 kg C m^{-2} y^{-1}), as were $I_{mineral}$ (0.003 ± 0.002

kg C m^{-2} y^{-1}) and $k_{active-layer}$ (0.0002 ± 0.0002 y^{-1}; Fig. 5b). For permafrost, we only used

equation (2) for the unburned mature stand. For the 2003 Burn and 1967 Burn, we used

simple linear accumulation, as the data did not conform to the exponential regression

function (Fig. 5c). As a result, we were able to calculate inputs across all three sites, but

only calculate $k_{permafrost}$ at the unburned site. $I_{permafrost}$ to the permafrost pool varied from

0.001 to 0.003 kg C m^{-2} y^{-1}. For the unburned stand, we estimated net C accumulation as

0.001 kg C m^{-2} y^{-1} and $k_{permafrost}$ as 0.0003 ± 0.0002 y^{-1}.

Modeling soil C dynamics

At end of the 6500-year model run, total OC stocks varied between 17 and 24 kg C m^{-2}, depending upon the stand age (Fig. 6). Whereas OC accumulation and loss in organic horizon was driven by fire dynamics, OC stocks in mineral soil were less sensitive directly to fire and more sensitive to changes in ALD. Based on the parameterization for our model verification (see Supplementary Figure 2), the OC in unfrozen mineral soil accumulated at a slow rate, with average input of 0.003 kg C m^{-2} y^{-1} and a turnover time of approximately 2500 years (Table 3). Permafrost OC stocks accumulated at an even slower rate, with input of 0.003 kg C m^{-2} y^{-1} and a turnover time of more than 3300 years (Table 3).

After 6500 years of landform and soil development, we observed significant changes in total OC stocks in response to different changes in the fire regime. In model scenarios where permafrost only partially thawed (i.e. first four scenarios), fire caused a sharp decline in total OC stocks from 17-24 kg C m^{-2} to 14-18 kg C m^{-2}, depending on the treatment (Fig. 6). The low frequency, low severity (FRI = 120 y, SEV = 64%) fire treatment resulted in the smallest reduction of total OC stocks, whereas the high frequency, high severity (FRI = 80 y, SEV = 77%) fire treatment resulted in the largest reductions of total OC stocks. Based on our model, the primary losses of soil OC stocks occurred in the deep organic horizon in response to high burn severities (Fig. 7a).

Approximately 500 years after the fire regime shift, total OC stocks began to re-accumulate, with C gains outpacing losses via decomposition and fire. These C gains were due in part to the stabilization of OC by permafrost across the first four model

scenarios (Fig. 7a). To evaluate the role of near-surface permafrost as a mode of stabilizing OC, we analyzed mineral OC accumulation "with permafrost" and "without permafrost". For scenarios with permafrost, we observed net increases in OC in mineral soil across all fire scenarios (Fig. 7a). For the scenario where fire induced deeper permafrost thaw, we observed a net loss of OC from mineral soil. From this analysis, we observed that total mineral OC stocks accumulate at a higher rate "with permafrost" than "without permafrost" (Fig. 7b). The difference in OC accumulation rates between treatments begins during historic times and is exacerbated following the fire regime shift, when mineral OC stocks "without permafrost" stop accumulating OC.

Discussion

Carbon accumulation and turnover in boreal soils

In this study, we demonstrate that the interaction between fire and permafrost governs OC accumulation in upland forest soils of the boreal region. Fire indirectly alters OC stocks in mineral soil by reducing organic horizon thickness, which in turn influences active layer depth (Fig. 1). In our model, active layer depth determines the proportion of mineral soil in a seasonally-thawed (i.e. active layer) or perennially-frozen (i.e. permafrost) state, and in turn, governs the susceptibility of OC in mineral soil to microbial decomposition. Our findings indicate that the presence of near-surface permafrost aids OC stabilization through the upward movement of the permafrost table between fire cycles, with ALD being driven by ecosystem recovery and moss re-growth. Thus, disturbance by fire interacts with permafrost to create a carbon "pump" from the

active layer to the near-surface permafrost, effectively arresting decomposition by transferring organic matter to the "freezer". This finding is consistent with the short-term dynamics captured in the modeling analyses of Yi *et al.* (2010), where CO_2 exchange shows a net efflux immediately following fire and net uptake several years post-fire.

We also illustrate that loss of permafrost following high-severity fires will result in a net loss of OC from deep mineral horizons through enhanced decomposition. These results imply that the vulnerability of deep OC stocks to future warming, and thus the magnitude of terrestrial carbon cycle feedbacks to the climate system from permafrost-dominated regions, is closely linked to the sensitivity of permafrost to wildfire disturbance. This finding is likely true for a wide variety of permafrost landscapes, although the water table and soil moisture will dictate both fire severity (and in response ALD) and rates of regeneration. For example, post-fire reduction of organic horizons and increase in ALD can greatly reduce water table height in well-drained black spruce stands, enhancing decomposition immediately following fire (Yi *et al.*, 2010). In poorly-drained black spruce stands, however, water table depth and decomposition tend to remain relatively stable across fire cycles (Yi *et al.*, 2010).

Mineral soils in black spruce ecosystems receive OC from a variety of sources, including roots, char, humic organic matter and leaching of dissolved organic matter. Our estimates of OC input rates to mineral soil (0.003 kg C m^{-2} y^{-1}; Table 2), as determined by the radiocarbon methodology, are lower than rates measured in other systems ($0.019 - 0.026$ 0.003 kg C m^{-2} y^{-1}; Richter *et al.*, 1999). Richter *et al.* (1999)

directly measured C inputs to mineral soil in a temperate forest. The difference between C inputs to mineral soil of a temperate and boreal forest was likely driven by variation in forest productivity between biomes (Jobbagy & Jackson, 2000), and by access of roots to mineral substrate. In permafrost systems, such access is limited by soil temperature and water state. Cryoturbation is another mechanism for incorporating soil C into mineral soil and permafrost at high-latitudes (Michaelson *et al.*, 1996; Bockheim, 2007), particularly mixing associated with the movement of fluid materials during thawing of ice-rich permafrost (Swanson *et al.*, 1999). We observed evidence of cryoturbated horizons in a number of soil profiles (e.g. Fig. 4a). Many studies have suggested that cryoturbation activity increases with warming (see review by Bockheim, 2007), but it is unclear how fire might influence rates of C burial by cryoturbation. Our estimates of OC input to the permafrost pool (Table 2) likely reflect a range of processes, including cryoturbation, the burial of OC through a rise of the permafrost table as a result of sedimentation (i.e. syngenetic permafrost aggradation), and OC incorporation into the permafrost pool in response to the upward movement of the permafrost table between fires (i.e. quasi-syngenetic permafrost aggradation).

Using radiocarbon techniques, we calculated low rates of organic matter decomposition in mineral soil, with turnover times ranging from 2500 to 3300 years for unfrozen and frozen soil, respectively. These turnover times reflect slow decomposition rates comparable to other published values for passive organic matter (Schimel *et al.*, 1994), and account for the net accumulation of OC in mineral soil observed in this study.

In our model, OC in mineral soil was distributed into either an unfrozen or frozen pool, depending upon the ALD. Prior studies have suggested that the processes governing decomposition are different in frozen and unfrozen soils (Mikan et al., 2002). Our findings indicate that the difference between $k_{permafrost}$ in near-surface permafrost and $k_{active-layer}$ in mineral soil of the active layer are relatively small. Nevertheless the transfer of C from the active layer to the permafrost pool is critical for slowing decomposition and increasing net accumulation rates in mineral soil. Slower rates of decomposition in near-surface permafrost are likely due to low unfrozen water content (Romanovsky & Osterkamp, 2000, Schimel & Mikan, 2005) and low microbial abundance and activity relative to active layer soils (Waldrop *et al.*, 2010).

We also observed large quantities of OC buried in deep loess deposits (i.e. yedoma; Figure 2 b). At Hess Creek, OC concentrations in yedoma averaged between 1 and 3% by weight, which (using bulk densities of 1.00-1.03 g cm^{-3}) translates to carbon densities of 17.00-17.03 kg C m^{-3}, consistent with values reported by other researchers (Dutta *et al.*, 2006; Ping *et al.*, 2008a; Schuur *et al.*, 2008; Khvorostyanov *et al.*, 2008). Yedoma sampling at Hess Creek revealed striking spatial variability in loess thickness, wedge ice volume and segregated ice volume (Shur *et al.*, 2010), which can greatly influence estimates of OC stocks. By stratifying our study area into ice-rich and ice-poor sections, we were better able to address the impact of ground ice on OC stocks. OC accumulation rates in permafrost varied among three profiles, which may reflect spatial variation in loess deposition, OC inputs or OC losses via decomposition from permafrost. In two profiles (2003 Burn and 1967 Burn), accumulation rates were linear, suggesting

that decomposition rates were low relative to OC inputs. In a third profile (Unburned

Mature), OC accumulation decreased with radiocarbon age, reflecting an increase in

decomposition relative to OC inputs over time.

Implications of future changes in climate, fire regime and permafrost stability

A number of recent studies have reported that future climate warming will likely

increase fire activity in the boreal region (Gillett *et al.*, 2004, Duffy *et al.*, 2005;

Flannigan *et al.*, 2009; Balshi *et al.*, 2009a). The vulnerability of permafrost to fire will

likely depend most on changes in burn severity (Fig. 6; Jorgenson *et al.* 2010) but also on

fire frequency and rates of ecosystem recovery between fire events (Shur & Jorgenson,

2007). Based on our modeling results, a shift in fire regime to both more frequent and

higher severity fires would cause the most significant response, with a shift from a net C

sink to a net C source to the atmosphere, primarily due to OC losses from deep organic

horizons (Fig. 7a). Additional OC losses may occur if near-surface permafrost

completely degrades, mobilizing old permafrost C. The results of these modeling

analyses could inform future investigations in boreal ecosystems underlain by permafrost,

particularly those experiencing climate-driven changes in the fire regime (Kasischke &

Turetsky, 2006; Flannigan *et al.*, 2009). Furthermore, similar responses to fire might be

possible in response to tundra fires in the continuous permafrost zone (e.g. Jones *et al.*,

2009).

Meanwhile, future increases in NPP could offset soil OC losses from changes in

the fire regime and subsequent permafrost thaw. To estimate how much NPP would have

to increase to maintain current ecosystem C budget, we calculated the difference between

mean OC stocks during the last fire cycle of the model spin-up (6350-6500 years) and

mean OC stocks after the next three fire cycles after the fire regime shift at 6500 years.

Our calculations suggest that moss and tree NPP would collectively have to increase by

7-14% in the next two to three centuries in order to offset soil C losses. Recent studies

suggest that NPP of the boreal region may indeed increase in response to increased

temperature, CO_2 fertilization, N availability, and increased fire frequency (Peng & Apps,

1999; Balshi *et al.*, 2009b). Recent findings suggest that permafrost thaw may increase

soil nitrogen availability (Schuur *et al.*, 2007), which if within the rooting zone can

partially offset OC losses from recently thawed soil (Schuur *et al.*, 2009). Furthermore,

severe fires can result in the conversion of black spruce forests to deciduous stands

(Johnstone *et al.*, 2009), which tend to have higher rates of NPP (Bond-Lamberty *et al.*,

2007). However, conversion to deciduous stands will likely reduce soil OC storage

through the loss of thick organic horizons and permafrost. Together with our findings,

these studies suggest that while productivity may increase in the future, soil carbon

turnover may also increase, resulting in a reduction of carbon storage in soils.

Active layer depth is also a function of summer air temperatures, precipitation,

snow depth and soil thermal properties (Romanovsky & Osterkamp, 2000; Yoshikawa *et

al.*, 2003; Nowinski *et al.*, 2010). However, we calculated active layer depth as a direct

function of organic horizon thickness and thus, values were constrained by our field

measurements across the fire chronosequence at our site and in today's climate (Fig. 1).

Fire did not cause deep thawing (> 1 meter) of near-surface permafrost, perhaps due to

low fire severities (Yoshikawa *et al.*, 2003), the presence of an ice-rich intermediate layer requiring high latent heat for thawing (Shur *et al.*, 2005), and/or the location of chronosequence sites on relatively cold, wet, north-facing slopes (Swanson, 1996). However, Viereck *et al.* (2008) observed deep thawing of permafrost in an open black spruce stand following a fire near Fairbanks, with a maximum thaw depth of 302 cm 24 years after the fire. Future fire regimes, together with warmer air temperatures, may result in similar deep thawing of permafrost at Hess Creek. To more accurately assess the future response of active layer depth to fire and air temperature, permafrost dynamics should be simulated using numerical (e.g. Marchenko *et al.* 2008) or process-based thermal models (e.g. Yi *et al.*, 2009b).

Finally, soil C dynamics are sensitive to changes in temperature and moisture (Lloyd & Taylor, 1994; Davidson & Janssens, 2006), and consequently, model parameters (e.g. *I, k*) should reflect these dynamics. Yi *et al.* (2010) show that immediately following fire, increased soil temperatures and ALD enhance decomposition and inorganic N availability to plants, which results in increased NPP in early successional stands. However, in mid-successional stands, decreased ALD and cooler soils lower decomposition rates, inorganic N availability, and rates of NPP (Yi *et al.* 2010). Kane & Vogel (2009) report that soil OC storage is reduced by nearly 50% with increasing soil degree-days, presumably due to the increased rates of decomposition at higher temperatures. In a synthesis of ecosystem warming experiments, aboveground NPP and soil respiration increased by similar magnitudes to sustained warming across biomes (Rustad *et al.*, 2001). However, there is still uncertainty regarding the

comparative response of NPP and soil respiration to warming in the boreal region, where

sensitivity analyses are complicated by fire disturbance and the presence of permafrost

(Zhuang *et al.*, 2003). In our model, decay constants (k) integrate the "apparent"

sensitivity of decomposition to temperature and moisture during past environmental

conditions as measured in the field. However, model forecasting needs to address the

response of decomposition to future warming and moisture dynamics. Thus, future

simulation of soil C dynamics in our model is limited by our ability to predict the

response of I and k to future climatic conditions. In the boreal region, researchers have

conducted short-term incubations to estimate temperature response quotients (Q_{10}) of

decomposition across a range of organic matter substrates (Wickland & Neff, 2007;

Waldrop *et al.*, 2010), which have aided parameterization of soil C models (Carrasco *et

al.*, 2006; Fan *et al.*, 2008). However, because soil C storage is a function of both inputs

and losses, changes in OC stocks will also depend upon production and the response of

plants to future warming (Heimann & Reichstein 2008; Balshi *et al.*, 2009b).

Conclusion

Wildfire in the boreal region will likely exacerbate rates of permafrost thaw, but

to date, has not been incorporated into climate models used for predicting loss of

permafrost. Loss of permafrost will enhance decomposition and loss of organic matter

stocks from both organic and mineral soil layers, accelerating feedbacks from terrestrial

ecosystems to the climate system. Such feedbacks invoke a soil carbon loss that is

transient for hundreds of years, after which time carbon accumulates slowly in permafrost layers. For context, we estimate that net primary production would have to increase by up to 14% relative to present-day rates following permafrost thaw in order for current C budgets to be maintained over such a regime shift.

Acknowledgements

References

Balshi MS, McGuire AD, Duffy P, Flannigan M, Walsh J, Melillo J (2009a) Assessing

the response of area burned to changing climate in western boreal North America

using a Multivariate Adaptive Regression Splines (MARS) approach. *Global*

Change Biology, **15**, 578-600, doi:10.1111/j.1365-2486.2008.01679.x.

Balshi MS, McGuire AD, Duffy P, Flannigan M, Kicklighter DW, Melillo J (2009b)

Vulnerability of carbon storage in North American boreal forests to wildfires

during the 21st century. *Global Change Biology*, doi:10.1111/j.1365-

2486.2009.01877.x.

Bockheim JG (2007) Importance of cryoturbation in redistributing organic carbon in

permafrost-affected soils. *Soil Science Society of America Journal*, **71**, 1335-

1342.

Bond-Lamberty, Peckham SD, Ahl DE, Gower ST (2007) Fire as the dominant driver of

central Canadian boreal forest carbon balance. *Nature*, **450**,

doi:10.1038/nature06272.

Carrasco JJ, Neff JC, Harden JW (2006) Modeling physical and biogeochemical controls

over carbon accumulation in a boreal forest soil. *Journal of Geophysical*

Research, **111**, G02004, doi:10.1029/2005JG000087.

Chapin FS III, Randerson JT, McGuire AD, Foley JA, Field CB (2008) Changing

feedbacks in the climate-biosphere system. *Frontiers in Ecology and the*

Environment, **6**, 313-320, doi:10.1890/080005.

Committee, CASC (1998) The Canadian System of Soil Classification. pp. 1-187. NRC
   Canada Research Press, Ontario, Canada.

Cox PM, Betts RA, Jones CD, Spall SA, Totterdell IJ (2000) Acceleration of global
   warming due to carbon-cycle feedbacks in a coupled climate model. *Nature*, **408**,
   184-187.

Davidson EA, Janssens IA (2006) Temperature sensitivity of soil carbon decomposition
   and feedbacks to climate change. *Nature*, **440**, doi:10.1038/nature04514.

Duffy PA, Walsh JE, Graham JM, Mann DH, Rupp TS (2005) Impacts of large scale
   atmospheric-ocean variability on Alaskan fire season severity. *Ecological
   Applications*, **15**, 1317-1330.

Dutta K, Schuur EAG, Neff JC, Zimov SA (2006) Potential carbon release from
   permafrost soils of Northeastern Siberia. *Global Change Biology*, **12**, 2336-2351,
   doi:10.1111/j.1365-2486.2006.01259.x.

Fan Z, Neff JC, Harden JW, Wickland KP (2008) Boreal soil carbon dynamics under a
   changing climate: A model inversion approach. *Journal of Geophysical Research*,
   113, G04016, doi:10.1029/2008JG000723.

Flannigan M, Stocks B, Turetsky M, Wotton M (2009) Impacts of climate change on fire
   activity and fire management in the circumboreal forest. *Global Change Biology*,
   15, 549-560, doi:10.1111/j.1365-2486.

Gillett NP, Weaver AJ, Zwiers FW, Flannigan MD (2004) Detecting the effect of climate
   change on Canadian forest fires. *Geophysical Research Letters*, **31**, L18211,
   doi:10.1029/2004GL020876.

Harden JW, O'Neill KP, Trumbore SE, Veldhuis H, Stocks BJ (1997) Moss and soil contributions to the annual net carbon flux of a maturing boreal forest. *Journal of Geophysical Research*, **102**, 28805-28816.

Harden JW, Trumbore SE, Stocks BJ, Hirsch A, Gower ST, O'Neill KP, Kasischke ES (2000) The role of fire in the boreal carbon budget. *Global Change Biology*, **6** (Suppl. 1), 174-184.

Hedges JI, Stern JH (1984) Carbon and nitrogen determinations of carbonate-containing solids. *Limnology and Oceanography*, **29**, 657-663.

Heimann M, Reichstein M (2008) Terrestrial ecosystem carbon dynamics and climate feedbacks. *Nature*, **451**, doi:10.1038/nature06591.

Jobbagy EG, Jackson RB (2000) The vertical distribution of soil organic carbon and its relation to climate and vegetation. *Ecological Applications*, **10**, 423-436.

Johnstone JF, Hollingsworth TN, Chapin FS III, Mack MC (2009) Changes in fire regime break the legacy lock on successional trajectories in Alaskan boreal forest. *Global Change Biology*, **16**, 1281-1295, doi:10.1111/j.1365-2486.2009.02051.x.

Jones BM, Kolden CA, Jandt R, Abatzoglou JT, Urban F, Arp CD (2009) Fire behavior, weather, and burn severity of the 2007 Anaktuvuk River tundra fire, North Slope Alaska. *Arctic, Antarctic, and Alpine Research*, **41**, 309-316.

Jorgenson MT, Racine CH, Walters JC, Osterkamp TE (2001) Permafrost degradation and ecological changes associated with a warming climate in central Alaska. *Climatic Change*, **48**, 551-579.

Jorgenson MT, Shur YL, Pullman ER (2006) Abrupt increase in permafrost degradation in Arctic Alaska. *Geophysical Research Letters*, **33**, L02503, doi:10.1029/2005GL024960.

Jorgenson MT, Romanovsky VE, Harden J, O'Donnell JA, Schuur EAG, Kanevskiy M (2010) Resilience and vulnerability of permafrost to climate change. *Canadian Journal of Forest Research*. In press.

Kane ES, Valentine DW, Schuur EAG, Dutta K (2005) Soil carbon stabilization along climate and stand productivity gradients in black spruce forests of interior Alaska. *Canadian Journal of Forest Research*, **35**, 2118-2129.

Kane ES, Kasischke ES, Valentine DW, Turetsky MR, McGuire AD (2007) Topographic influences on wildfire consumption of soil organic carbon in interior Alaska: implications for black carbon accumulation. *Journal of Geophysical Research*, **112**, G03017, doi:10.1029/2007JG000458.

Kane ES, Vogel JG (2009) Patterns of total ecosystem carbon storage with changes in soil temperature in boreal black spruce forests. *Ecosystems*, **12**, 322-335, doi:10.1007/s10021-008-9225-1.

Kasischke ES, Christensen NL, Stocks BJ (1995) Fire, global warming, and the carbon balance of boreal forests. *Ecological Applications*, **5**, 437-451.

Kasischke ES, Turetsky MR (2006) Recent changes in the fire regime across the North American boreal region – Spatial and temporal patterns of burning across Canada and Alaska. *Geophysical Research Letters*, **33**, L09703, doi:10.1029/2006GL025677.

Khvorostyanov DV, Krinner G, Ciais P, Heimann M, Zimov SA (2008) Vulnerability of
permafrost carbon to global warming. Part I: model description and role of heat
generated by organic matter decomposition. *Tellus B*, **60**, 250-264,
doi:10.1111/j.1600-0889.2007.00333.x.

Komada T, Anderson MR, Dormeier CL (2008) Carbonate removal from coastal
sediments for the determination of organic carbon and its isotopic signatures, $\delta^{13}C$
and $\Delta^{14}C$: comparison of fumigation and direct acidification by hydrochloric acid.
Limnology and Oceanography: Methods, **6**, 254-262.

Kuhry P, Ping CL, Tarnocai C, Schuur EAG, Zimov S (2009) Report from the
International Permafrost Association: Carbon pools in permafrost regions.
Permafrost and Periglacial Processes, 10.1002/ppp.648.

Lloyd J, Taylor JA (1994) On the temperature dependence of soil respiration. *Functional
Ecology*, **8**, 351-323.

Manies KL, Harden JW, Silva SR, Briggs PH, Schmidet BM (2004) Soil data from *Picea
mariana* stands near Delta Junction, AK of different stand ages and soil drainage
type. *US Geological Survey Open File Report*, **2004-1271**, 1-19.

Manies KL, Harden JW, Veldhuis H (2006) Soil data from a moderately well and
somewhat poorly drained fire chronosequence near Thompson, Manitoba,
Canada. *US Geological Survey Open File Report*, **2006-1291**, 1-17.

Marchenko S, Romanovksy V, Tipenko G (2008) Numerical modeling of spatial

   permafrost dynamics in Alaska. In: *Proceedings of the Ninth International

   Conference on Permafrost*, July 29-July 3, 2008, (eds Kane DL, Hinkel KM), pp.

   1-6. Fairbanks, AK, USA.

McGuire AD, Hayes DJ, Kicklighter DW, Manizza M, Zhuang Q, Chen M, Follows MJ,

   Gurney KR, McClelland JW, Melillo JM, Peterson BJ, Prinn R (2010) An

   analysis of the carbon balance of the Arctic Basin from 1997 to 2006. *Tellus*. In

   press.

Michaelson GJ, Ping CL, Kimble JM (1996) Carbon storage and distribution in tundra

   soils of arctic Alaska. *Arctic and Alpine Research*, **28**, 414-424.

Mikan CJ, Schimel JP, Doyle AP (2002) Temperature controls of microbial respiration in

   arctic tundra soils above and below freezing. *Soil Biology & Biochemistry*, **34**,

   1785-1795.

Nowinski NS, Taneva L, Trumbore SE, Welker JM (2010) Decomposition of old organic

   matter as a result of deeper active layers in a snow depth manipulation

   experiment. *Oecologia*, doi:10.1007/s00442-009-1556-x.

Osterkamp TE, Romanovsky VE (1999) Evidence for warming and thawing of

   discontinuous permafrost in Alaska. *Permafrost and Periglacial Processes*, **10**,

   17-37.

Peng C, Apps MJ (1999) Modelling the response of net primary productivity (NPP) of

   boreal forest ecosystems to changes in climate and fire disturbance regimes.

   Ecological Modelling, **122**, 175-193.

Ping CL, Michaelson GJ, Jorgenson MT, Kimble JM, Epstein H, Romanovsky VE,
Walker DA (2008a) High stocks of soil organic carbon in the North American
Arctic region. *Nature Geoscience*, **1**, 615-619, doi:10.1038/ngeo284.

Ping CL, Michaelson GJ, Kimble JM, Romanovsky VE, Shur YL, Swanson DK, Walker
DA (2008b) Cryogenesis and soil formation along a bioclimate gradient in Arctic
North America. *Journal of Geophysical Research*, **113**, G03S12,
doi:10.1029/2008JG000744.

Richter DD, Markewitz D, Trumbore SE, Wells CG (1999) Rapid accumulation and
turnover of soil carbon in re-establishing forest. *Nature*, **400**, 56-58.

Romanovsky VE, Osterkamp TE (2000) Effects of unfrozen water on heat and mass
transport processes in the active layer and permafrost. *Permafrost and Periglacial
Processes*, **11**, 219-239.

Rustad LE, Campbell JL, Marion GM, Norby RJ, Mitchell MJ, Hartley AE, Cornelissen
JHC, Gurevitch J, GCTE-NEWS (2001) A meta-analysis of the response of soil
respiration, net nitrogen mineralization, and aboveground plant growth to
experimental warming. *Oecologia*, **126**, 543-562, doi:10.1007/s004420000544.

Schimel DS, Braswell BH, Holland EA, McKeown R, Ojima DS, Painter TH, Parton WJ,
Townsend AR (1994) Climatic, edaphic, and biotic controls over storage and
turnover of carbon in soils. *Global Biogeochemical Cycles*, **8**, 279-293.

Schimel JP, Mikan C (2005) Changing microbial substrate use in Arctic tundra soils
through a freeze-thaw cycle. *Soil Biology & Biochemistry*, **37**, 1411-1418.

Schirrmeister L, Siegert C, Kuznetsova T, Kuzmina S, Andreev A, Kienast F, Meyer H,

    Bobrov A (2002) Paleoenvironmental and paleoclimatic records from permafrost

    deposits in the Arctic region of Northern Siberia. *Quaternary International*, **89**,

    97-118.

Schuur EAG, Crummer KG, Vogel JG, Mack MC (2007) Plant species composition and

    productivity following permafrost thaw and thermokarst in Alaskan tundra.

    Ecosystems, **10**, 208-292, doi:10.1007/s10021-007-9024-0.

Schuur EAG, Bockheim J, Canadell JG, Euskirchen E, Field CB, Goryachkin SV,

    Hagemann S, Kuhry P, Lafleur PM, Lee H, Mazhitova G, Nelson FE, Rinke A,

    Romanovsky VE, Shiklomanov N, Tarnocai C, Venevsky S, Vogel JG, Zimov SA

    (2008) Vulnerability of permafrost carbon to climate change: implications for the

    global carbon cycle. *Bioscience*, **58**, 701-714.

Schuur EAG, JG Vogel, KG Crummer, H Lee, JO Sickman, and TE Osterkamp (2009)

    The effect of permafrost thaw on old carbon release and net carbon exchange

    from tundra. *Nature*, **459**, 556-559, doi:10.1038/nature08031.

Shur Y, Hinkel KM, Nelson FE (2005) The transient layer: implications for geocryology

    and climate-change science. *Permafrost and Periglacial Processes*, **16**, 5-17.

Shur YL, Jorgenson MT (2007) Patterns of permafrost formation and degradation in

    relation to climate and ecosystems. *Permafrost and Periglacial Processes*, **18**, 7-

    19.

Shur YL, Kanevskiy M, White DM, Connor B (2010) Geotechnical investigations for the Dalton Highway Innovation Project as a case study of the ice-rich syngenetic permafrost. *AUTC assigned project #207122*, February 25, 2010.

Southon J, Santos G, Druffel-Rodriguez K, Druffel E, Trumbore S, Xu X, Griffin S, Ali S, Mazon M (2004) The Keck Carbon Cycle AMS laboratory, University of California Irvine: initial operation and background surprise. *Radiocarbon*, **46**, 41-49.

Staff SS (1998) Keys to soil taxonomy. pp 599. Pocahontas Press, Inc., Blacksburg, VA, USA.

Stuiver M, Polach HA (1977) Discussion: reporting of ^{14}C data. *Radiocarbon*, **19**, 355-363.

Swanson DK (1996) Susceptibility of permafrost soils to deep thaw after forest fires in interior Alaska, USA. *Arctic and Alpine Research*, **28**, 217-227.

Swanson DK, Ping CL, Michaelson GJ (1999) Diapirism in soils due to thaw of ice-rich material near the permafrost table. *Permafrost and Periglacial Processes*, **10**, 349-367.

Tarnocai C, Canadell JG, Schuur EAG, Kuhry P, Mahitova G, Zimov S (2009) Soil organic carbon pools in the northern circumpolar permafrost region. *Global Biogeochemical Cycles*, **23**, GB2023, doi:10.1029/2008GB003327.

Tomirdiaro SV, Arslanov KA, Chernenkiy BI, Tertychnaya TV, Prokhorova TN (1984) New data on formation of loess-ice sequences in Northern Yakutia and ecological conditions of mammoth fauna in the Arctic during the late Pleistocene. *Reports Academy of Sciences USSR*, **278**, 1446-1449 (in Russian).

Trumbore SE, Harden JW (1997) Accumulation and turnover of carbon in organic and mineral soils of the BOREAS northern study area. *Journal of Geophysical Research*, **102**, 28817-28830.

Trumbore SE, Czimczik CI (2008) An uncertain future for soil carbon. *Science*, **321**, 1455-1456.

Viereck LA, Dyrness CT, Batten AR, Wenzlick KJ (1992) The Alaska vegetation classification. *General Technical Report PNW-GTR-286*, U.S. Department of Agriculture, Forest Service, Pacific Northwest Research Station.

Viereck LA, Werdin-Pfisterer NR, Adams PC, Yoshikawa K (2008) Effect of wildfire and fireline construction on the annual depth of thaw in a black spruce permafrost forest in interior Alaska: a 36-year record of recovery. In: Proceedings of the Ninth International Conference on Permafrost, July 29-July 3, 2008, (eds Kane DL, Hinkel KM), pp. 1845-1850. Fairbanks, AK, USA.

Waldrop MP, Wickland K, White R III, Berhe AA, Harden J, Romanovsky V (2010) Molecular investigations into a globally important carbon pool: permafrost-protected carbon in Alaskan soils. *Global Change Biology*, doi:10.1111/j.1365-2486.2009.02141.x.

Walter KM, Zimov SA, Chanton JP, Verbyla D, Chapin FS III (2006) Methane bubbling

from Siberian thaw lakes as a positive feedback to climate warming. *Nature*, **443**,

doi:10.1038/nature05040.

Wickland KP, Neff JC (2007) Decomposition of soil organic matter from boreal black

spruce forest: environmental and chemical controls. *Biogeochemistry*,

doi:10.1007/s10533-007-9166-3.

Xu X, Trumbore SE, Zheng S, Southon JR, McDuffee KE, Luttgen M, Liu JC (2007)

Modifying a sealed tube zinc reduction method for preparation of AMS graphite

targets: Reducing background and attaining high precision. *Nuclear Instruments*

and Methods in Physics Research B, **259**, 320-329.

Yi S, Manies K, Harden J, McGuire AD (2009a) Characteristics of organic soil in black

spruce forests: Implications for the application of land surface and ecosystem

models in cold regions. *Geophysical Research Letters*, **36**, L05501,

doi:10.1029/2008GL037014.

Yi S, McGuire AD, Harden JW, Kasischke E, Manies K, Hinzman L, Lilgedahl A,

Randerson J, Liu H, Romanovsky V, Marchenko S, Kim Y (2009b) Interactions

between soil thermal and hydrological dynamics in the response of Alaska

ecosystems to fire disturbance. *Journal of Geophysical Research*, **114**, G02015,

doi:10.1029/2008JG000841.

Yi S, McGuire AD, Kasischke ES, Harden JW, Manies KL, Mack M, Turetsky MR

    (2010) A dynamic organic soil biogeochemical model for analyzing carbon

    responses in black spruce forests in Interior Alaska. *Journal of Geophysical*

    Research. In review.

Yoshikawa K, Bolton WR, Romanovsky VE, Fukuda M, Hinzman LD (2003) Impacts of

    wildfire on the permafrost in the boreal forests of Interior Alaska. *Journal of*

    Geophysical Research, **108**, D1, doi:10.1029/2001JD000438.

Zhuang Q, McGuire AD, O'Neill KP, Harden JW, Romanovsky VE, Yarie J (2003)

    Modeling soil thermal and carbon dynamics of a fire chronosequence in interior

    Alaska. Journal of Geophysical Research, 108, doi:10.1029/2001JD001244.

Tables

Table 1. Summary of soil chemistry across different soil horizons

Field Horizon Type	Sample Size	Bulk Density (g cm^{-3})	Field VWC (%)	Organic C (%)	Organic N (%)	Inorganic C (%)
surface organic horizons						
live moss	16	0.05 ± 0.01	16 ± 4	39.8 ± 0.7	0.97 ± 0.07	0.00 ± 0.00
fibrous	32	0.05 ± 0.01	14 ± 3	41.7 ± 1.1	0.95 ± 0.05	0.00 ± 0.00
amorphous	25	0.23 ± 0.05	39 ± 4	35.3 ± 2.3	1.08 ± 0.06	0.00 ± 0.00
mineral soil in active layer						
A/B/C	63	1.23 ± 0.06	56 ± 2	3.4 ± 0.7	0.17 ± 0.02	0.10 ± 0.07
permafrost						
fC (< 1m)	29	0.70 ± 0.06	78 ± 2	1.51 ± 0.23	0.10 ± 0.01	0.32 ± 0.13
fC (1-2 m)	79	0.92 ± 0.03	68 ± 1	1.32 ± 0.13	0.11 ± 0.01	0.44 ± 0.03
fC (2-5 m)	45	0.99 ± 0.04	66 ± 2	2.55 ± 0.39	0.21 ± 0.03	0.41 ± 0.05
fC (5-10 m)	59	0.91 ± 0.04	72 ± 2	1.78 ± 0.17	0.14 ± 0.01	0.56 ± 0.07
fC (10-20 m)	17	0.99 ± 0.06	72 ± 2	1.78 ± 0.27	0.13 ± 0.02	0.30 ± 0.05

Note: Reported values reflect means ± standard error.

Table 2. Summary of input and decomposition rates of organic matter in surface organic horizons, active layer, and permafrost.

Site Description	Cumulative C kg C m^{-2}	Inputs kg C m^{-2} yr^{-1}	k (yr-1)	Net accumulation/loss rate kg C m^{-2} yr^{-1}
Recent C Accumulation (organic soil above char layer)				
Hess Creek Chronosequence	2.03 ± 1.08	0.050 ± 0.011	0.0173 ± 0.0056	0.015
C accumulation in mineral soil of the active layer				
2003 Burn	6.28 ± 4.73	0.003 ± 0.002	0.0002 ± 0.0002	0.002
C accumulation in near-surface permafrost				
Unburned Mature	6.26 ± 4.65	0.003 ± 0.0003	0.0003 ± 0.0002	0.001
2003 Burn	10.72 ± 6.14	0.002 ± 0.0004	-	-0.001
1967 Burn	7.42	0.001 ± 0.00007	-	-0.001

Data represent mean values ± 1 standard deviation.

Table 3. Parameters used in fire-permafrost interaction model.

Model Parameters	Description	Calculated Values	Units	Model Input	Source
$I_{shallow}$	inputs to shallow organic horizon	0.050 (0.011)	kg C m^{-2} y^{-1}	0.06	Hess Creek chronosequence
$k_{shallow}$	decay constant for shallow organic horizon	0.017 (0.06)	y^{-1}	0.024	Hess Creek chronosequence
k_{deep}	decay constant for deep organic horizon	-	y^{-1}	0.0025	model validation from this study
$I_{mineral}$	inputs to mineral horizons	0.003 (0.002)	kg C m^{-2} y^{-1}	0.003	^{14}C accumulation model
$k_{active\text{-}layer}$	decay constant for thawed mineral horizons	0.0002 (0.0002)	y^{-1}	0.0004	^{14}C accumulation model
$k_{permafrost}$	decay constant for permafrost	0.0003 (0.0002)	y^{-1}	0.0003	^{14}C accumulation model
FRI	fire return interval	148 (50)	y	150	Mature stand ages at Hess Creek
SEV	burn severity	65 (8)	%	41	Harden *et al.*, 2006

Calculated values represent means ± 1 standard deviation (in parentheses)

Figures
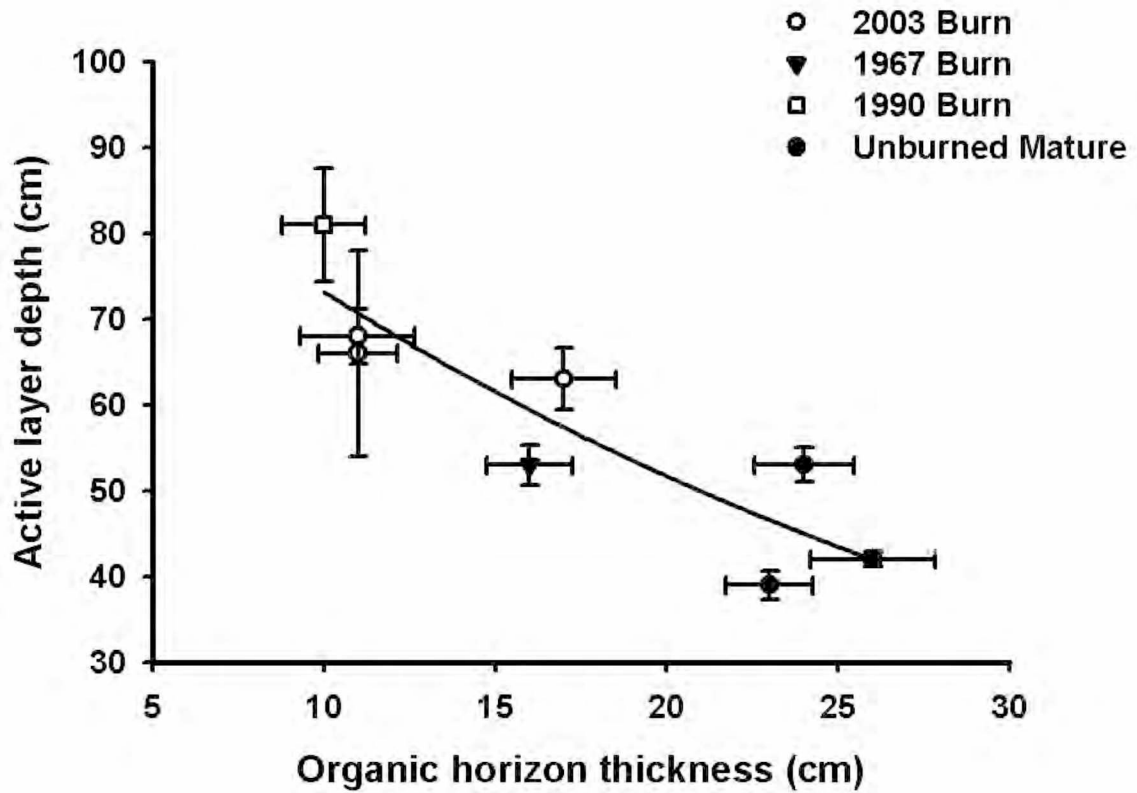
Figure 1. Relationship between active layer depth and organic horizon thickness

measured across chronosequence at Hess Creek. The curve is represented by the

following exponential equation: $ALD = 103.7537 * e^{(-0.0349*OHT)}$. OHT and ALD

measurements were drawn from replicate 2003 Burn (n = 3) and Unburned Mature (n =

3) stands, and individual 1967 Burn and 1990 Burn stands.
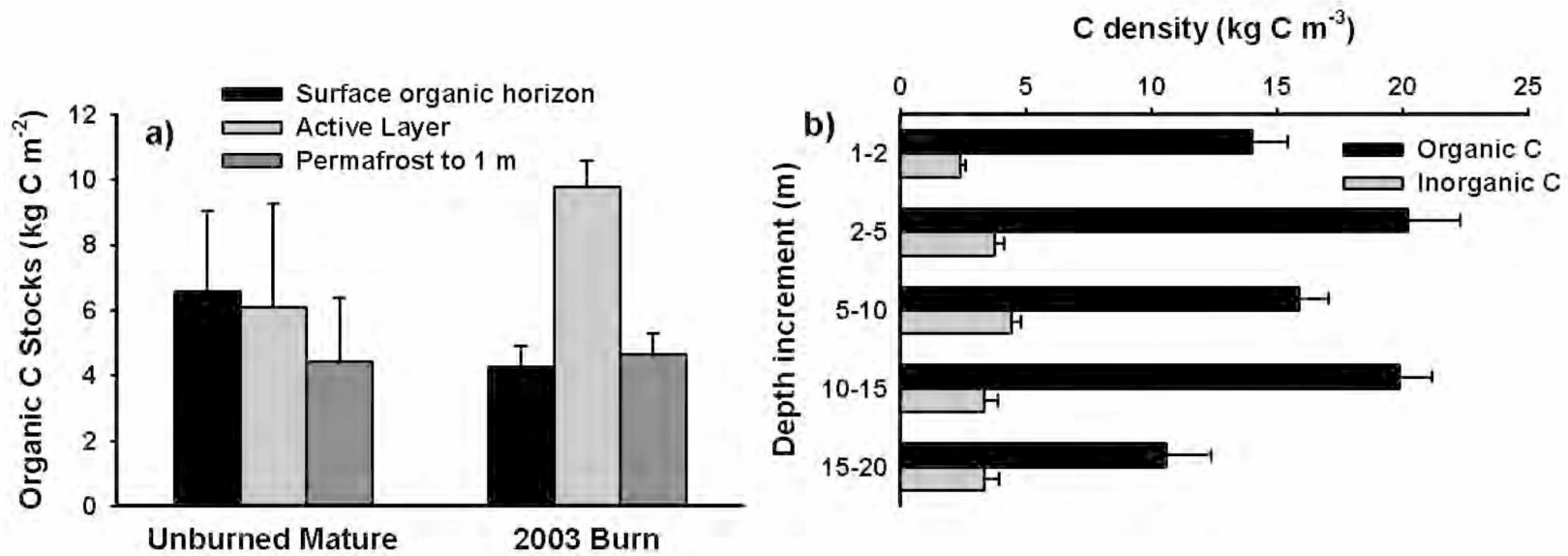
Figure 2. **(a)** OC stocks in organic horizons, mineral soil of the active layer, and permafrost down to 1 meter in a mature and recently burned stand. **(b)** OC and IC density with depth in frozen loess deposits at Hess Creek. Data are means (± 1 standard error).
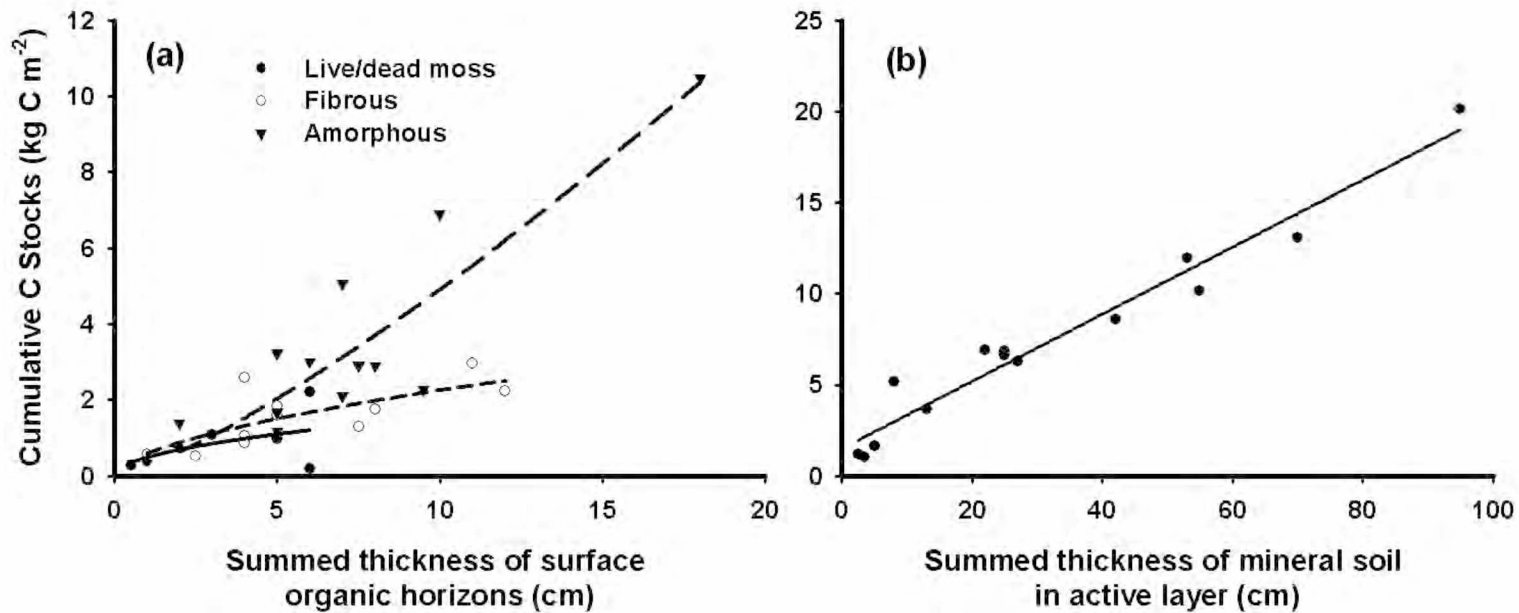
Figure 3. Relationship between cumulative OC stocks (kg C m-2) and **(a)** summed thickness of individual organic horizons and **(b)**.summed thickness of mineral horizons in the active layer ($R^2 = 0.95$; $P < 0.0001$) . In Fig (a), exponential curves (Equation 3) are fit to live/dead moss (solid line; a = 0.49; b = 0.50); $R^2 = 0.27$; $P = 0.19$), fibrous organic matter (short-dashed line; a = 0.59, b = 0.59; $R^2 = 0.52$; $P = 0.01$), and amorphous organic matter (long-dashed line; a = 0.26; b = 1.27; $R^2 = 0.77$; $P = 0.0002$).
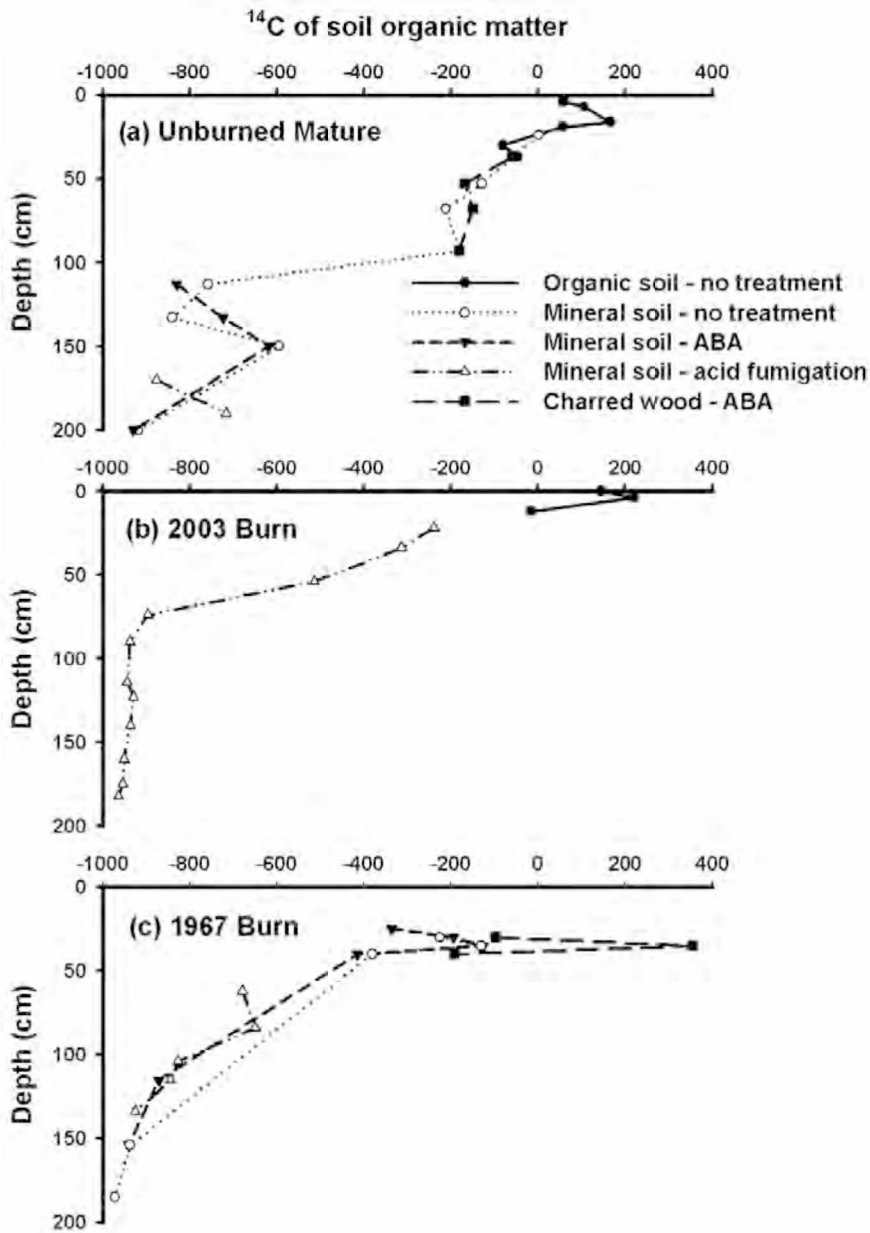
Figure 4. Patterns of Δ^{14}C of soil organic matter with depth across three stand ages near Hess Creek, Alaska. ABA refers to "acid-base-acid" treatment, which was conducted to remove organic matter and inorganic C from the surface of soil particles.
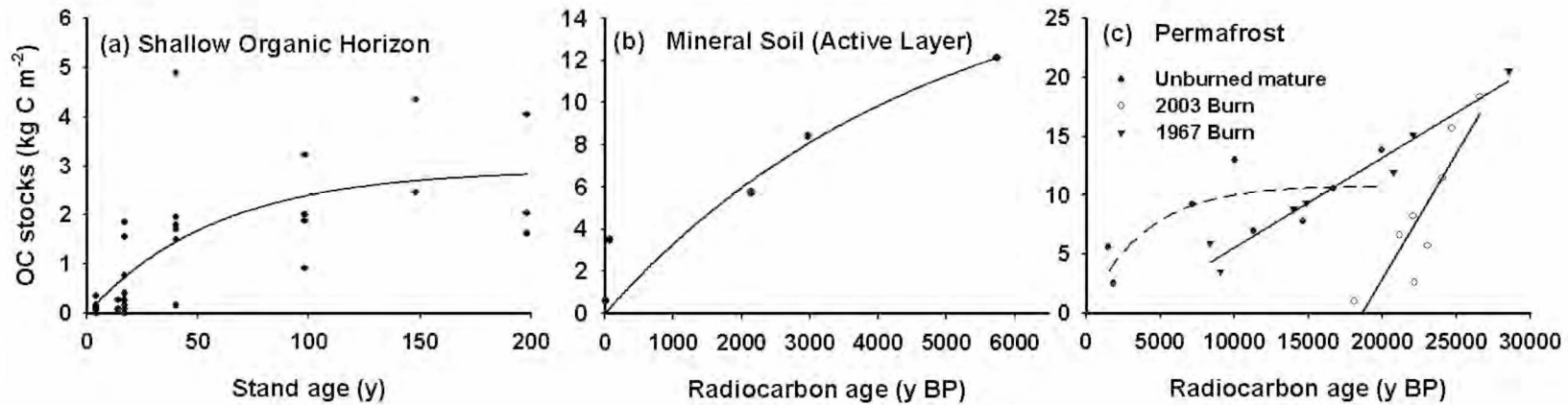
Figure 5. Soil OC accumulation in different soil horizons at Hess Creek. For the shallow organic horizons **(a)**, OC stocks above char (i.e. C recovery) is plotted versus stand age as measured across the upland fire-thaw chronosequence. Here, we fit an exponential curve (equation 2) to the data following Harden *et al.* (1997) to estimate inputs (i.e. NPP) and a decay constant (*k*) for the shallow organic horizon. For mineral soil in the active layer **(b)**, OC stocks are plotted versus radiocarbon age and fit with an exponential curve following Trumbore & Harden (1997). For permafrost **(c)**, OC stocks are also plotted versus radiocarbon age. The dashed line represents an exponential curve, while the solid lines represent a linear fit to the data. Inputs, decay constants and net C accumulation rates estimated from these approaches are summarized in Table 2.
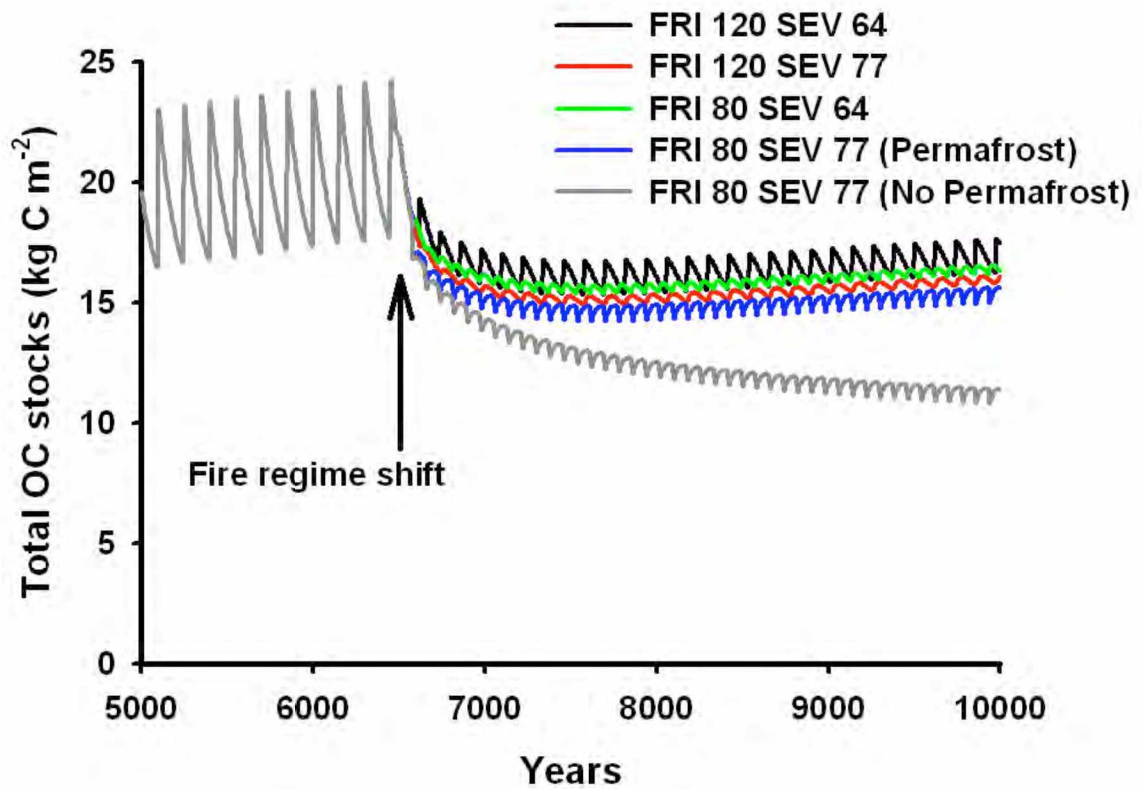
Figure 6. The sensitivity of total OC stocks to a change in fire regime. The five colored lines reflect different fire scenarios that vary with respect to fire return interval (120 and 80 years) and burn severity (64 and 77% of organic matter combusted). The gray line represents a scenario where all of the permafrost thawed following a fire regime shift (FRI 80, SEV 77).
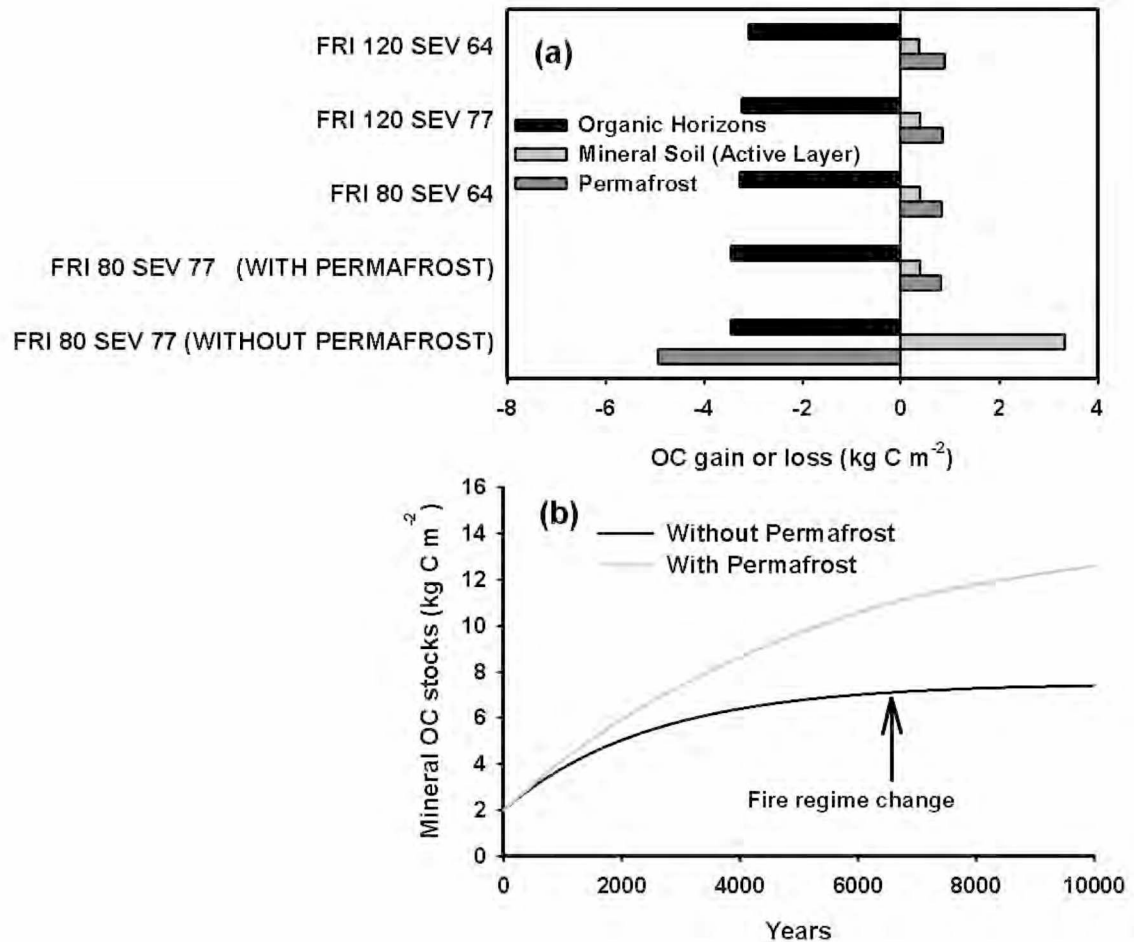
Figure 7. (a) Changes in OC stocks across four fire treatments relative to average OC stocks during the last fire cycle of the spin-up (years 6350-6500). A positive value reflects a net OC gain, while a negative value reflects a net OC loss. (b) Comparison of mineral OC accumulation between a fire scenario with near-surface permafrost and when near-surface permafrost completely thaws.

Supplemental Material

Here, we provide a brief description of the model (see Harden *et al.* (2000) for more detailed description) and focus primarily on the modifications made for this particular study. The model examines net changes in soil C storage over time (dC/dt) as governed by C inputs (net primary production (NPP) from moss and trees) and losses (heterotrophic respiration and fire). We prescribed a constant value for tree stem + branch NPP (0.07 kg C m^{-2} y^{-1}), as reported by prior field and modeling studies (Bond-Lamberty *et al.*, 2004; Manies *et al.*, 2005). NPP from tree wood (stem + branch) varies with stand age, ranging from 0.005 to 0.146 kg C m^{-2} y^{-1} in a feather moss-dominated black spruce ecosystem in Manitoba, Canada (Bond-Lamberty *et al.*, 2004). For our study, a constant NPP reflects the average value across stand ages.

The soil organic horizon is partitioned into a shallow layer ($C_{shallow}$) that accumulates between fire cycles and a deep layer (C_{deep}) that is buried by the regrowth of moss (in the $C_{shallow}$ layer) following fire. In this study, $C_{shallow}$ consists primarily of live and dead feather moss, fibrous organic matter, plant litter and fine roots, all of which decompose at a first order rate constant, $k_{shallow}$. C_{deep} consists of roots, amorphous organic matter (mesic and humic horizons), dead wood and char, all of which decompose at a first order rate constant, k_d. During fire events, a proportion of tree C stocks and $C_{shallow}$ burns and is lost to the atmosphere. The charred and unburned intact remains decompose for one fire cycle at rate $k_{shallow}$ and are then transferred into C_{deep}, where they

decompose at rate k_d. However, as k_d is unconstrained by our radiocarbon measurements, k_d was solved through model calibration.

Carbon dynamics in the fire-permafrost interaction model were parameterized using OC input and loss estimates derived from our measurements of OC recovery across the chronosequence and radiocarbon inventories. We assigned fixed parameters for OC input and decay constants so that net OC accumulation during the model simulation was a good fit for measured OC stocks in each soil horizon. For shallow organic horizons, we assigned mean values of $I_{shallow}$ and $k_{shallow}$ as determined by measurements of C recovery across the chronosequence. For mineral horizons, we assigned the mean value of $I_{mineral}$ as estimated from the OC and radiocarbon inventories at the 2003 burn. Depending upon ALD, a proportion of $C_{mineral}$ were then decomposed as a function of either $k_{active-layer}$ or $k_{permafrost}$, which were assigned as fixed parameters based on OC and radiocarbon inventories.

To test the model, we compared simulated and measured OC stock values for each soil horizon ($C_{shallow}$, C_{deep}, $C_{active-layer}$, $C_{permafrost}$) across our fire chronosequence at the Hess Creek study region (Supplementary Figure 1). The model was run from the approximate arrival of black spruce in the interior Alaskan landscape about 6500 years ago (Lynch *et al.*, 2003) to the present at 10-year time steps. In addition to the above parameters, we ran the model with a fire return interval of 150 years, based on the average age of tree cores measured from three mature black spruce stands at Hess Creek. We also prescribed a burn severity of 41% (percentage of organic horizon combusted

during fire) as reported by Harden *et al.* (2006) for a similar black spruce site near Delta Junction, AK, to reflect historic combustion of soil organic horizons by fire. Meanwhile, to determine k_{deep}, which was unconstrained by our radiocarbon measurements, we conducted a sensitivity test to evaluate how variations in k_{deep} govern C accumulation in deep organic horizons. The sensitivity test revealed that k_{deep} exerts considerable influence on OC accumulation in deep organic horizons (Supplementary Figure 2), and that a k_{deep} of 0.005 y^{-1} in the model most closely approximates measured target OC stocks in the deep organic horizon (Supplementary Figure 3).

We observed two distinct zig-zag patterns for OC stocks in shallow and deep organic horizons (Supplementary Figure 2a), as initially reported by Harden *et al.* (2000). For the shallow organic horizon, the zig-zag pattern represents the net accumulation of organic matter (from moss growth and leaf litter inputs) between fire cycles and the loss of organic matter via combustion during fire events. For the deep organic horizons, the zig-zag pattern represents the inputs of dead and burned material from shallow to deep layers and the subsequent decline of organic matter stocks due to decomposition.

Supplemental Tables

Supplemental Table 1. Parameters and statistics from linear equations used to predict

OC stocks from organic horizon thickness.

Horizon Type	β	n	R^2	*P-value*
	(g C cm^{-1})			
Live moss	0.0083	89	0.18	< 0.0001
Dead moss	0.0141	101	0.41	< 0.0001
Burned dead moss	0.0203	17	0.18	0.008
Fibric	0.0149	162	0.36	< 0.0001
Burned fibric	0.0429	23	0.72	< 0.0001
Mesic	0.0412	114	0.42	< 0.0001
Humic	0.0626	55	68	< 0.0001
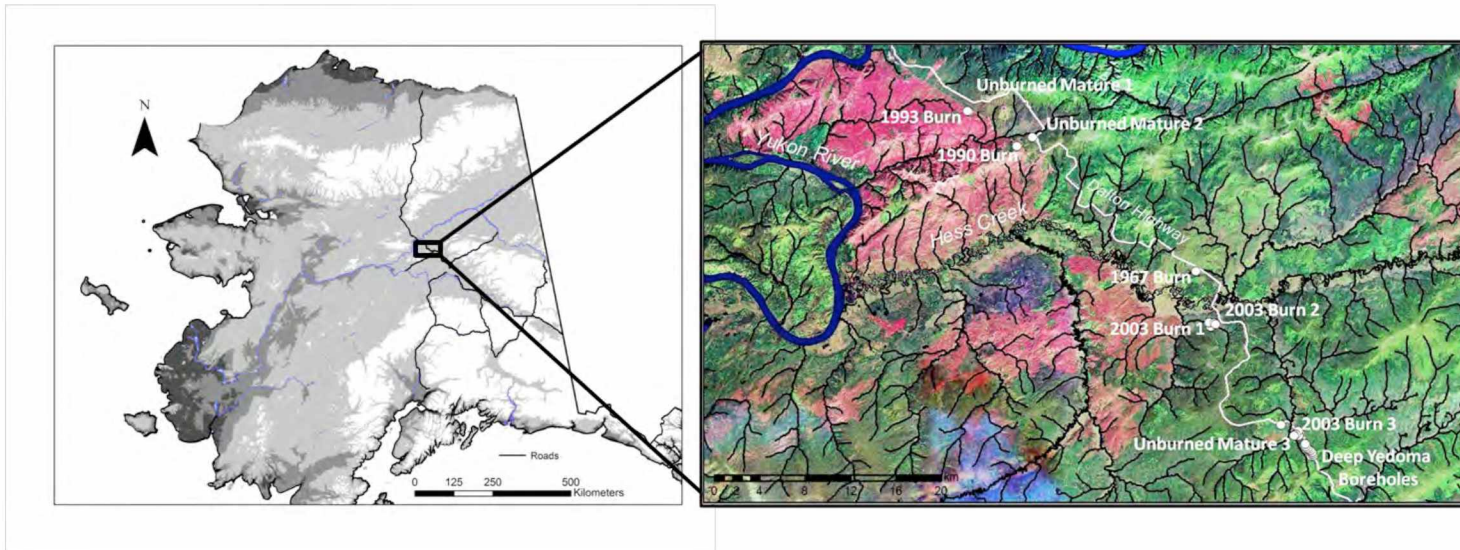
Supplemental Figure 1. Map of Alaska (left panel) and study sites across fire chronosequence near Hess Creek (right panel).
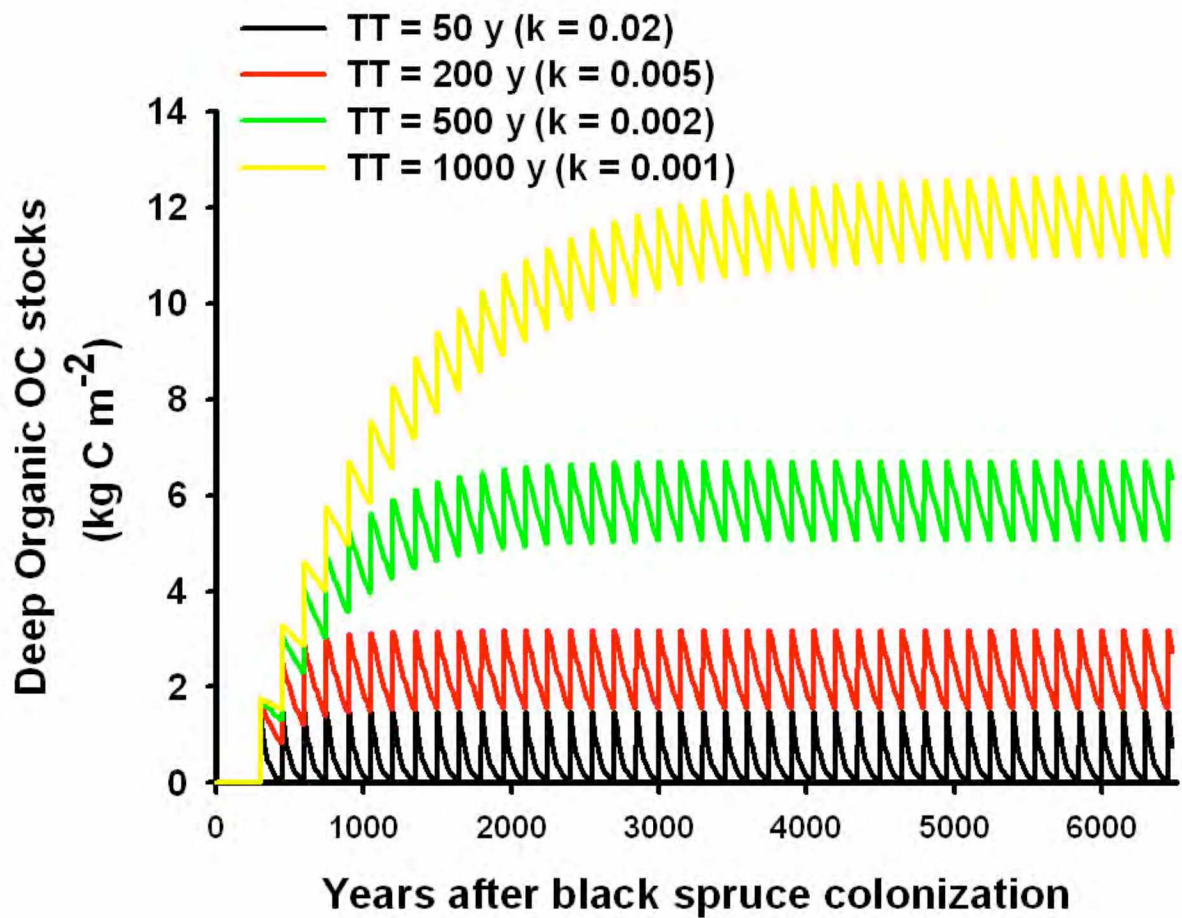
Supplemental Figure 2. Sensitivity test to analyze the effect of k_{deep}, and thus turnover time (TT) on deep organic OC stocks.
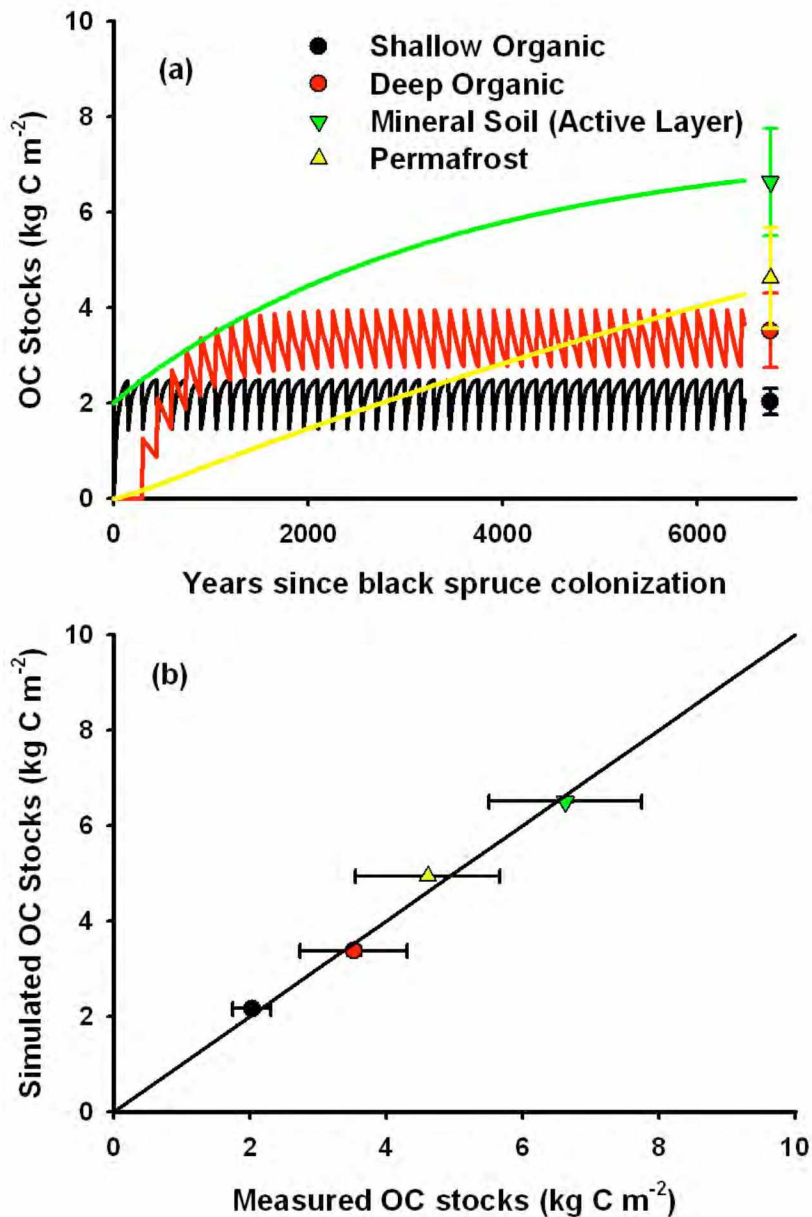
Supplemental Figure 3. Verification of soil OC accumulation model. **(a)** Results of model simulation for the first 6500 years since black spruce colonization on the interior Alaskan landscape. **(b)** Comparison of simulated and measured OC stocks. Simulated OC stocks reflect the mean (± 1 standard error) during the last fire cycle of the model run.

References

Bond-Lamberty B, Wang C, Gower ST (2004) Net primary production and net ecosystem

    production of a boreal black spruce wildfire chronosequence. *Global Change*

    Biology, **10**, 473-487, doi:10.1111/j.1529-8817.2003.0742.x.

Harden JW, Trumbore SE, Stocks BJ, Hirsch A, Gower ST, O'Neill KP, Kasischke ES

    (2000) The role of fire in the boreal carbon budget. *Global Change Biology*, **6**

    (Suppl. 1), 174-184.

Harden JW, Manies KL, Turetsky MR, Neff JC (2006) Effects of wildfire and permafrost

    on soil organic matter and soil climate in interior Alaska. *Global Change Biology*,

    12, 2391-2403, doi: 10.1111/j.1365-2486.2006.01255.x.

Lynch JA, Clark JS, Bigelow NH, Edwards ME, Finnery BP (2003) Geographic and

    temporal variations in fire history in boreal ecosystems of Alaska. *Journal of*

    Geophysical Research, **108**, doi:10.1029/2001JD000332.

Manies KL, Harden JW, Bond-Lamberty BP, O'Neill KP (2005) Woody debris along an

    upland chronosequence in boreal Manitoba and its impact on long-term carbon

    storage. *Canadian Journal of Forest Research*, **35**, 472-482.

Chapter 3: The effect of moisture content on the thermal conductivity of moss and organic soil horizons from black spruce ecosystems in Interior Alaska[2]

Abstract

Organic soil horizons function as important controls on the thermal state of near-surface soil and permafrost in high-latitude ecosystems. The thermal conductivity of organic horizons is typically lower than mineral soils and is closely linked to moisture content, bulk density and water phase. In this study, we examined the relationship between thermal conductivity and soil moisture for different moss and organic horizon types in black spruce ecosystems of interior Alaska. We sampled organic horizons from feather moss-dominated and *Sphagnum*-dominated stands and divided horizons into live moss, fibrous and amorphous organic matter. Thermal conductivity measurements were made across a range of moisture contents using the transient line heat source method. Our findings indicate a strong positive and linear relationship between thawed thermal conductivity (K_t) and volumetric water content. We observed similar regression parameters (β or slope) across moss types and organic horizons types and small differences in β_0 (*y*-intercept) across organic horizon types. Live *Sphagnum spp.* had a higher range of K_t than live feather moss due to the field capacity (lab-based) of live *Sphagnum spp.* In northern regions, the thermal properties of organic soil horizons play a critical role in mediating the effects of climate warming on permafrost conditions.

Findings from this study could improve model parameterization of thermal properties in organic horizons and enhance our understanding of future permafrost and ecosystem dynamics.

Introduction

Moss and organic soil horizons function as important controls on soil temperature and the thermal state of permafrost in high latitude ecosystems (Dyrness, 1982; Bonan and Shugart, 1989; Yoshikawa et al., 2003; Nicolsky et al., 2007a). In general, organic soil horizons have low thermal conductivity values relative to mineral soil (Farouki, 1981), and consequently, reduce vertical heat fluxes through the soil column and insulate permafrost from warm summer air temperatures. Recent climate warming at high latitudes has resulted in warming and thawing of permafrost (Lachenbruch and Marshall, 1986; Jorgenson et al., 2006), particularly in the discontinuous permafrost zone (Osterkamp and Romanovsky, 1999; Jorgenson et al., 2001), where soil temperatures are near 0 °C. However, the thermal properties of organic soil horizons may function to minimize the effects of climate warming on the ground thermal regime (Shur and Jorgenson, 2007; Yi et al., 2007), slowing rates of soil warming and permafrost degradation.

The thermal conductivity of unfrozen organic soil horizons is influenced by soil moisture, bulk density and decomposition state of the organic matter (Farouki, 1981; Yoshikawa et al., 2003). Organic soil horizons have very high porosity (Yi et al., 2009a),

and thus, the thermal conductivity of organic horizons can fluctuate widely with moisture content. Prior studies have illustrated that the thermal conductivity of peat increases with moisture content (Johansen, 1975; Andersland and Anderson, 1978; Farouki, 1981). Andersland and Anderson (1978) reported a non-linear relationship between the thermal conductivity of unfrozen peat and gravimetric moisture content, whereas Johansen (1975) reported a linear relationship between the square root of thermal conductivity and the degree of saturation. Thermal conductivity of organic matter also increases with bulk density (Andersland and Anderson, 1978), and bulk density typically increases with decomposition of soil organic matter (Manies et al., 2004). As a result, thermal conductivity should increase with decomposition and humification of soil organic matter.

To accurately predict future changes in permafrost extent and thickness, climate models have begun to include explicit thermal and hydrologic properties of soil organic horizons in high-latitude regions (Euskirchen et al., 2006; Nicolsky et al., 2007a; Lawrence et al., 2008; Yi et al., 2009b). In earlier studies, soil thermal models and ecosystem process-based models prescribed a constant average thermal conductivity value for thawed and frozen peat (Zhuang et al., 2001; Romanovsky and Osterkamp, 2000), but did not account for the effect of interannual and seasonal variability in moisture content on thermal conductivity, even though it was recognized as a necessary next step (Romanovsky and Osterkamp, 1997). Indeed, variability in the thermal conductivity of surface organic horizons can have a profound effect on simulated soil temperatures at depth (Bonan, 1991). More recently, several studies have used Kersten numbers to calculate thermal conductivity as a function of moisture content (Lawrence

and Slater, 2008; Yi et al., 2009b). The Kersten number is a normalized thermal conductivity value used to weight the saturated and dry thermal conductivities values of a given substrate (Kersten, 1949; Farouki 1981). The incorporation of thermal conductivity as a moisture-affected variable in climate and ecosystem models is an important step forward in understanding high-latitude permafrost dynamics. To further enhance projections of high-latitude permafrost dynamics, it will be critical to include parameterizations for multiple organic horizons, based on improved *in situ* soil moisture measurements and more accurate thermal conductivity parameters (Nicolsky et al., 2007b).

The aim of this study is to examine the relationship between thermal conductivity and moisture content in different organic horizons from black spruce (*Picea mariana* (Mill.) BSP) ecosystems of interior Alaska. Black spruce is the dominant forest type in interior Alaska, covering approximately 44 % of the landscape (Van Cleve et al., 1983), and is typically underlain by permafrost. Mosses dominate forest floor cover in black spruce ecosystems (Barney and Van Cleve, 1973; Beringer et al., 2001). Moss species vary with soil drainage in black spruce ecosystems. Feather moss-dominated stands often occur in somewhat poorly drained conditions, but are generally quite pervasive across drainage classes (Harden et al., 1997; Bisbee et al., 2001), whereas *Sphagnum*-dominated stands typically occur in poorly drained conditions. To evaluate the effect of moisture content on thermal conductivity, we collected samples from the organic horizons of both feather moss-dominated and *Sphagnum*-dominated black spruce ecosystems. Organic samples were divided into three horizons (live moss, fibrous, amorphous) that differ with

respect to physical properties and extent of decomposition, and we measured thermal

conductivity across a range of moisture contents. Relationships derived from these data,

which will allow for the calculation of thermal conductivity directly from *in situ*

measures of soil moisture in surface organic horizons, are useful for modeling how the

soil temperature regime of black spruce forests will respond to climate variability and

change.

Materials and Methods

Soil samples were collected from three somewhat poorly-drained and two poorly

drained black spruce forests in interior Alaska. Somewhat poorly-drained sites are

typically located in areas with limited slope (< 15%), silt-dominated mineral soil texture,

and permafrost that is typically present in the top 1 m. We sampled somewhat poorly-

drained sites at the Bonanza Creek Experimental Forest (BCEF; www.lter.uaf.edu), Delta

Junction, AK (DFCC site; see Harden et al., 2006), and in the uplands of the Washington

Creek watershed (25 km north of Fairbanks, AK). Poorly-drained sites are typically

underlain by permafrost, with a shallow active layer depth (30 to 50 cm) and a water

table is typically within 20-30 cm of the moss surface. We sampled poorly-drained sites

that included a *Sphagnum*-dominated site at the BCEF and a site in the valley bottom of

the Washington Creek watershed. Feather mosses (*Hylocomium splendens and*

Pleurozium schreberi) were the dominant moss species in the somewhat-poorly drained

stands, whereas *Sphagnum spp.* (most commonly *Sphagnum fuscum)* dominated forest

floor cover in the poorly drained stands. Field measurements of moisture content in fibrous organic horizons of black spruce ecosystems indicate that typical moisture values are greater in *Sphagnum-* than feathermoss-dominated forest floors (Figure 1; O'Donnell et al., 2009).

Organic soils were sampled by hand to ensure accurate volume and bulk density measurements. Using a variety of soil knives, saws, and scissors, samples were cut into small blocks and measured for volume. Samples were divided into live moss, fibrous organic matter (slightly decomposed), and amorphous organic matter (moderate to highly decomposed) for both moss types, following the stratified approach of Yi et al. (2009a). Samples were then transferred into small Tupperware containers and stored in a cooler until returned to the laboratory for further analysis. In the lab, all samples (n = 5 per site per horizon, total = 75 samples) were saturated with deionized water and allowed to drain for 24 hours. After 24 hours, we removed any excess water from the Tupperware containers that had drained from the samples. Herein, we refer to this initial moisture content as "field capacity (lab-based)," based on the definition of field capacity as "the amount of water held in the soil after the excess gravitational water has drained away and the downward movement of water has materially decreased" (Veihmeyer and Hendrickson, 1931; Cassel and Nielsen, 1986).

We began measuring thawed thermal conductivity (K_t) using the KD2 Pro Thermal Properties Analyzer (Decagon Devices, Inc., Pullman, WA, USA). The KD2 Pro takes measurements using the transient line heat source method (Bristow et al.,

1994). Briefly, the measurement cycles consist of a 30 second equilibrium time, a 30 second heating time and a 30 second cooling time. Temperature measurements are made every second during heating and cooling, and then temperature measurements are fit with an exponential integral function using nonlinear least squares procedure. On average, samples were relatively thin (3-4 cm thick), insuring uniform distribution of water throughout each sample. Measurements were made by inserting the KD2 Pro probe horizontally into the middle of each soil sample. Samples were allowed to air dry at room temperature (23 °C) from the soil surface. We took daily measurements to generate a K_t – moisture content relationship for each sample from each horizon type. Repeated measurements of thermal conductivity at similar moisture contents varied by approximately six percent. Unreasonably high or low values for thermal conductivity were omitted from our data collection and analysis.

To determine moisture content, we weighed each sample at the time of each thermal conductivity measurement. After the samples were air dried, we oven dried each sample at 65 °C for 48 hours and weighed each sample again after drying. Bulk density was calculated by dividing the oven dry sample weight by sample volume. Gravimetric moisture content was calculated for each sample and then converted to volumetric moisture content by multiplying gravimetric moisture content by the oven-dry bulk density.

Analysis of variance (ANOVA) techniques were used to evaluate the effects of moss type and organic horizon type on bulk density, field capacity, and porosity.

ANOVA was also used to evaluate the effects of moss type, organic horizon type, and water phase on average thermal conductivity values. Tukey's post-hoc comparisons were used to evaluate statistical differences among treatments. Linear regression techniques were used to assess the relationship between thermal conductivity and moisture content for different organic matter types. All data are reported as means ± one standard deviation. All statistical analyses were conducted in either Sigma Plot Version 10.0 (Systat Software, Inc., San Jose, CA, USA) or Statistica Version 7.0 (StatSoft, Inc., Tulsa, OK, USA).

Results

Physical characteristics of soil organic matter

The bulk density and field capacity (lab-based) of organic horizons differ between feather moss- and *Sphagnum*-dominated black spruce ecosystems (Table 1). Bulk density varied as a function of moss type (ANOVA; df = 1; F = 4.28; P = 0.04) and organic horizon type (df = 2, F = 35.48; P < 0.0001). In general, bulk density increased with extent of organic matter decomposition. For instance, live feather moss had significantly lower bulk density than feather moss-derived amorphous horizons, averaging 0.02 ± 0.01 and 0.12 ± 0.06 g cm^{-3}, respectively (Tukey's post-hoc; P = 0.0001). Similarly, live *Sphagnum* averaged 0.04 ± 0.03 g cm^{-3} and amorphous organic matter derived from *Sphagnum* averaged 0.17 ± 0.10 g cm^{-3} (P = 0.0001).

Field capacity (lab-based) values were governed by the interaction of moss type and organic horizon type (df = 2; F = 5.16; P = 0.008; Table 1). Among feather moss

horizons, field capacity (lab-based) increased from 27.5 ± 8.0 % in live samples to 65.0 ± 13.6 % in amorphous samples (P = 0.008). Among *Sphagnum* samples, field capacity (lab-based) was not significantly different among organic horizon types (P > 0.05), ranging from 60 to 70 % among all horizons. Field capacity (lab-based) values also varied between moss types, where values were more than double in live *Sphagnum* than live feather moss (P = 0.0002). However, the field capacity (lab-based) of fibrous (P = 0.44) and amorphous (P = 0.99) organic matter was not significantly different between feather moss and *Sphagnum* samples.

Soil porosity was governed by organic horizon type (df = 2; F = 81.20; P < 0.0001), but was not significantly different between moss types (P = 0.98; Table 1). For both feather moss and *Sphagnum* samples, porosity decreased with decomposition extent. For instance, the porosity of live feather moss was significantly greater than amorphous horizons derived from feather moss, averaging 98.9 ± 1.1 % and 88.3 ± 8.0 %, respectively (P < 0.0001).

The effect of moisture content on thermal conductivity

We observed strong positive and linear relationships between K_t and VWC across moss types and organic horizon types (Table 2; Figure 2). We did not observe significant differences among regression parameters (β) across moss types or organic horizons types, with β averaging 0.0051 ± 0.0005, collectively (Table 2). However, we did observe small variations in $β_0$ across organic horizon types (Table 2), indicating that minimum K_t

values under dry conditions are variable across organic horizon types. We also observed

higher maximum K_t in live *Sphagnum* than in live feather moss (Figure 2), due to the

higher field capacity in live *Sphagnum* moss relative to live feather moss (Table 1).

Discussion

Controls on thermal conductivity of organic horizons

Soil thermal dynamics in organic horizons are strongly governed by soil moisture

content (Figure 2). Dry organic horizons have considerably lower thermal conductivity

than wet organic horizons and thus, function as good insulators against warm air

temperatures. Wet organic horizons also dampen the amplitude of seasonal temperature

variations through the absorption and release of latent heat during phase transitions

(Romanovsky and Osterkamp, 2000). Both feathermoss- and *Sphagnum*-derived organic

horizons have high porosity (Table 1), and consequently, changes in soil moisture content

largely determine variability in thermal conductivity values. Based on our findings, there

is nearly a five- to eight-fold difference in thermal conductivity of dry and wet feather

moss-derived organic horizons, and a 10-fold difference between dry and wet *Sphagnum*-

derived organic horizons. Maximum K_t ranged from 0.5 and 0.6 W m^{-1} K^{-1}, considerably

lower than the values suggested by Brown and Williams (1972; 1.1 W m^{-1} K^{-1}), but

consistent with measurements by Andersland and Anderson (1978). Our measurements

are also consistent with the K_t values suggested by Bonan (1991), who used 0.023 W m^{-1}

K^{-1} for dry moss and 0.291 W m^{-1} K^{-1} for saturated moss in Alaskan ecosystems. Sharratt

(1997) measured *in situ* thermal conductivity in black spruce forests of interior Alaska, and reported values for relatively dry moss ranging from 0.03 to 0.09 W m^{-1} K^{-1} over the growing season, which are consistent with our measurements at low moisture content (< 20 % by volume). Minimum K_t values measured in this study are also consistent with *in situ* thermal conductivity measurements of *Sphagnum* peat by Kettridge and Baird (2007). Our results are also in a good agreement with the estimates of Romanovsky and Osterkamp (2000, Table 1) based on interpretation of high resolution and high precision temperature measurements from a black spruce forest site in the Bonanza Creek LTER research area (0.1 W m^{-1} K^{-1} for the living moss, 0.3 W m^{-1} K^{-1} for the dead moss, and 0.5 W m^{-1} K^{-1} for the peat layer). Our measurements and calculations of organic horizon physical properties were also consistent with other reported values for bulk density (O'Neill et al., 2003), porosity (Raaflaub and Valeo, 2009), and field capacity (Yoshikawa et al., 2003).

We observed substantive differences in K_t values between moss types, which can, in part, be explained by differences in physical and ecophysiological properties of each moss. *Sphagnum spp.* can absorb and retain more water than feather mosses, as indicated by higher field capacity (lab-based) values (Table 1; also see Yoshikawa et al., 2003). In the field, *Sphagnum spp.* can wick and obtain moisture from deep in the soil profile through capillary action (Bisbee et al., 2001), whereas feather mosses depend on precipitation inputs and dew formation for moisture. Despite this difference in maximum K_t, minimum K_t values were similar between moss types, as both mosses are easily

subject to desiccation on warm and sunny days (Skre et al., 1983; Bonan and Shugart, 1989).

Soil thermal dynamics and climate change at high-latitudes

Improved parameterization of soil thermal dynamics in organic horizons is essential for modeling future permafrost and ecosystem dynamics in high-latitude ecosystems (Yi et al., 2009b). The thermal properties of organic horizons help to mediate and slow the effects of future climate warming on permafrost degradation (Shur and Jorgenson, 2007). Atmospheric warming may stimulate the release of carbon dioxide and methane from boreal ecosystems (Zhuang et al., 2006), which currently harbor large stores of organic carbon in near surface soils and permafrost (Schuur et al., 2008). Incorporation of organic horizon thermal properties into large-scale model simulations has improved our understanding of future permafrost dynamics (Euskirchen et al., 2006; Nicolsky et al., 2007a; Lawrence et al., 2008), and as a result, will improve our ability to predict the fate of organic carbon in northern soils.

Incorporation of organic horizon thermal properties, as measured in this study, could improve model simulations of future climate change and ecosystem dynamics in the boreal region. In particular, the inclusion of specific thermal conductivity-soil moisture relationships for different organic horizon and moss types will improve current predictions of permafrost vulnerability to climate warming. Future studies could use these relationships to calculate thermal conductivity directly from *in situ* moisture

measurements in organic soil horizons or from the soil moisture content values calculated in coupled permafrost-hydrological models. The redistribution of surface and soil water in response to permafrost thaw (Jorgenson et al., 2001) or regional drying (Smith et al., 2005; Goetz et al., 2005) will clearly influence thermal conductivity of organic horizons, and can be easily represented in models based on our measurements. In our related study (Jorgenson et al., 2010), we showed that changes in the organic horizon moisture content and related changes in thermal conductivity may not only result in changes in permafrost temperature but also can lead to a long-term permafrost thawing and disappearance. Future vegetation and moss dynamics in black spruce ecosystems may also alter soil thermal properties (Potter 2004) either through changes in or loss of moss types. Our findings suggest that a shift towards *Sphagnum-* from feather moss-dominated ecosystems could enhance heat conduction through organic horizons via wetter soil conditions, causing a thickening of the active layer and even thawing of permafrost. Alternatively, moss species abundance may decline in response to changing vascular plant composition or resource availability (Hart and Chen, 2006), which would likely reduce organic horizon thickness and protective insulation for permafrost.

Conclusions

Considerable uncertainties still exist regarding the fate of permafrost at high-latitudes in response to climate warming (Burn and Nelson, 2006; Lawrence and Slater, 2006), largely due to the complex interactions among climatic, ecosystem and

disturbance controls on permafrost stability (Shur and Jorgenson, 2007). Thermal properties of soil organic matter play a critical role in mediating the effects of climate change, particularly in the discontinuous permafrost zone. Here, we illustrate the importance of moisture content on the thermal conductivity of soil organic horizons. Our findings suggest that this thermal conductivity-moisture relationship is consistent across moss type and decomposition state of soil organic horizons.

Acknowledgements

References

Andersland, O. B., and D. M. Anderson. 1978. Geotechnical engineering for cold regions. McGraw-Hill, New York.

Barney, R. J., and K. Van Cleve. 1973. Black spruce fuel weights and biomass in two interior Alaska stands. Can. J. For. Res. 3: 304-311.

Beringer, J., A. H. Lynch, F. S. Chapin III, M. Mack, and G. B. Bonan. 2001. The representation of arctic soils in the land surface model: The importance of mosses. J. Clim. 14: 3324-3335.

Bisbee, K. E., S. T. Gower, J. M. Norman, and E. V. Nordheim. 2001. Environmental controls on ground species composition and productivity in a boreal black spruce forest. Oecologia 129: 261-270.

Bonan, G. B., and H. H. Shugart. 1989. Environmental factors and ecological processes in boreal forests. Annu. Rev. Ecol. Syst. 20: 1-28.

Bonan, G. B. 1991. A biophysical surface energy budget analysis of soil temperature in the boreal forests of interior Alaska. Water Resour. Res. 27: 767-781.

Bristow, K. L., R. D. White, and G. J. Kluitenberg. 1994. Comparison of single and dual-probes for measuring soil thermal properties with transient heating. Aust. J. Soil Res. 32: 447-464.

Brown, R. J. E., and G. P. Williams. 1972. The freezing of peatland. National Research Council of Canada, Technical Paper No. 381.

Burn, C. R., and F. E. Nelson. 2006. Comment on "A projection of severe near-surface permafrost degradation during the 21st century" by David M. Lawrence and Andrew G. Slater. Geophys. Res. Lett. 33: doi: 10.1029/2006GL027077.

Cassel, D.K., and D.R. Nielsen. 1986. Field capacity and available water capacity. *In*: Methods of Soil Analysis. Part 1: Physical and Mineralogical Methods. A. Klute (ed). American Society of Agronomy and Soil Science Society of America, Inc. Publishers, Madison, WI, pp. 901-926.

Dyrness, C. T. 1982. Control of depth to permafrost and soil temperature by forest floor in black spruce/feather moss communities. US Department of Agriculture Research Note PNW-396.

Euskirchen, E. S., A. D. McGuire, D. W. Kicklighter, Q. Zhuang, J. S. Clein, R. J. Dargaville, D. G. Dye, J. S. Kimball, K. C. McDonald, J. M. Melillo, V. E. Romanovsky, and N. V. Smith. 2006. Importance of recent shifts in soil thermal dynamics on growing season length, productivity and carbon sequestration in terrestrial high-latitude ecosystems. Global Change Biol. 12: 731-750.

Farouki, O. T. 1981. Thermal properties of soils. CRREL Monograph 81-1. Cold Regions Research and Engineering Laboratory, Hanover, NH.

Goetz, S. J., A. G. Bunn, G. J. Fiske, and R. A. Houghton. 2005. Satellite-observed photosynthetic trends across boreal North America associated with climate and fire disturbance. Proc. Natl. Acad. Sci. 102: 13521-13525.

Harden, J. W., K. P. O'Neill, S. E. Trumbore, H. Veldhuis, and B. J. Stocks. 1997. Moss and soil contributions to the annual net carbon flux of a maturing boreal forest. J. Geophys. Res. 102: 28805-28816.

Harden, J. W., K. L. Manies, M. R. Turetsky, and J. C. Neff. 2006. Effects of wildfire and permafrost on soil organic matter and soil climate in interior Alaska. Global Change Biol. 12: 2391-2403.

Hart, S. A., and H. Y. H. Chen. 2006. Understory vegetation dynamics of North American boreal forests. Crit. Rev. Plant Sci. 25: 381-397.

Johansen, O. 1975. Thermal conductivity of soils. Ph.D. Thesis, University of Trondheim, Trondheim, Norway. CRREL Draft English Translation 637. US Army Corps of Engineers, Cold Regions Research and Engineering Laboratory, Hanover, NH.

Jorgenson, M. T., C. H. Racine, J. C. Walters, and T. E. Osterkamp. 2001. Permafrost degradation and ecological changes associated with a warming climate in Central Alaska. Clim. Change 48: 551-579.

Jorgenson, M. T., Y. L. Shur, and E. R. Pullman. 2006. Abrupt increase in permafrost degradation in Arctic Alaska. Geophys. Res. Lett. 33: doi:10.1029/2005GL024960.

Jorgenson, M. T, V. E. Romanovsky, J. Harden, Y. L. Shur, J. A. O'Donnell, T. Schuur, and M. Kanevskiy. 2010. Resilience and vulnerability of permafrost to climate change. Canadian Journal of Forest Research 40: 1219-1236.

Kersten, M. S. 1949. Thermal properties of soils. University of Minnesota Engineering Experiment Station Bulletin 28.

Kettridge, N., and A. Baird. 2007. In situ measurements of thermal properties of a northern peatland: Implications for peatland temperature models. Journal of Geophysical Research 112, F02019, doi:10.1029/2006JF000655.

Lachenbruch, A. H., and B. V. Marshall. 1986. Changing climate: Geothermal evidence from permafrost in the Alaskan Arctic. Science 234: 689-696.

Lawrence, D. M., and A. G. Slater. 2005. A projection of severe near-surface permafrost degradation during the 21st century. Geophys. Res. Lett. 32: doi: 10.109/2005GL025080.

Lawrence, D. M., and A. G. Slater. 2006. Reply to comment by CR Burn and FE Nelson on "A projection of near-surface permafrost degradation during the 21st century". Geophys. Res. Lett. 33: doi: 10.1029/2006GL027955.

Lawrence, D. M., and A. G. Slater. 2008. Incorporating organic soil into a global climate model. Climate Dynamics 30: 145-160.

Lawrence, D. M., A. G. Slater, V. E. Romanovsky, and D. J. Nicolsky. 2008. Sensitivity of a model projection of near-surface permafrost degradation to soil column depth

and representation of soil organic matter. J.Geophys. Res. 113, F02011, doi:10.1029/2007JF000883.

Manies, K. L., J. W. Harden, S. R. Silva, P. H. Briggs, and B. M. Schmid. 2004. Soil data from *Picea mariana* stands near Delta Junction, Alaska of different ages and soil drainage type. US Geological Survey Open File Report 2004-1271.

McDonald, K. C., J. S. Kimball, E. Njoku et al. 2004. Variability in springtime thaw in the terrestrial high latitudes: monitoring a major control on the biospheric assimilation of atmospheric CO2 with spaceborne microwave remote sensing. Earth Interactions 8: 1-23.

Nicolsky, D. J., V. E. Romanovsky, V. A. Alexeev, and D. M. Lawrence. 2007a. Improved modeling of permafrost dynamics in a GCM land-surface scheme. Geophys. Res. Lett. 34, L08501, doi:10.1029/2007GL029525.

Nicolsky, D. J., V. E. Romanovsky, and G. S. Tipenko. 2007b. Using in-situ temperature measurements to estimate saturated soil thermal properties by solving a sequence of optimization problems. The Cryosphere 1: 41-58.

O'Neill, K.P., E.S. Kasischke, and D.D. Richter. 2003. Seasonal and decadal patterns of soil carbon uptake and emission along an age sequence of burned black spruce stands in interior Alaska. Journal of Geophysical Research 108, doi:10.1029/2001JD000443.

Osterkamp, T. E., and V. E. Romanovsky. 1999. Evidence for warming and thawing of discontinuous permafrost in Alaska. Permafrost and Periglacial Processes 10: 17-37.

O'Donnell, J. A., M. R. Turetsky, J. W. Harden, K. L. Manies, L. E. Pruett, G. Shetler, and J. C. Neff . 2009. Interactive effects of fire, soil climate, and moss on CO_2 fluxes in black spruce ecosystems of interior Alaska. Ecosystems 12: 57-72.

Potter, C. 2004. Predicting climate change effects on vegetation, soil thermal dynamics, and carbon cycling in ecosystems of interior Alaska. Ecological Modeling 175: 1-24.

Raaflaub, L., and C. Valeo. 2009. Hydrological properties of duff. Water Resources Research 45, W05502, doi:10.1029/2008WR007396.

Romanovsky, V.E., and T.E. Osterkamp. 1997. Thawing of the active layer on the coastal plain of the Alaskan Arctic. Permafrost and Periglacial Processes 8: 1-22.

Romanovsky, V. E., and T. E. Osterkamp. 2000. Effects of unfrozen water on heat and mass transport processes in the active layer and permafrost. Permafrost and Periglacial Processes 11: 219-239.

Schuur, E. A. G., J. Bockheim, J. G. Canadell, E. Euskirchen, C. B. Field, S. V. Goryachkin, S. Hagemann, P. Kuhry, P. M. Lafleur, H. Lee, G. Mazhitova, F. E. Nelson, A. Rinke, V. E. Romanovsky, N. Shiklomanov, C. Tarnocai, S. Venesky,

and J. G. Vogel. 2008. Vulnerability of permafrost carbon to climate change: Implications for the global carbon cycle. BioScience 58: 701-714.

Sharratt, B. S. 1997. Thermal conductivity and water retention of a black spruce forest floor. Soil Science 162: 576-582.

Shur, Y. L., and M. T. Jorgenson. 2007. Patterns of permafrost formation and degradation in relation to climate and ecosystems. Permafrost and Periglacial Processes 18: 7-19.

Skre, O., W. C. Oechel, and P. M. Miller. 1983. Moss leaf water content and solar radiation at the moss surface in a mature black spruce stand in central Alaska. Can. J. For. Res. 13: 860-68.

Smith, L. C., Y. Sheng, G. M. MacDonald, and L. D. Hinzman. 2005. Disappearing Arctic lakes. Science 308: 1429.

Van Cleve, K., C. T. Dyrness, L. A. Viereck, J. Fox, and F. S. Chapin III. 1983. Taiga ecosystems of interior Alaska. Bioscience 33: 39-44.

Veihmeyer, F.J., and A.H. Hendrickson. 1931. The moisture equivalent as a measure of the field capacity of soils. Soil Science 32: 181-194.

Yi, S., M. K. Woo, and A. M. Arain. 2007. Impacts of peat and vegetation on permafrost degradation under climate warming. Geophys. Res. Lett. 34, L16504, doi:10.1029/2007/GL030550.

Yi, S., K. Manies, J. Harden, and A. D. McGuire. 2009a. Characteristics of organic soil in

black spruce forests: Implications for the application of land surface and

ecosystem models in cold regions. Geophys. Res. Lett. 36: doi:

10.1029/2008GL037014.

Yi, S., A. D. McGuire, J. Harden, E. Kasischke, K. Manies, L. Hinzman, A. Liljedahl, J.

Randerson, H. Liu, V. Romanovsky, S. Marchenko, and Y. Kim. 2009b.

Interactions between soil thermal and hydrological dynamics in the response of

Alaska ecosystems to fire disturbance. J.Geophys. Res. 114, G02015,

doi:10.1029/2008JG000841.

Yoshikawa, K., W. R. Bolton, V. E. Romanovsky, M. Fukuda, and L. D. Hinzman. 2003.

Impacts of wildfire on the permafrost in the boreal forests of Interior Alaska. J.

Geophys. Res. 108: doi: 10.1029/2001JD000438.

Zhuang, Q., V. E. Romanovsky, and A. D. McGuire. 2001. Incorporation of a permafrost

model into a large-scale ecosystem model: Evaluation of temporal and spatial

scaling issues in simulating soil thermal dynamics. J. Geophys. Res. 106: 33649-

33670.

Zhuang, Q., J. M. Melillo, M. C. Sarofin, D. W. Kicklighter, A. D. McGuire, B. S. Felzer,

A. Sokolov, R. G. Prinn, P. A. Steudler, and S. Hu. 2006. CO_2 and CH_4 exchanges

between land ecosystems and the atmosphere in northern high latitudes over the

21st century. Geophys. Res. Lett. 33, L17403, doi: 10.1029/2006GL026972.

Figures
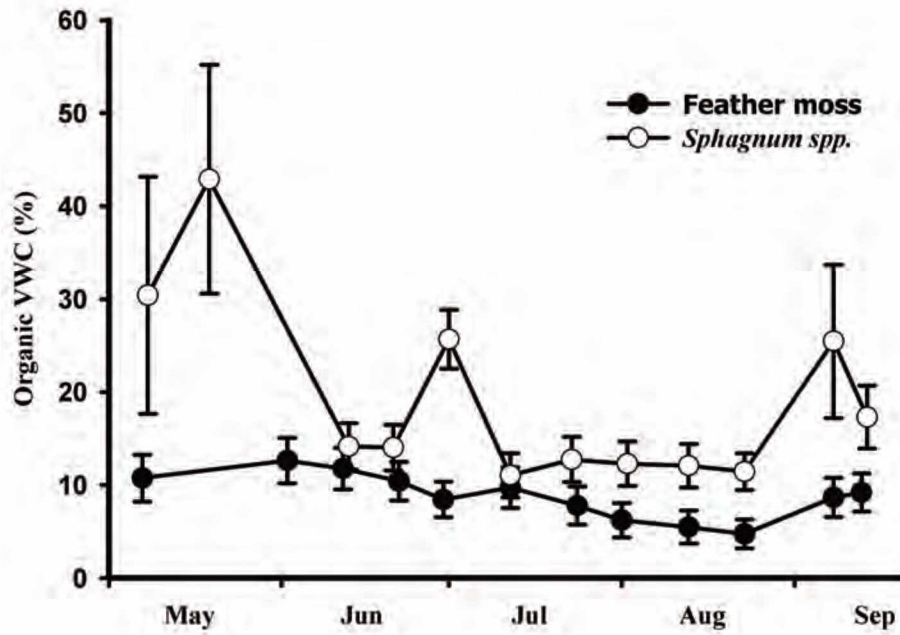
Figure 1. Seasonal variation in volumetric water content of shallow organic soils (10 cm below the ground surface) near Erickson Creek, Alaska (re-plotted from O'Donnell *et al.* 2009).
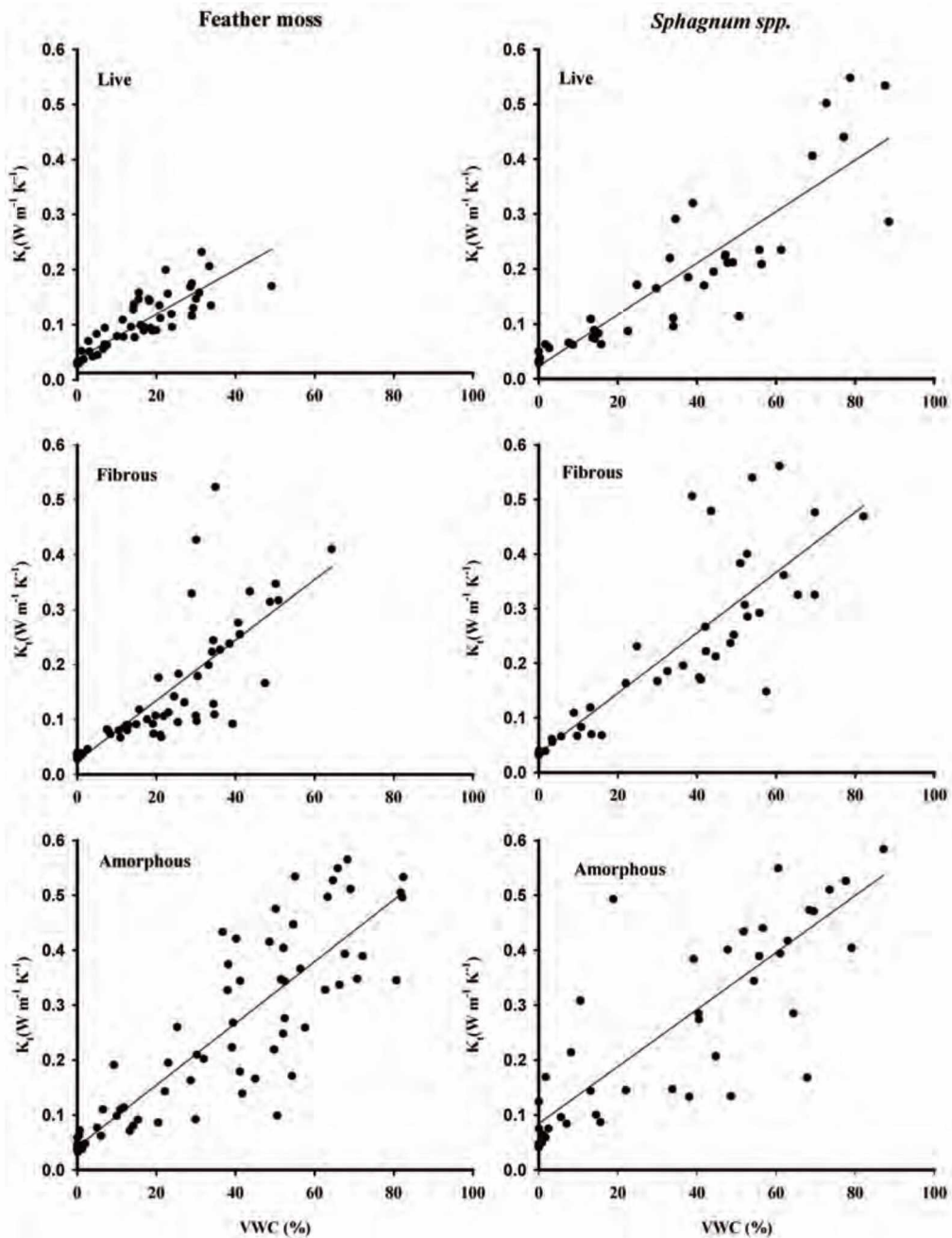
Figure 2. The relationship between thawed thermal conductivity (K_t) and volumetric water content (VWC) within different moss and organic matter types. Regression techniques revealed a positive linear relationship between K_t and VWC for all samples types. Detailed regression statistics are reported in Table 2.

Tables

Table 1. Bulk density, field capacity (lab-based), and porosity of different organic horizon types in somewhat poorly- and poorly-drained black spruce ecosystems. Values in parentheses indicate sample size.

	Live	Fibrous	Amorphous
Feather moss (somewhat poorly drained)			
bulk density (g cm-3)	0.02 ± 0.01 (15)	0.06 ± 0.02 (15)	0.12 ± 0.06 (15)
field capacity (lab-based; %)	27.5 ± 8.0 (15)	39.0 ± 10.5 (15)	65.0 ± 13.6 (15)
porosity (%)*	98.9 ± 1.1 (32)	96.5 ± 2.6 (94)	88.3 ± 8.0 (45)
Sphagnum spp. **(poorly drained)**			
bulk density (g cm-3)	0.04 ± 0.03 (10)	0.06 ± 0.02 (8)	0.17 ± 0.10 (9)
field capacity (lab-based; %)	60.6 ± 19.0 (9)	62.7 ± 10.0 (9)	70.6 ± 10.5 (9)
porosity (%)*	98.2 ± 0.9 (8)	97.4 ± 1.3 (30)	88.1 ± 7.4 (26)

*Porosity values were calculated from Yi et al. (2009a).

Table 2. Results from linear regression between thawed thermal conductivity and volumetric moisture content for all six organic matter types.

	β	β_0	t	r^2	P
Feather moss					
Live	0.0041	0.0377	15.39	0.79	< 0.0001
Fibrous	0.0055	0.0243	11.67	0.67	< 0.0001
Amorphous	0.0056	0.0420	17.60	0.79	< 0.0001
Sphagnum spp.					
Live	0.0047	0.0233	13.97	0.81	< 0.0001
Fibrous	0.0055	0.0347	11.09	0.74	< 0.0001
Amorphous	0.0052	0.0844	8.48	0.61	< 0.0001

Chapter 4: Exploring the sensitivity of soil carbon dynamics to climate change, fire disturbance and permafrost thaw in a black spruce ecosystem[3]

Abstract

In the boreal region, soil organic carbon (OC) dynamics are strongly governed by the interaction between wildfire and permafrost. Using a combination of field measurements, numerical modeling of soil thermal dynamics, and process-based modeling of OC dynamics, we tested the sensitivity of soil OC storage to a suite of individual climate factors (air temperature, soil moisture, and snow depth) and fire severity. We also conducted sensitivity analyses to explore the combined effects of fire-moisture interactions and snow seasonality on OC storage. OC losses were calculated as the difference in OC stocks after three fire cycles (~450 years) following a prescribed step-change in climate and/or fire. Across single-factor scenarios, our findings indicate that warmer air temperatures resulted in the largest soil OC losses (5.3 kg C m^{-2}), whereas dry soil conditions alone (in the absence of wildfire) resulted in the smallest carbon losses (0.1 kg C m^{-2}). Increased fire severity resulted in carbon loss of 3.3 kg C m^{-2}, whereas changes in snow depth resulted in smaller OC losses (2.1-2.2 kg C m^{-2}). Across multiple climate factors, we observed larger OC losses than for single-factor scenarios. For instance, high fire severity regime associated with warmer and drier

---

[3] O'Donnell JA, JW Harden, AD McGuire, and VE Romanovsky. 2010 (in review). Exploring the sensitivity of soil carbon dynamics to climate change, fire disturbance and permafrost thaw in a black spruce ecosystem. Submitted to Biogeosciences.

conditions resulted in OC losses of 6.1 kg C m^{-2}, whereas a low fire severity regime

associated with warmer and wetter conditions resulted in OC losses of 5.6 kg C m^{-2}. A

longer snow-free season associated with future warming resulted in OC losses of 5.4 kg

C m^{-2}. Soil climate was the dominant control on soil OC loss, governing the sensitivity

of microbial decomposers to fluctuations in temperature and soil moisture; this control, in

turn, is governed by interannual changes in active layer depth. Transitional responses of

the active layer depth to fire regimes also contributed to OC losses, primarily by

determining the proportion of OC in frozen and unfrozen soil layers. Carbon cycle

feedbacks from the boreal region to the climate system will clearly depend upon these

interactions among climate drivers, fire regime characteristics, and permafrost dynamics.

Introduction

High-latitude soils store large quantities of organic carbon (OC), accounting for

nearly 50% of the global belowground OC pool (Tarnocai et al., 2009). Accumulation of

soil OC in many northern soils is governed by the presence of permafrost, which

functions as a large reservoir for OC (Zimov et al., 2006). Recent warming at high

latitudes has caused localized thawing of permafrost (Osterkamp and Romanovsky, 1999;

Romanovsky et al., 2010), resulting in the release of old OC from terrestrial ecosystems

(Schuur et al., 2009). Permafrost thaw also can alter local soil thermal and hydrologic

conditions (Jorgenson et al., 2001; Yi et al., 2009a), which can influence rates of

microbial activity and OC loss from decomposition. Modeling analyses project

widespread thawing of permafrost in the next century (Euskirchen et al., 2006; Lawrence

et al. 2008), but considerable uncertainty exists regarding the fate of soil OC following thaw (Limpens et al., 2008; Schuur et al., 2008).

Wildfire has the potential to exacerbate rates of permafrost thaw (Yoshikawa et al., 2003) and OC losses (Harden et al., 2000) from soils of the boreal region. Through the combustion of surface organic horizons, wildfire reduces thermal insulation and increases active layer depth (ALD; Burn, 1998; Yoshikawa et al., 2003; Johnstone et al., 2010). Re-accumulation of the organic horizon between fire cycles can allow for the recovery of ALD to pre-fire depths (Yi et al., 2010). This interaction between wildfire and permafrost can have a profound influence on soil OC accumulation and loss (O'Donnell et al., 2010). ALD fluctuations across fire cycles determine the proportion of OC in unfrozen or frozen mineral soil, and thus, rates of OC accumulation or loss in deep soil horizons (O'Donnell et al., 2010). In this manner, ALD functions as a control on substrate (i.e. OC) availability to microbial decomposers in unfrozen soils. Furthermore, the magnitude of the ALD effect on soil OC loss is closely linked to fire regime characteristics, such as fire severity (O'Donnell et al., 2010).

Soil OC dynamics are also governed by the sensitivity of microbial decomposition to changes in soil climate, which in the boreal region is governed by complex interactions among physical drivers, soil properties and disturbance (Jorgenson et al., 2010). For example, increased soil temperatures following fire can stimulate decomposition rates (Richter et al., 2000; O'Neill et al., 2002). However, the temperature sensitivity of decomposition may be reduced due to post-fire changes in soil

moisture or OC quality (Neff et al., 2005; O'Donnell et al., 2009a). Wildfire can increase soil moisture content via reduced rates of evapotranspiration and interception (Moody and Martin 2001), but can also result in decreased soil moisture content (O'Neill et al., 2002). Similarly, permafrost thaw has caused both wetting and drying of terrestrial ecosystems, depending upon topographic position and ground ice content (Jorgenson et al., 2001; Jorgenson and Osterkamp, 2005). Increased snow depth can enhance soil warming and permafrost thaw (Nowinski et al., 2010), whereas decreases in snow-depth can promote rapid freezing during cooling periods (Goodrich, 1982; Stieglitz et al., 2003). The relative sensitivity of soil thermal conditions to these climatic drivers and disturbances will ultimately govern rates of decomposition, and, in turn, will determine OC storage across the boreal landscape.

Here, we build on prior field and modeling studies (Harden et al., 2000; O'Donnell et al., 2010) to assess the relative sensitivity of ALD and soil climate effects on soil OC storage in a black spruce ecosystem of interior Alaska. To achieve this objective, we used a combination of field measurements of soil temperature, moisture and snow dynamics, numerical modeling of soil thermal dynamics, and process-based modeling of soil OC dynamics. Using this approach, we addressed the following questions; 1) What is the sensitivity of ALD and soil climate to air temperature, soil moisture, snow depth, and fire severity? 2) What is the sensitivity of soil OC storage to air temperature, soil moisture, snow depth, and fire severity? 3) What are the relative effects of ALD, soil climate, and ALD-soil climate interactions on soil OC losses across

climate and fire scenarios? By addressing these questions, we aim to refine our

understanding of the mechanisms underlying soil OC dynamics in relation to wildfire and

permafrost thaw in the boreal region.

Methods

Experimental design

Previous work demonstrated the fundamental importance of active layer depth

(ALD) (O'Donnell et al., 2010) and soil temperature (Carrasco et al., 2006) in governing

the net C balance of boreal soils. For this study, we combined field observations of

temperature and soil moisture, numerical modeling, and process-based modeling to

quantify the relative effects of individual and combined climate/fire factors on net soil

OC accumulation and loss (Figure 1; Table 1). In this study, we modified the Fire-C

model (Harden et al., 2000; O'Donnell et al., 2010) to improve simulations of ALD and

OC dynamics in order to (1) account for deeper permafrost OC stocks, and (2)

incorporate in more detail the temperature and moisture controls on decomposition. In

previous work, thermal conductivity of the organic horizon was measured across a range

of moisture contents (O'Donnell et al., 2009b) and ALD was calculated as a function of

organic horizon thickness across an upland fire chronosequence near Hess Creek, AK

(see O'Donnell et al., 2010). For this study, we used the Geophysical Institute

Permafrost Laboratory (GIPL) model (Romanovsky and Osterkamp, 1997; Nicolsky et

al., 2007; Marchenko et al., 2008) to assess the sensitivity of ALD and soil temperature to

a wide range of climatic factors (air temperature, moisture, snow, and fire severity) both

as separate and combined. We then used output from these sensitivity analyses to assess the effects of ALD and soil climate on organic matter decomposition and soil OC accumulation using a simple process-based, long-term model (O'Donnell et al., 2010).

Modeling soil carbon dynamics

The soil OC dynamics model used in this study was originally developed by Harden et al. (2000) to track long-term trends in soil carbon inventories of shallow and deep organic horizons across fire cycles. This model was subsequently modified to include inputs from coarse woody debris (Manies et al., 2005), to operate on annual or monthly time-steps (Carrasco et al., 2006), and to include OC dynamics in mineral soil of the active layer and near-surface permafrost (O'Donnell et al., 2010). Briefly, the model examines net changes in soil OC storage over time (dC/dt) as governed by OC inputs (net primary production (NPP) from moss and trees) and losses (heterotrophic respiration and fire). Here we discuss further improvements and modifications to the model, which include GIPL-modeled active layer dynamics, and temperature and moisture regulation of decomposition.

Active layer dynamics - In the modeling study by O'Donnell et al. (2010), active layer depth was calculated simply as a function of organic horizon thickness at time *t* (in years) for the study area near Hess Creek. To more precisely represent active layer dynamics in the model, we reconstructed active layer depth vs. organic horizon thickness regression curves across a range of climate conditions using the GIPL model (as discussed in the *Modeling soil temperature dynamics* section below). The equations

derived from these relationships were then used to inform the soil OC dynamics model across different climatic scenarios.

Deep soil carbon - In a prior version of the model, we tracked soil C inventories between the ground surface and a depth of one meter (O'Donnell et al., 2010). Here, we have parameterized the model to track soil OC inventories in the top two meters. In most mature forests in Alaska, soil OC between one and two meters resides in the permafrost pool (Tarnocai et al., 2009). However, post-fire thawing of near-surface permafrost can result in thaw depths exceeding one meter (e.g. Viereck et al., 2008), which might impact deeper OC stocks (> one meter).

Temperature and moisture controls on decomposition - In a prior version of the model (O'Donnell et al., 2010), decomposition constants (*k*) were derived using chronosequence and radiocarbon methodologies. In that study, *k* reflected the apparent decomposability of soil organic matter (see Davidson and Janssens, 2006), integrating the effects of temperature, soil moisture and organic matter quality on decomposition during historic times. However, future climate scenarios require that *k* respond to fluctuations in soil temperature and moisture.

We used the following equation to calculate an inherent *k*, which integrates the decomposability of a substrate based on its molecular structure at ambient temperature:

$$K_{base} = ke^{rT} * f(\theta) \qquad (1)$$

where K_{base} is the apparent decomposition constant as reported in O'Donnell et al. (2010),

k is the inherent decomposition constant, r is a parameter describing the temperature

sensitivity of decomposition, T is the mean monthly soil temperature for the month of

August (as measured or calculated across the fire chronosequence), when maximum thaw

depth occurs during the year, and $f(\theta)$ is a soil moisture scalar that depends on

gravimetric moisture content. The function $f(\theta)$ is a value between 0 and 1, with optimal

decomposition occurring when $f(\theta)$ is around 0.6, and was calculated following the

equations of Frolking et al. (1996) for a feather moss-dominated black spruce forest. To

determine a value for r, we used a temperature sensitivity quotient (Q_{10}) equation:

$$Q_{10} = e^{r10} \qquad (2)$$

We used a different Q_{10} value for each soil layer, as reported in the literature. For

shallow organic horizons, we prescribed a Q_{10} of 1.9, as reported by Wickland and Neff

(2007) for fibric organic matter. For deep organic horizons (i.e. mesic or humic

horizons), we prescribed a Q_{10} value of 4.4, as reported by Dioumaeva et al. (2003). For

unfrozen mineral soil of the active layer, we prescribed a Q_{10} of 2.0, as reported in other

studies (Clein and Schimel, 1995; Frolking et al., 1996; Carrasco et al., 2006). For near-

surface permafrost, we lowered the Q_{10} value of unfrozen mineral soil to 30% of its

value, following the work of Dioumaeva et al. (2003) and Fan et al. (2008), to account for

reduced microbial activity at temperatures below freezing. We then used soil

temperature output from the GIPL model (see *Modeling soil thermal dynamics* section for

details) to calculate T across all climate and fire sensitivity analyses (Figure 1). The

function $f(\theta)$ was only re-calculated for the two climate scenarios in which we prescribed wetter or drier conditions.

Field measurements of soil temperature, moisture and snow depth

We measured soil temperature, soil moisture, and ALD and snow depth at three stand ages (Unburned Mature, 2003 Burn, 1967 Burn) from the fire chronosequence of O'Donnell et al. (2010). These different stand ages provide a natural gradient in soil properties such as organic horizon thickness, soil thermal dynamics, ALD, and soil OC stocks. From September 2007 to September 2009, we monitored soil temperature every two hours using HOBO Pro V2 two-channel dataloggers (Onset Computer Corporation, Pocasset, MA, USA). We also used HOBO Smart Temperature sensors to monitor temperature at a single depth at each site. Temperature probes were installed at the ground surface, at the top of the permafrost (i.e. TTOP), near two meters below the ground surface, and also at the interface of key organic soil horizons. Soil moisture of organic soil horizons was also logged every two hours at each stand age using ECH$_2$O Smart Soil Moisture probes routed to a HOBO microstation (Onset Computer Corporation, Pocasset, MA, USA). Soil moisture probes were installed within distinct organic soil horizons. In addition to temperature and soil moisture, we conducted snow surveys over two winters. At each stand age, we measured snow depth every 6 meters across a 30 m linear transect on November 13th, February 25th, and April 3rd, 2007 and 2008 and we also measured snow depth on April 2, 2009.

Modeling soil temperature dynamics

We used the GIPL model to simulate the depth of seasonal freezing and thawing by solving a one-dimensional non-linear heat equation with phase change (Nicolsky et al., 2007). To calibrate the GIPL thermal model for the Hess Creek study sites, we combined field measurements of soil temperature (Supplemental Figures 1 and 2), soil moisture (Supplemental Figure 3), ALD, snow depth, field descriptions of soil horizon thickness (O'Donnell et al., 2010), and empirical calculations of thermal conductivity (O'Donnell et al., 2009b). For each study site (Unburned Mature, 2003 Burn, 1967 Burn), the measured soil temperature data were used to calibrate the model, which in turn was used to reconstruct the one-dimensional temperature field in the active layer and near-surface permafrost. We used air temperature and snow depth measurements from Hess Creek to drive model simulations of soil temperature. For soil parameterizations, we divided the organic horizon into three layers: live/dead moss, fibrous organic matter, and amorphous organic matter (Table 2), following the approach of Yi et al. (2009b). Mineral soil horizons were divided into active layer soil, frozen loess, and frozen bedrock. We prescribed soil moisture content for organic horizons based on mean volumetric water content (VWC) measured during the summer of 2008 (Table 3; Supplemental Figure 3). Unfrozen thermal conductivity values for organic horizons were calculated from measured VWC values (O'Donnell et al., 2009b; Table 3). Frozen thermal conductivity, volumetric heat capacity, and volumetric unfrozen water content

parameters were prescribed following previous studies (Romanovsky and Osterkamp, 1997, 2000).

Following model calibration, we used the GIPL model to determine the sensitivity of ALD and soil temperatures to changes in air temperature, snow dynamics, soil moisture, and fire severity (Figure 1; Table 1). For all sensitivity analyses, we introduced a step-change in climate or fire disturbance in order to evaluate effects on soil thermal conditions at the year 2100 relative to the present day. Using the step-change approach, we compared the importance of various factors in governing soil thermal dynamics in a black spruce ecosystem. Climate and fire factors were considered both in isolation and as combined effects. These simulations were designed to explore the underlying mechanisms controlling OC loss from boreal soils, and not to provide an exact estimate of future permafrost thaw. For a more precise estimation of ALD and soil temperature responses to future climate and fire, a transient simulation from the present day to 2100 (e.g. Lawrence et al., 2008) would be more appropriate.

To assess the effect of atmospheric warming, we increased mean daily air temperature (as measured at Hess Creek) to match predicted air temperatures under the A2 (business as usual) and B1 (reduced greenhouse gas emissions) warming scenarios (Christensen et al., 2007; Figure 2). To assess the effects of future wetting or drying scenarios on active layer depth, we increased and decreased soil moisture content of organic horizons by 25% relative to present-day measurements (Supplementary Figure 3), with concomitant changes in thermal conductivity following O'Donnell et al. (2009b).

We also ran two alternate snow scenarios where daily snow depth was increased by 25% and decreased by 25% relative to present-day measurements. To assess the sensitivity of ALD and soil temperatures to fire severity, we first prescribed a moderate fire severity (64% of organic matter combusted) and high fire severity (77% of organic matter combusted, following Kane et al., 2007) relative to present-day fire severity (41% of organic matter combusted; Harden et al., 2006).

We also ran scenarios to test the combined effects of climate and fire severity. For instance, we ran two scenarios to test the interactive effects of fire severity (high, low), moisture (wet, dry) and warming (A2 scenario; Table 1) relative to the present day. We also ran a scenario to reflect changes in snow seasonality associated with future warming. Following estimates of temporal snow dynamics by Euskirchen et al. (2009), our simulations reflected snow conditions at the year 2100, with snowmelt occurring 21 days earlier in the spring and snow return occurring 20 days later in the fall as compared to present-day conditions. The A2 warming scenario was also used as driving data for the changing snow seasonality treatment.

Sensitivity of soil carbon to future climate and fire scenarios

To assess the sensitivity of soil OC to future climate and fire scenarios, we used output (ALD, soil temperature) from the GIPL model to drive OC storage and decomposition in the Fire-C model (Figure 1). Other studies have coupled thermal and ecosystem models to investigate soil OC dynamics in northern ecosystems (Zhuang et al., 2001, 2002; Khvorostyanov et al., 2008; Yi et al., 2009a). Our approach here is unique in

that it incorporates field and laboratory parameterizations (O'Donnell et al., 2009b, 2010) into a modeling framework in which we explicitly evaluate fire-permafrost interactive effects on soil OC across a range of future climate conditions. At this stage, the model does not consider the effects of talik development on decomposition of soil organic matter. For the model spin-up (0-6500 years), we ran the Fire-C model following parameterizations of O'Donnell et al. (2010), which reflect historic climatic conditions and fire regimes. At the year 6500, we modified Fire-C parameters to reflect future climatic conditions and fire regimes. We tested the sensitivity of soil OC to air temperature (A2 vs B1 scenarios), soil moisture (wetter vs. drier), snow depth (deeper vs. shallower), and fire severity (low severity, or 25% vs high severity, or 77%). We also tested the sensitivity of soil OC to the combined climate and fire effects. Specifically, we evaluated the effects of increased fire severity associated with drier and warmer condition, decreased fire severity with wetter and warmer conditions, and changes in snow seasonality associated with future warming. The net change in OC storage for each scenario was calculated as the difference between total OC stocks (top two meters) at 6500 (i.e. present day) and 7000 years (i.e. after 3 fire cycles).

Model simulations were run to assess the magnitude of both ALD and soil climate effects on soil OC dynamics. To isolate the ALD effect on soil OC, we first ran the Fire-C model by only changing the relationship between ALD and organic horizon thickness, as simulated by the GIPL model. To isolate the soil climate effect on soil OC, we then ran the Fire-C model by only changing the soil temperature (as simulated by GIPL) and

moisture controls on decomposition rates. To assess the interactive effects of ALD and soil climate on soil OC, we ran the Fire-C model a third time changing both ALD dynamics and soil climate controls on decomposition rates. For each effect (ALD, soil climate, ALD + soil climate), we calculated the net effect on soil OC accumulation or loss.

Results

Thermal model calibration

Field measurements of air temperature and snow depth were used to calibrate the GIPL model. Air temperature varied seasonally (black line in Figure 2), with maxima occurring during July (monthly mean = 14.9 °C) and minima during January (monthly mean = -25.3 °C). Snow depth varied across survey dates but not among study sites across the fire chronosequence (Figure 3a). Minimum snow depths were measured in November, ranging between 7 and 9 cm across study sites. Maximum snow depths were measured in April and varied between years. In winter 2007-2008, maximum snow depths averaged between 41 and 48 cm, whereas in winter 2008-2009, maximum snow depths averaged between 60 and 67 cm. We observed a good relationship between snow depths at Hess Creek and at a long-term monitoring site near Fairbanks, AK (Figure 3b), described by the equation: y = -4.0822 + 0.8502x (R^2 = 0.78; P = 0.12). We used this relationship to calculate daily snow depth at Hess Creek during model calibration.

We observed good agreement between measured and modeled soil temperatures (Figure 4) and ALD (Supplemental Figure 4) at sites across the Hess Creek fire chronosequence. At the ground surface, modeled mean daily temperature (MDT) closely tracked observed MDT during winter, summer and during seasonal transitions (e.g. snowmelt). Deeper in the soil profile, we observed small differences (< 0.5 °C) during winter and summer between modeled and observed ground temperatures (Figure 4b-d). The differences were most pronounced during periods of cooling in the fall/early winter and warming during spring/early summer. The differences in ground temperature during periods of cooling have been attributed to the influence of unfrozen water content (Romanovsky and Osterkamp 1997, 2000). During periods of warming in spring, ground temperatures were likely influenced by infiltration and re-freezing of snowmelt waters. These processes typically result in the formation of a "zero-degree curtain" at the ground surface, which we observed at our study sites during spring. Following the completion of snowmelt, thawing of the active layer began with ground temperatures > 0 °C. Modeled ALD was within 3 cm of the observed ALD across the three study sites (Supplemental Figure 4).

Modeling the sensitivity of active layer depth and soil climate to climate and fire

Warmer air temperatures alone had a large impact on ALD (Figure 5a; Table 4), with the A2 scenario increasing ALD by an average of 37 ± 3 cm relative to present-day air temperatures across a range of organic horizon thicknesses. The B1 scenario resulted in considerably smaller increases in ALD, averaging 9 ± 1 cm across a range of organic

horizon thicknesses. Changes in soil moisture had a moderate influence on ALD (Figure 5b), with wetter conditions driving an average ALD increase of 5.4 ± 0.7 cm and drier conditions driving an average ALD decrease of 7.0 ± 1.2 cm across a range of organic horizon thicknesses. Snow depth had a very small impact on ALD, with average ALD increasing or decreasing by 2 ± 0 cm with deeper or shallow snowpack, respectively (Figure 5c). High fire severity caused an average increase in ALD of 18 ± 5 cm, whereas low fire severity caused an average decrease in ALD of 7 ± 1 cm (Figure 5d).

In addition to driving changes in ALD, individual climate and fire factors caused changes in soil temperature in the active layer and near-surface permafrost (Figure 6). Warming associated with the A2 scenario increased soil temperature by 3.5-4.5 °C for August MMT in active layer soils. The B1 scenario resulted in higher soil temperatures by 0.7 to 1.0 °C relative to present-day climate conditions. Soil moisture also had a moderate influence on August MMT in the active layer, as wetter conditions resulted in an increase of 0.3-0.6 °C and drier conditions resulted in decrease of up to 0.5 °C relative to present-day conditions. Deeper snowpack resulted in slight increases and shallower snowpack resulted in slight decreases in August MMT relative to present-day conditions. Increased fire severity (as prescribed through changes in organic horizon thickness) increased August MMT by 0.4 to 1.5 °C, whereas decreased fire severity cooled August MMT by up to 0.3 °C relative to present-day conditions.

When considered as combined effects, we found that high fire severity, drier soils and warmer air temperatures resulted in the largest increase in ALD (mean = 56 ± 6 cm;

Figure 7a; Table 4) and August MMT (4.7-5.5°C increase in active layer soils; Figure

7b). The combined effects of low severity fires, wetter soils and warmer air temperatures

resulted in more modest increases in ALD (mean = 37 ± 4 cm) and August (3.6-5.0 °C

increase in active layer soils). Longer snow-free seasons associated with future warming

also resulted in large increases in ALD (mean = 39 ± 3 cm) and August MMT (3.6-4.6 °C

increase in active layer soils).

Modeling the sensitivity of soil carbon to climate and fire

Of the individual climate factors, the A2 warming scenario (no change in fire

severity) resulted in the largest OC losses from soil (5.3 kg C m^{-2}; Figure 8), whereas the

drier soil moisture scenario resulted in the smallest losses (0.06 kg C m^{-2}). After the A2

scenario, the high fire severity treatment resulted in the largest OC losses (3.3 kg C m^{-2}).

Changes in snow depth and increases in soil moisture resulted in minimal OC losses,

ranging from 2.1-2.2 kg C m^{-2}. When the model was run for three fire cycles under the

present-day climate (with no changes in snow, moisture or fire), we also observed an OC

loss of 2.1 kg C m^{-2}. Across individual climate scenarios, interannual changes in ALD

(i.e. the ALD effect) accounted for 61% of the total OC losses, whereas changes in soil

temperature and/or moisture (i.e. the soil climate effect) accounted for 82% of total OC

losses.

When multiple climate factors were considered as combined effects, we generally

observed larger OC losses from soil relative to the individual factor analyses (Figure 9).

The high fire severity scenario associated with drier soil and warmer air temperature

resulted in a soil OC loss of 6.1 kg C m^{-2}. The low fire severity scenario associated with wetter soil and warmer air temperature resulted in a soil OC loss of 5.6 kg C m^{-2}. The scenario reflecting longer snow-free season and warmer air temperatures resulted in a soil OC loss of 5.4 kg C m^{-2}. Across combined-effect scenarios, the ALD effect accounted for 39% of total OC losses, while the soil climate effect accounted for 79% of total OC losses.

Discussion

Effects of air temperature on active layer depth, soil climate and soil carbon

Terrestrial ecosystems have the potential to act as a positive feedback to the climate system in response to warmer air temperatures (e.g. Friedlingstein et al., 2006), given the temperature sensitivity of heterotrophic respiration and subsequent CO_2 release from soils. In this study, we illustrate the importance of higher air temperatures for OC loss from boreal soil. When compared to other individual factors (soil moisture, snow depth, fire severity), higher air temperatures caused the largest OC losses from soil in an upland black spruce ecosystem. Through our modeling analyses, we were able to identify two mechanisms underlying OC losses. First, higher air temperatures resulted in warmer soil temperatures, which stimulated microbial decomposition of soil organic matter following Q_{10} value for each soil horizon. Second, higher air temperatures, and in particular the A2 warming scenario, resulted in large increases in active layer depth (ALD), which transferred considerable amounts of OC from the permafrost to a thawed C pool (e.g. Schuur et al., 2008), where decomposition rates were higher (Mikan et al.,

2002). Above 0 °C, decomposition rates are typically described by an exponential

relationship with temperature (Lloyd and Taylor, 1994; Kirschbaum, 2000), whereas

decomposition rates below 0 °C are indirectly related to temperature, constrained by the

availability of unfrozen water (Rivkina et al., 2000; Romanovsky and Osterkamp, 2000).

This complex interaction between physical and biological processes has contributed to

the ongoing uncertainty regarding the temperature sensitivity of decomposition and

carbon cycle feedbacks to the climate system (Davidson and Janssens, 2006;

Kirschbaum, 2006; Heimann and Reichstein, 2008). Explicit consideration of freeze-

thaw fronts (e.g. Yi et al., 2009a) and phase change effects on soil OC dynamics in

ecosystem models will help in reducing these uncertainties. Furthermore, increased

heterotrophic respiration associated with warming will likely be accompanied by

increased nitrogen availability and plant production (Mack et al., 2004), although the net

C balance is likely to favor an increase of CO_2 relative to pre-disturbance conditions

(Bond-Lamberty et al., 2007).

Effects of fire severity versus warming

In a prior study, O'Donnell et al. (2010) illustrated the importance of fire severity

on soil OC loss from deep soil horizons using the Fire-C model. Here, we show that the

direct effects of increased fire severity on soil OC storage, while substantial, are

generally smaller than the direct effects of warmer air temperatures. In reality, greater

fire severity always results in warmer soils because of the insulating effect of organic

layers on soil temperatures and active layer depth. For example, using the GIPL model,

we showed that high severity fires result in increased ALD and soil temperatures following deep combustion of organic soil horizons (Figure 5d), which enhanced OC losses from soil. These findings are consistent with other sensitivity analyses conducted in other black spruce ecosystems in the boreal region. In a recent analysis, Yi et al. (2010) illustrate that this post-fire soil warming and increases in ALD enhance soil decomposition and N mineralization in early succesional stands. Zhuang et al. (2002) illustrated that soil OC stocks in black spruce ecosystems are highly sensitive to fire severity, with large OC losses associated with high severity burns. Therefore, as future warming will likely increase the size and severity of wildfires in the boreal region (Balshi et al., 2009; Flannigan et al., 2009), increases in OC loss from boreal soils will result.

We also showed that soil OC stocks were also sensitive to changes in soil moisture. Under drier soil conditions (in the absence of fire), we observed relatively low OC losses from soil, a response driven by both physical and biological factors. Decreased soil moisture reduced the thermal conductivity of organic soil horizons, which is a dominant control on ALD in black spruce ecosystems (Bonan, 1989; Yi et al., 2009a; Jorgenson et al., 2010). By reducing ALD, a larger proportion of OC stocks in mineral soil were reincorporated into the near-surface permafrost pool, where decomposition is essentially arrested. Together, cooler temperatures and drier conditions reduced decomposition rates, resulting in smaller OC losses relative to other scenarios. Under higher moisture conditions, we generally observed the opposite effect, with increased ALD, soil temperatures and decomposition.

Interactions between fire and soil drainage class will likely govern the extent of permafrost thaw and magnitude of soil OC losses following fire in the boreal region (Harden et al., 2001; Kane et al., 2007; Yi et al., 2009b). We conducted additional simulations to assess the combined effects of fire severity (high, low), soil moisture (wet, dry) and warming on permafrost and soil OC dynamics. Surprisingly, we observed a similar magnitude of OC loss from both the high severity-dry treatment and the low-severity-wet treatment. This finding is likely due to a shift in the dominant mechanism driving soil temperature and OC dynamics between treatments. For instance, under the low severity-wet treatment, soil OC dynamics appear to be more sensitive to increased soil moisture and heat transfer than to the large reduction in organic horizon thickness than the decrease in soil moisture. In contrast, under the high severity-dry treatment, soil OC dynamics appear to be more sensitive to the large reduction in organic horizon thickness than to the decrease in soil moisture. Prior studies have documented the importance of organic horizon thickness and moisture on soil temperatures at the ground surface (Harden et al., 2006) and in near-surface permafrost (Jorgenson et al., 2010). The response of OC and permafrost dynamics in black spruce ecosystems to future climate and fire regimes will likely depend on these feedbacks among organic horizon thickness, soil drainage, and soil temperature and permafrost dynamics (Johnstone et al., 2010).

The interactive effects of fire and soil moisture on soil OC dynamics may depend on localized conditions relating to parent material and ground ice content (Jorgenson et al., 2010). Across the fire chronosequence at Hess Creek, soil moisture increased in surface soil horizons immediately following fire and persisted for at least 40 years after

the burn (Supplemental Figure 4). This observation is counter to the findings of Yoshikawa et al. (2003), who for a range of burned stands in interior Alaska observed higher moisture content immediately following fire but lower moisture content in maturing stands. Sites examined by Yoshikawa et al. (2003) were typically underlain by mica schist with a thin loess mantel (Rieger et al., 1972, Ping et al., 2005), whereas our study sites were underlain by thick loess deposits (O'Donnell et al., 2010). Furthermore, we observed cryostructures consistent with syngenetic permafrost and the common occurrence of an ice-rich intermediate layer (Shur et al., 2010), which mediates thaw of deep permafrost due to the high-latent heat content of ice (Shur et al., 2005). This ice-rich layer may have influenced post-fire soil conditions by both contributing thaw water to the active layer and by minimizing deep thaw, and thus attenuating reductions in soil moisture.

Effects of snow dynamics on active layer depth, soil climate and soil carbon

Increased duration of the snow-free season associated with future warming had a profound impact on ALD, soil climate and soil OC dynamics, although changes in snow depth alone had minimal effects. The longer snow-free season resulted in greater warming of soil, thawing of the near-surface permafrost, and soil OC losses relative to present-day conditions. However, our model simulations did not consider feedbacks associated with changes to snow seasonality, such as mid-summer drought (Welp et al., 2007) and increases in wildfire frequency (Kasischke and Turetsky, 2006). To more accurately assess the net effect of snow on soil OC dynamics in the boreal region, models

are needed that consider the combined effects of snow, disturbance and hydrology (e.g. Yi et al., 2010).

Variation in snow dynamics across boreal successional sequences has received little attention in the literature (see Euskirchen et al., 2009). Field measurements in this study show that winter soil temperatures were consistently warmer at the 2003 Burn relative to the Unburned Mature stand and the 1967 Burn (Supplementary Figure 1), despite similar snow depths and seasonal dynamics across sites (Figure 3a). These observations indicate that the magnitude of insulation is affected by the thermal properties of not only the snow, but also the underlying soil layers (Lachenbruch, 1959). This phenomenon is characterized by the parameter μ (Sazonova and Romanovsky, 2003), which quantifies the difference in thermal properties (heat capacity, thermal conductivity) between snow and the underlying soil layer. Higher μ values reflect increased insulation, and as a result, the thermal effect of snow should be more pronounced in recently burned stands (with thin organic horizons) than in mature stands (with thick organic horizons). These observations highlight the overriding importance of organic horizon thickness (Figure 5), and thus stand age and fire severity, as important controls on soil thermal dynamics during winter and summer.

Comparing the effects of active layer depth and soil climate on soil carbon loss

The combined effect of ALD and soil climate on soil OC was generally less than the sum of each individual effect (ALD effect + soil climate effect; Figure 8 and 9), suggesting that these factors are not distinct but have overlapping properties. While

many studies in the boreal region have documented the soil climate effect on decomposition (Dioumaeva et al., 2003; Wickland and Neff, 2007; O'Donnell et al., 2009a; Karhu et al., 2010), the nature and importance of the ALD effect is less clear. We suggest that the ALD effect integrates three factors that govern soil OC cycling in the northern permafrost region. First, the ALD effect reflects the distribution of OC into unfrozen and frozen soil, which in turn, determines the size of the OC pool (C) and contributes to the decomposition rate ($-kC$; O'Donnell et al., 2010). Second, the ALD effect incorporates the impact of soil phase (i.e. frozen vs. unfrozen) on the temperature sensitivity of decomposition rates (see Rivkina et al., 2000; Mikan et al., 2002). Third, the ALD effect also reflects differences in the inherent decomposability of organic matter substrates in unfrozen ($k_{active-layer}$) and frozen mineral soil ($k_{permafrost}$; Waldrop et al., 2010). While the first property of the ALD effect is distinct from the soil climate effect, the other two properties overlap with the soil climate effect. Inter-annual variability in ALD likely drives small changes in the distribution OC between unfrozen and frozen pools, whereas periodic disturbances (e.g. wildfire, erosion) may result in large transfers of OC from permafrost to and from the active layer.

Conclusions

    Recent field studies and modeling efforts have helped shape our understanding of soil OC dynamics in relation to wildfire and permafrost dynamics in the boreal region (Carrasco et al., 2006; Harden et al., 2006; Fan et al., 2008; Yi et al., 2009b, 2010; O'Donnell et al., 2010). Our findings illustrate that atmospheric warming and increased

fire severity will likely drive larger OC losses from boreal soils than from changes in snow depth or soil moisture. Moreover, our findings explore the complex interactions among climate and disturbance factors, and in turn draw attention to how these interactions function to increase soil OC loss. For instance, future increases in fire severity associated with a warmer and drier climate resulted in large OC losses through the deep combustion of organic soil horizons and subsequent warming and thawing of permafrost soils. Future decreases in fire severity associated with a warmer and wetter climate also resulted in similar OC losses, both by alleviating the moisture limitation of decomposition and by increasing heat conduction through wet organic soils. In each case, OC loss was governed by interannual changes in active layer depth, which determines the OC pool size in frozen and unfrozen mineral soil, and by the response of soil microbes to changing soil climate. Together, these findings highlight the need for modeling frameworks that consider the combined effects of fire, soil hydrology, permafrost and snow dynamics (e.g. Yi et al., 2010).

References

Balshi, M. S., McGuire, A. D., Duffy, P., Flannigan, M., Walsh, J., and Melillo, J.: Assessing the response of area burned to changing climate in western boreal North America using a Multivariate Adaptive Regression Splines (MARS) approach, Global Change Biol., 15, 578-600, 2009.

Bonan, G. B.: A computer model of the solar radiation, soil moisture, and soil thermal regimes in boreal forests, Ecol. Model., 45, 275-306, 1989.

Bond-Lamberty, B., Peckham, S. D., Ahl, D. E., and Gower, S. T.: Fire as the dominant driver of central Canadian boreal forest carbon balance, Nature, 450, 89-92, doi:10.1038/nature06272, 2007.

Burn, C. R.: The response (1958-1997) of permafrost and near-surface ground temperatures to forest fire, Takhini River valley, southern Yukon Territory, Can. J. Earth Sci., 35, 184-199, 1998.

Carrasco, J. J., Neff, J. C., and Harden, J. W.: Modeling physical and biogeochemical controls over carbon accumulation in a boreal forest soil, J. Geophys. Res-Biogeo., 111, G02004, doi:10.1029/2005JG000087, 2006.

Christensen, J. H., Hewitson, B., Busuioc, A., Chen, A., Gao, X., Held, I., Jones, R., Kolli, R. K., Kwon, W.-T., Laprise, R., Magaña, Rueda V., Mearns, L., Menéndez, C. G., Räisänen, J., Rinke, A., Sarr, A., and Whetton, P.: Regional Climate Projections, in: Climate Change 2007: The Physical Science Basis. Contribution of Working Group I to the Fourth Assessment Report of the Intergovernmental Panel on Climate Change. S. Solomon, D. Qin, M. Manning, Z. Chen, M. Marquis, K. B. Averyt, M. Tignor and H. L. Miller, editors. Cambridge University Press, Cambridge, United Kingdom and New York, NY, USA, 2007.

Clein, J. S. and Schimel, J. P.: Microbial activity of tundra and taiga soils at sub-zero temperatures, Soil Biol. Biochem., 27, 1231-1234, 1995.

Davidson, E. A. and Janssens, I. A.: Temperature sensitivity of soil carbon decomposition and feedbacks to climate change, Nature, 440, 165-173, 2006.

Dioumaeva, I., Trumbore, S., Schuur, E. A. G., Goulden, M. L., Litvak, M., and Hirsch, A. I.: Decomposition of peat from upland boreal forest: temperature dependence and sources of respired carbon, J. Geophys. Res-Atmos., 108, 8222, doi:10.1029/2001JD000848, 2003.

Euskirchen, E. S., McGuire, A. D., Kicklighter. D. W., Zhuang, Q., Clein, J. S., Dargaville, R. G., Dye, D. G., Kimball, J. S., McDonald, K. C., Melillo, J. M., Romanovsky, V. E., and Smith, N. V.: Importance of recent shifts in soil thermal dynamics on growing season length, productivity and carbon sequestration in terrestrial high-latitude ecosystems, Global Change Biol., 12, 731-750, 2006.

Euskirchen, E. S., McGuire, A. D., Rupp, T. S., Chapin, F. S. III, and Walsh, J. E.:
Projected changes in atmospheric heating due to changes in fire disturbance and
the snow season in the western Arctic, 2003-2100, J. Geophys. Res-Biogeo., 114,
G04022, doi:10.1029/2009JG001095, 2009.

Fan, Z., Neff, J. C., Harden, J. W., and Wickland, K. P.: Boreal soil carbon dynamics
under a changing climate: A model inversion approach, J. Geophys. Res-Biogeo.,
113, G04016, doi:10.1029/2008JG000723, 2008.

Flannigan, M., Stocks, B., Turetsky, M., and Wotton, M.: Impacts of climate change on
fire activity and fire management in the circumboreal forest, Global Change Biol.,
15, 549-560, 2009.

Friedlingstein, P., Cox, P., Betts, R., Bopp, L., von Bloh, W., Brovkin, V., Cadule, P.,
Doney, S., Eby, M., Fung, I., Bala, G., John, J., Joos, F., Kato, T., Kawamiya, M.,
Knorr, W., Lindsay, L., Matthews, H. D., Raddatz, T., Rayner, P., Reick, C.,
Roeckner, E., Schnitzler, K.-G., Schnur, R., Strassmann, K., Weaver, A. J.,
Yoshikawa, C., and Zeng, N.: Climate-carbon cycle feedback analysis: results
from the C^4MIP model intercomparison, J. Climate, 19, 3337-3353, 2006.

Frolking, S., Goulden, M. L., Wofsy, S. C., Fan, S.-M., Sutton, D. J., Munger, J. W.,
Bazzazz, A. M., Daube, B. C., Crill, P. M., Aber, J. D., Band, L. E., Wang, X.,
Savage, K., Moore, T., and Harris, R. C.: Modeling temporal variability in the
carbon balance of a spruce/moss boreal forest, Global Change Biol., 2, 343-366,
1996.

Goodrich, L. E.: The influence of snow cover on the ground thermal regime, Can. Geotech. J., 19, 421-432, 1982.

Harden, J. W., O'Neill, K. P., Trumbore, S. E., Velhuis, H., and Stocks, B. J.: Moss and soil contributions to the annual net carbon flux of a maturing boreal forest, J. Geophys. Res-Atmos., 102, 28805-28816, 1997.

Harden, J. W., Trumbore, S. E., Stocks, B. J., Hirsch, A., Gower, S. T., O'Neill, K. P., and Kasischke, E. S.: The role of fire in the boreal carbon budget. Global Change Biol., 6 (Suppl. 1), 174-184, 2000.

Harden, J. W., Meier, R., Silapaswan, C., Swanson, D. K., and McGuire, A. D.: Soil drainage and its potential for influencing wildfires in Alaska, US Geological Survey Professional Paper, 1678, 139-144, 2001.

Harden, J. W., Manies, K. L., Turetsky, M. R., and Neff, J. C.: Effects of wildfire and permafrost on soil organic matter and soil climate in interior Alaska, Global Change Biol., 12, 2391-2402, 2006.

Heimann, M. and Reichstein, M.: Terrestrial ecosystem carbon dynamics and climate feedbacks, Nature, 451, 289-292, 2008.

Johnstone, J. F., Chapin, F. S. III, Hollingsworth, T. N., Mack, M. C., Romanovsky, V., and Turetsky, M.: Fire, climate change, and forest resilience in interior Alaska, Can. J. Forest Res., 40, 1302-1312, 2010.

Jorgenson, M. T., Racine, C. H., Walters, J. C., and Osterkamp, T. E.: Permafrost degradation and ecological changes associated with a warming climate in central Alaska, Climatic Change, 48, 551-579, 2001.

Jorgenson, M. T. and Osterkamp, T. E.: Response of boreal ecosystems to varying modes
of permafrost degradation, Can. J. Forest Res., 35, 2100-2111, 2005.

Jorgenson, M. T., Romanovsky, V., Harden, J., Shur, Y., O'Donnell, J., Schuur, E. A. G.,
Kanevskiy, M., and Marchenko, S.: Resilience and vulnerability of permafrost to
climate change, Can. J. Forest Res., 40, 1219-1236, 2010.

Kane, E. S., Kasischke, E. S., Valentine, D. W., Turetsky, M. R., and McGuire, A. D.:
Topographic influences on wildfire consumption of soil organic carbon in interior
Alaska: implications for black carbon accumulation, J. Geophys Res-Biogeo.,
112, G03017, doi:10.1029/2007JG000458, 2007.

Karhu, K., Fritze, H., Hamalainen, K., Vanhala, P., Jungner, H., Oinonen, M., Sonninen,
E., Tuomi, M., Spetz, P., Kitunen, V., and Liski, J.: Temperature sensitivity of
soil carbon fractions in boreal forest soil, Ecology, 91, 370-376, 2010.

Kasischke, E. S., and Turetsky, M. R.: Recent changes in the fire regime across the North
American boreal region – Spatial and temporal patterns of burning across Canada
and Alaska, Geophys. Res. Lett., 33, L09703, doi: 10.1029/2006GL025677, 2006.

Khvorostyanov, D. V., Krinner, G., Ciais, P., and Heimann, M.: Vulnerability of
permafrost carbon to global warming. Part I: model description and role of heat
generated by organic matter decomposition, Tellus B, 60, 250-264, 2008.

Kirschbaum, M. U. F.: Will changes in soil organic carbon act as a positive or negative
feedback on global warming?, Biogeochemistry, 48, 21-51, 2000.

Kirschbaum, M. U. F.: The temperature dependence of organic matter decomposition –
still a topic of debate, Soil Biol. Biochem., 38, 2510-2518, 2006.

Lachenbruch, A. H.: Periodic heat flow in a stratified medium with applications to permafrost problems, US Geological Survey Bulletin 1083-A, 1959.

Lawrence, D. M., Slater, A. G., Romanovsky, V. E., and Nicolsky, D. J.: Sensitivity of a model projection of near-surface permafrost degradation to soil column depth and representation of soil organic matter, J. Geophys. Res-Earth., 113, F02011, doi:10.1029/2007JF000883, 2008.

Limpens, J., Berendse, F., Blodau, C., Canadell, J. G., Freeman, C., Holden, J., Roulet, N., Rydin, H., and Schaepman-Strub, G.: Peatlands and the carbon cycle: from local processes to global implications – a synthesis, Biogeosciences, 5, 1475-1491, 2008.

Lloyd, J. and Taylor, J.A.: On the temperature dependence of soil respiration, Funct. Ecol., 8, 315-323, 1994.

Mack, M. C., Schuur, E. A. G., Bret-Harte, M. S., Shaver, G. R., and Chapin III, F. S.: Ecosystem carbon storage in arctic tundra reduced by long-term nutrient fertilization, Nature, 431, 440-443, 2004.

Manies, K. L., Harden, J. W., Bond-Lamberty, B. P., and O'Neill, K. P.: Woody debris along an upland chronosequence in boreal Manitoba and its impact on long-term carbon storage, Can. J. Forest Res., 35, 472-482, 2005.

Marchenko, S., Romanovsky, V., and Tipenko, G.: Numerical modeling of spatial permafrost dynamics in Alaska. Proceedings of Ninth International Conference on Permafrost, Ninth International Conference on Permafrost, Fairbanks, Alaska, USA, 29 June – 3 July 2008, 1125-1130, 2008.

Mikan, C. J., Schimel, J. P., and Doyle, A. P.: Temperature controls of microbial respiration in arctic tundra soils above and below freezing, Soil Biol. Biochem., 34, 1785-1795, 2002.

Moody, J. A. and Martin, D. A.: Post-fire rainfall intensity-peak discharge relations for three mountainous watersheds in the western USA, Hydrol. Proc., 15, 2981-2993, 2001.

Neff, J. C., Harden, J. W., and Gleixner, G.: Fire effects on soil organic matter content, composition, and nutrients in boreal interior Alaska. Can. J. Forest Res., 35: 2178-2187, 2005.

Nicolsky, D. J., Romanovsky, V. E.,and Tipenko, G. S.: Using in-situ temperature measurements to estimate saturated soil thermal properties by solving a sequence of optimization problems, The Cryosphere, 1, 41-58, 2007.

Nowinski, N. S., Taneva, L., Trumbore, S. E., and Welker, J. M.: Decomposition of old organic matter as a result of deeper active layers in a snow depth manipulation experiment, Oecologia, 163, 785-792, 2010.

O'Donnell, J. A., Turetsky, M. R., Harden, J. W., Manies, K. L., Pruett, L. E., Shetler, G., and Neff, J. C.: Interactive effects of fire, soil climate, and moss on CO_2 fluxes in black spruce ecosystems of Interior Alaska, Ecosystems, 12, 57-72, 2009a.

O'Donnell, J. A., Romanovsky, V. E., Harden, J. W., and McGuire, A. D.: The effect of moisture content on the thermal conductivity of moss and organic soil horizons from black spruce ecosystems in interior Alaska, Soil Sci., 174, 646-651, 2009b.

O'Donnell, J. A., Harden, J. W., McGuire, A. D., Kanevskiy, M. Z., Jorgenson, M. T., and Xu, X.: The effect of fire and permafrost interactions on soil carbon accumulation in an upland black spruce ecosystem of interior Alaska: implications for post-thaw carbon loss, Global Change Biol., In press.

O'Neill, K. P., Kasischke, E. S., and Richter, D. D.: Environmental controls on soil CO2 flux following fire in black spruce, white spruce, and aspen stands of interior Alaska, Can. J. Forest Res., 32, 1525-1541, 2002.

Osterkamp, T. E. and Romanovsky, V. E.: Evidence for warming and thawing of discontinuous permafrost in Alaska, Permafrost Periglac., 10, 17-37, 1999.

Ping, C.-L., Michaelson, G. J., Packee, E. C., Stiles, C. A., Swanson, D. K., and Yoshikawa, K.: Soil catena sequences and fire ecology in the boreal forest of Alaska, Soil Sci. Soc. Am. J., 69, 1761-1772, 2005.

Richter, D. D., O'Neill, K. P., and Kasischke, E. S.: Stimulation of soil respiration in burned black spruce (*Picea mariana* L.) forest ecosystems: a hypothesis, in: Fire, climate change, and carbon cycling in the North American boreal forest, Ecological Studies 138, Springer, New York, New York, USA, 167-178, 2000.

Rieger, S., C. E. Furbush, C. E., Shoephorster, D. B., Summerfield Jr., H., and Geiger, L.
C.: Soils of the Caribou-Poker Creeks Research Wateshed, Interior Alaska, Cold
Regions Research and Engineering Laboratory, Hanover, New Hampshire, USA,
Technical Report 236, 1972.

Rivkina, E., Friedmann, E., McKay, C., and Gilichinsky, D.: Metabolic activity of
permafrost bacteria below the freezing point, Appl. Environ. Microb., 66, 3230-
3233, 2000.

Romanovsky, V. E. and Osterkamp, T. E.: Thawing of the active layer on the coastal
plain of the Alaskan Arctic, Permafrost Periglac., 8, 1-22, 1997.

Romanovsky, V. E. and Osterkamp, T. E.: Effects of unfrozen water on heat and mass
transport processes in the active layer and permafrost, Permafrost Periglac., 11,
219-239, 2000.

Romanovsky, V. E., Smith, S. L., and Christiansen, H. H.: Permafrost thermal state in the
polar northern hemisphere during the International Polar Year 2007-2009: a
Synthesis, Permafrost Periglac., 21, 106-116, 2010.

Sazonova, T. S. and Romanovsky, V. E.: A model for regional-scale estimation of
temporal and spatial variability of active layer thickness and mean annual ground
temperatures, Permafrost Periglac., 14, 125-139, 2003.

Schuur, E. A. G., Bockheim, J., Canadell, J. G., Euskirchen, E., Field, C. B., Goryachkin, S. V., Hagemann, S., Kuhry, P, Lafleur, P. M., Lee, H., Mazhitova, G., Nelson, F. E., Rinke, A., Romanovsky, V. E., Shiklomanov, N., Tarnocai, C., Venevsky, S., Vogel, J. G., and Zimov, S. A.: Vulnerability of permafrost carbon to climate change: implications for the global carbon cycle, Bioscience, 58, 701-714, 2008.

Schuur, E. A. G., Vogel, J. G., Crummer, K. G., Lee, H., Sickman, J. O., and Osterkamp, T. E.: The effect of permafrost thaw on old carbon release and net carbon exchange from tundra, Nature, 459, 556-559, 2009.

Shur, Y., Hinkel, K. M., and Nelson, F. E.: The transient layer: implications for geocryology and climate-change science, Permafrost Periglac., 16, 5-17, 2005.

Shur, Y. L., Kanevskiy, M., White, D. M., and Connor, B.: Geotechnical investigations for the Dalton Highway Innovation Project as a case study of the ice-rich syngenetic permafrost, Alaska Department of Transporation, AUTC assigned project 207122, 2010.

Stieglitz, M., Dery, S. J., Romanovsky, V. E., and Osterkamp, T. E.: The role of snow cover in the warming of arctic permafrost, Geophys. Res. Lett., 30, 1721, doi:10.1029/2003GL017337, 2003.

Swanson, D. K.: Susceptibility of permafrost soils to deep thaw after forest fires in interior Alaska, USA, and some ecological implications, Arctic Alpine Res., 28, 217-227, 1996.

Tarnocai, C., Canadell, J. G., Schuur, E. A. G., Kuhry, P., Mazhitova, G., and Zimov, S.: Soil organic carbon pools in the northern circumpolar permafrost region, Global Biogeochem. Cy., 23, GB2023, doi:10.1029/2008GB003327, 2009.

Trumbore, S. E. and Harden, J. W.: Accumulation and turnover of carbon in organic and mineral soils of the BOREAS northern study area, J. Geophys. Res-Atmos., 102, 28817-28830, 1997.

Viereck, L. A., Werdin-Pfisterer, N. R., Adams, P. C., Yoshikawa, K.: Effect of wildfire and fireline construction on the annual depth of thaw in a black spruce permafrost forest in interior Alaska: A 36-year record of recovery, Proceedings of Ninth International Conference on Permafrost, Ninth International Conference on Permafrost, Fairbanks, Alaska, USA, 29 June – 3 July 2008, 1125-1130, 2008.

Waldrop, M. P., Wickland, K. P., White III, R., Behre, A. A., Harden, J. W., Romanovsky, V. E. 2010. Global Change Biology, doi:10.1111/j.1365.-2486.2009.02141.x.

Welp, L. R., Randerson, J. T., and Liu, H. P.: The sensitivity of carbon fluxes to spring warming and summer drought depends on plant functional types in the boreal forest ecosystems, Agr. Forest Meteorol., 47, 172-185, 2007.

Wickland, K. P. and Neff, J. C.: Decomposition of soil organic matter from boreal black spruce forest: environmental and chemical controls, Biogeochemistry, 87, 29-47, 2007.

Yi, S., McGuire, A. D., Harden, J. W., Kasischke, E., Manies, K., Hinzman, L., Liljedahl, A., Randerson, J., Liu, H., Romanovsky, V., Marchenko, S., and Kim, Y.: Interactions between soil thermal and hydrological dynamics in the response of Alaska ecosystems to fire disturbance, J. Geophys. Res–Biogeo., 114, G02015, doi:10.1029/2008JG000841, 2009a.

Yi, S., Manies, K., Harden, J., and McGuire, A. D.: Characteristics of organic soil in black spruce forests: Implications for the application of land surface and ecosystem models in cold regions, Geophys. Res. Lett., 36, L05501, doi:10.1029/2008GL037014, 2009b.

Yi, S., McGuire, A. D., Kasischke, E., Harden, J. W., Manies, K. L., Mack, M., and Turetsky, M. R.: A dynamic organic soil biogeochemical model for simulating the effects of wildfire on soil environmental conditions and carbon dynamics of black spruce forests, J. Geophys. Res–Biogeo., In press.

Yoshikawa, K., Bolton, W. R., Romanovsky, V. E., Fukuda, M., and Hinzman, L. D.: Impacts of wildfire on the permafrost in the boreal forests of interior Alaska, J. Geophys. Res-Atmos., 108, doi:10.1029/2001JD000438, 2003.

Zhuang, Q., Romanovsky, V. E., and McGuire, A. D.: Incorporation of a permafrost model into a large-scale ecosystem model: Evaluation of temporal and spatial scaling issues in simulating soil thermal dynamics, J. Geophys. Res-Atmos., 106, 33649-33670, 2001.

Zhuang, Q., McGuire, A. D., O'Neill, K. P., Harden, J. W., Romanovsky, V. E., and

    Yarie, J.: Modeling soil thermal and carbon dynamics of a fire chronosequence in

    interior Alaska, J. Geophys. Res-Atmos., 108, 8147, doi:10.1029/2001JD001244,

    2002.

Zimov, S. A., Schuur, E. A. G., and Chapin III, F. S.: Permafrost and the global carbon

    budget, Science, 312, 1612-1613, 2006.

Tables

Table 1. Climate and disturbance scenarios tested using GIPL and Fire-C models.

Climate/Disturbance Scenarios	Description	*Source Data*
Air Temperature		
A2 Scenario	"Business as usual" scenario following IPCC (Christensen et al. 2007)	Figure 2
B1 Scenario	Reduced greenhouse gas emission following IPCC (Christensen et al. 2007)	Figure 2
Soil Moisture		
Wetter	25% increase in VWC of organic soil horizons relative to present-day values	Supplemental Figure 3
Drier	25% decrease in VWC of organic soil horizons relative to present-day values	Supplemental Figure 3
Snow Dynamics		
Deeper Snowpack	25% increase in snow depth relative to present-day values	Figure 3
Shallower Snowpack	25% decrease in snow depth relative to present-day values	Figure 3
Fire Severity		
Lower Severity	25% of organic horizon combusted during fire	Harden et al. (2000)
Higher Severity	77% of organic horizon combusted during fire	Kane et al. (2007)
Multiple Factors		
High Severity x Drying x Warming	Interactive effects of high severity fires (77%), warming (A2), and drying	
Low Severity x Wetting x Warming	Interactive effects of low severity fires (25%), warming (A2), and wetting	
Longer Snow-free Season	Snowmelt 21 days earlier, snow return 20 days later than present day (Euskirchen et al. 2009)	Figure 3

Table 2. Organic horizon thicknesses and active layer depths across upland fire chronosequence.

Site	n	Live/Dead Moss (cm)	Fibric (cm)	Mesic/Humic (cm)	Organic Horizon (cm)	Active Layer Depth (cm)
Unburned Mature	33	6 ± 2	8 ± 4	10 ± 6	24 ± 5	45 ± 8
2003 Burn	23	3 ± 4	5 ± 4	6 ± 3	14 ± 5	66 ± 12
1990 Burn	10	4 ± 3	4 ± 5	2 ± 3	9 ± 4	77 ± 19
1967 Burn	11	4 ± 2	4 ± 3	6 ± 2	15 ± 4	54 ± 7

Table 3. GIPL model parameterizations at three study sites across fire chronosequence at Hess Creek, AK.

Site	Horizon thickness[a] (cm)	Volumetric water content[b] (%)	Unfrozen thermal conductivity[c] ($W\,m^{-1}\,K^{-1}$)	Frozen thermal conductivity[d] ($W\,m^{-1}\,K^{-1}$)
Unburned Mature				
live/dead moss	5	20	0.07	0.15
Fibric	11	25	0.15	0.20
mesic/humic	8	30	1.40	2.00
2003 Burn				
Fibric	8	49	0.26	0.75
mesic/humic	5	55	0.25	0.75
1967 Burn				
live/dead moss	6	20	0.25	1.20
Fibric	5	25	0.25	1.50
mesic/humic	9	68	0.40	1.40

NOTE: Parameterizations for specific heat capacity and unfrozen water content for each horizon were taken from calibration conducted by Romanovsky and Osterkamp (2000).

[a] Horizon thickness reflect average measurements for each horizon type as measured across the Hess Creek chronosequence (O'Donnell et al. 2010).

[b]VWC values vary with one standard deviation of the summer mean VWC, as measured in this study (Supplemental Figure 3). VWC data calibrated following O'Donnell et al. (2009a).

[c]Unfrozen thermal conductivity values were calculated from the VWC measurements following the equations by O'Donnell et al. (2009b).

[d]Frozen thermal conductivity values were prescribed following Romanovsky and Osterkamp (2000).

Table 4. Exponential equation parameters and statistics for the relationship between active layer depth (ALD) and organic horizon thickness across climate and fire scenarios.

Climate/Disturbance Scenario	ALD x Organic Horizon Thickness			
	a	*b*	R^2	*P*
Present-Day Climate				
2007-2009	116.9490	0.0282	0.93	< 0.0001
Air Temperature				
A2 Scenario	163.6927	0.0234	0.85	0.0010
B1 Scenario	127.0604	0.026	0.89	0.0004
Soil Moisture				
Wetter	118.3910	0.0245	0.92	0.0002
Drier	113.9505	0.0332	0.93	0.0001
Snow Dynamics				
Deeper Snowpack	116.6501	0.0275	0.90	0.0003
Shallower Snowpack	114.8101	0.0287	0.92	0.0002
Fire Severity				
Lower Severity (25%)	116.1617	0.0294	0.9	0.0003
Higher Severity (75%)	103.884	0.0121	0.42	0.0833
Climate-disturbance Interactions				
High Severity x Warming x Drier	145.9954	0.0113	0.36	0.1160
Low Severity x Warming x Wetter	167.3116	0.0216	0.84	0.0014
Snow Seasonality	165.4936	0.0233	0.86	0.0010

Figures
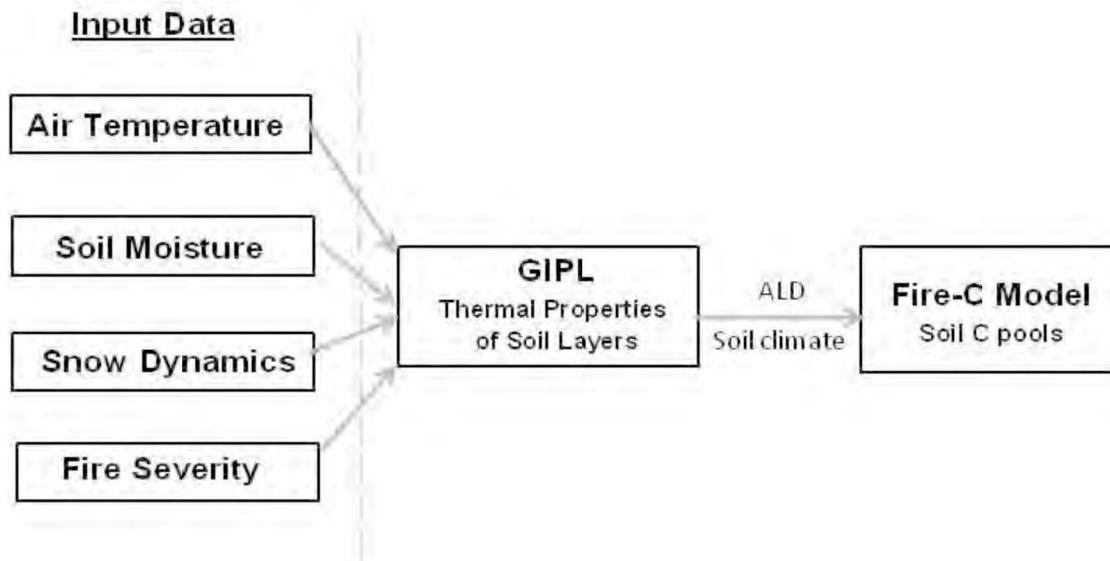
Figure 1. The modeling framework of this study in which Geophysical Institute Permafrost Laboratory (GIPL) model was calibrated from measured temperature input data. GIPL was then used to simulate active layer depth (ALD) and soil temperature profiles over a variety of climate and soil conditions. The Fire-C model used GIPL results to simulate changes in soil OC storage over multiple fire cycles based on ALD and soil temperature (August mean monthly temperature). Input data include air temperature, soil moisture, snow depth and fire severity (carbon fraction combusted during a fire event) from the Hess Creek study area collected from 2007-2009. Sensitivity analyses were conducted (see Table 1 for scenario details) using the GIPL model to assess the impact of input variables on ALD and soil temperatures. ALD and soil temperature data were then used to drive soil C turnover in the Fire-C model.
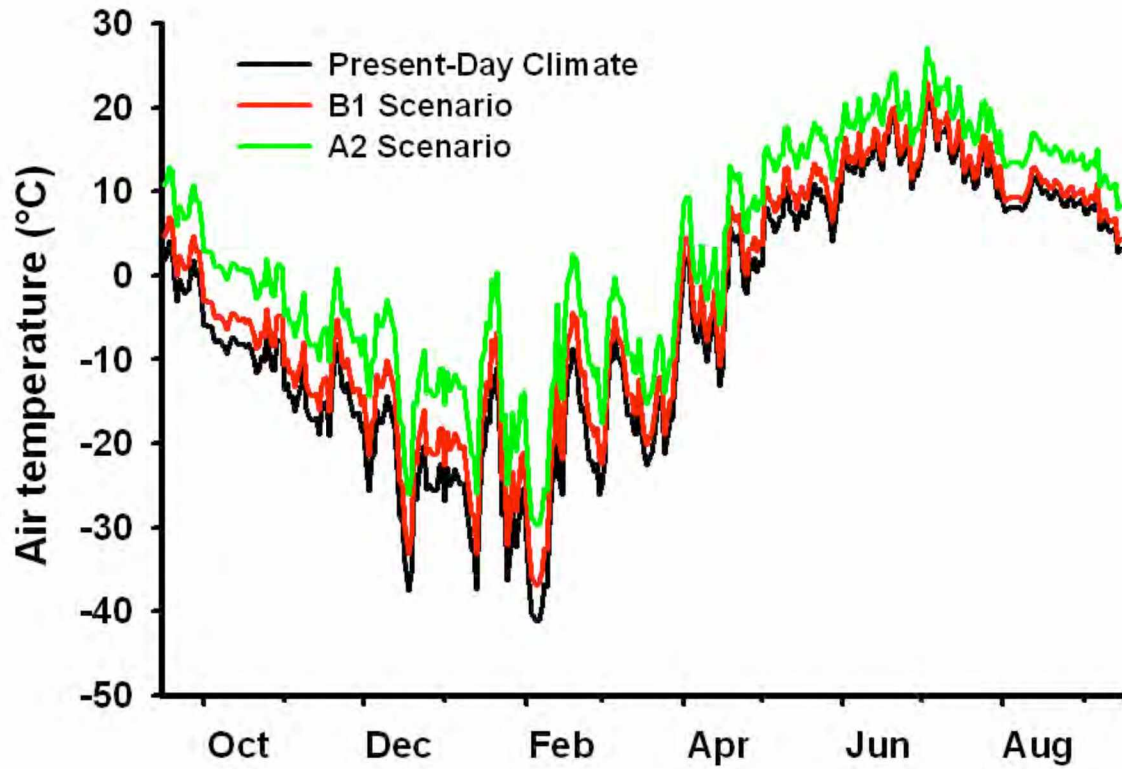
Figure 2. Future air temperature scenarios for the year 2100 relative to present-day climate at Hess Creek study region. The B1 scenario reflects future air temperatures under reduced carbon emissions, whereas the A2 scenario reflects carbon emissions following "business as usual" trends.
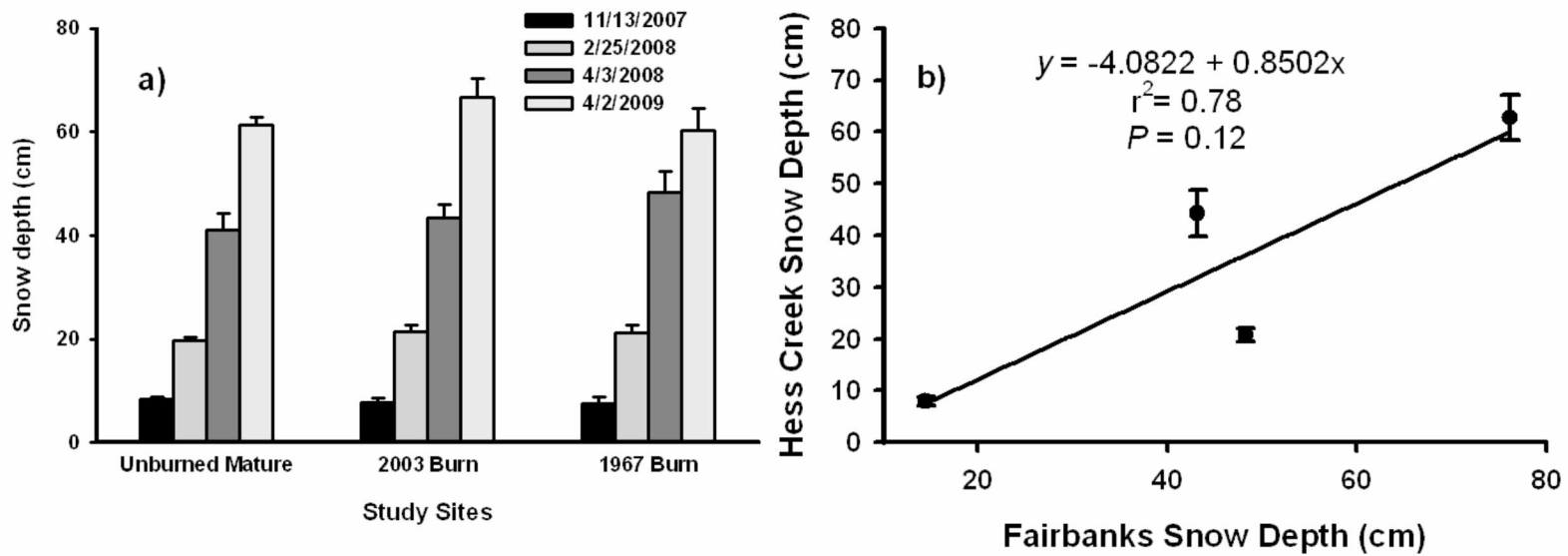
Figure 3. a) Results from snow surveys conducted the winter of 2007-2008 and April 2009 at the Hess Creek study sites. b)

Linear curve fit between snow depth measured at Hess Creek and near Fairbanks (data from Bonanza Creek Long-Term

Ecological Research Station, www.lter.uaf.edu).
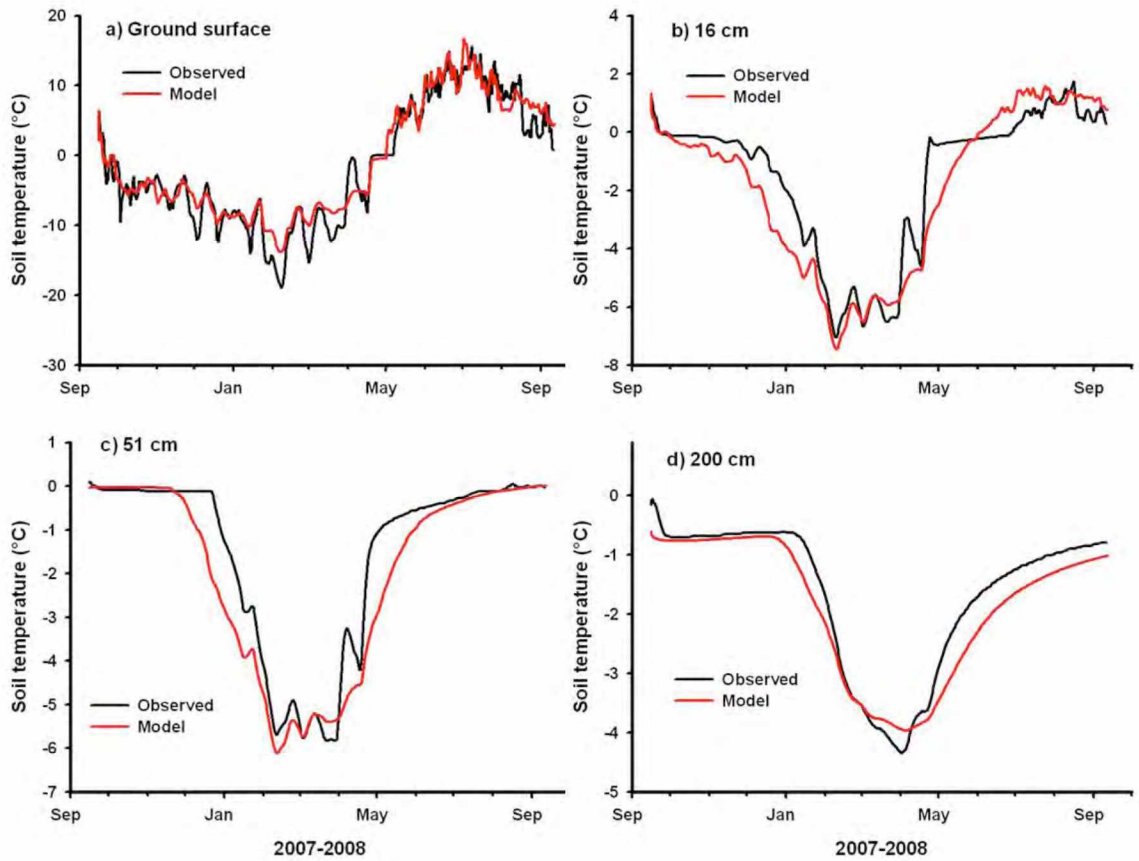
Figure 4. Comparison of model soil temperature outputs (from GIPL2) and observed soil temperatures at different depths at the unburned mature site near Hess Creek. Model was separately parameterized for 2003 Burn and 1967 Burn soil profiles.
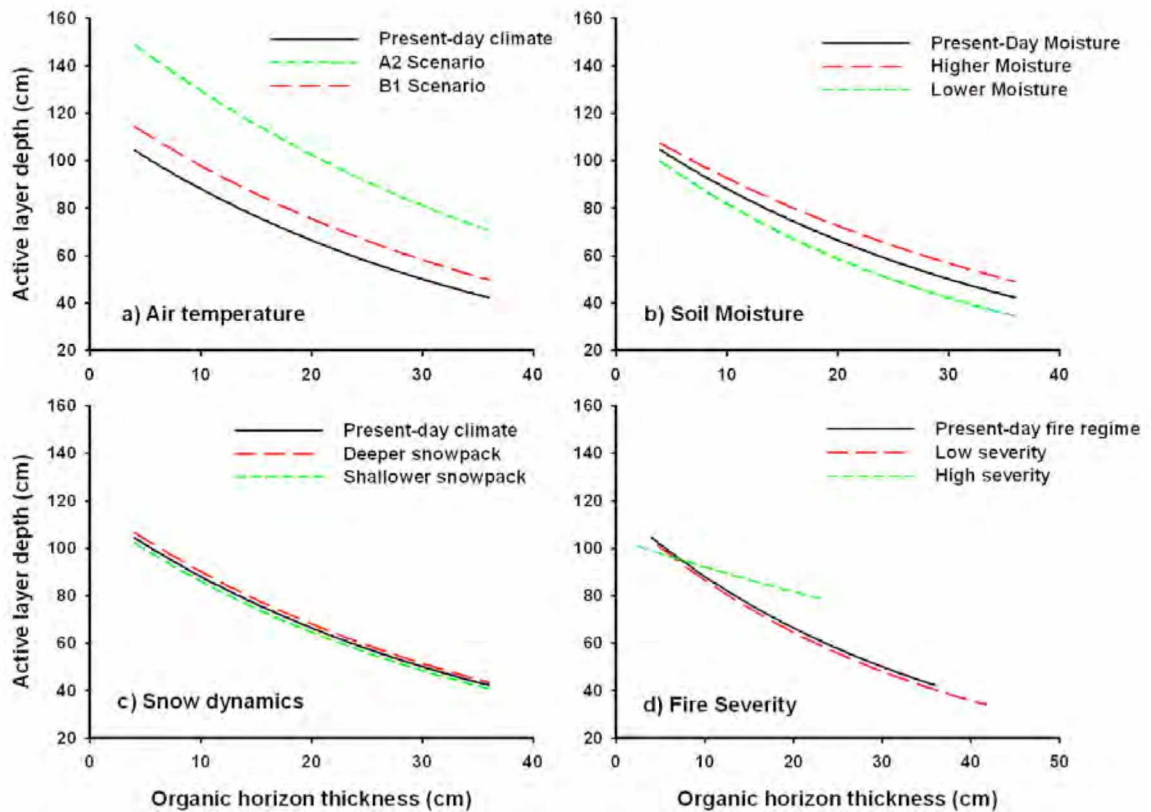
Figure 5. Sensitivity of the active layer depth (ALD) to temperature, soil moisture, snow dynamics and fire severity. The relationship between ALD and organic horizon thickness was modeled using GIPL across a range of future air temperatures (a; IPCC scenarios), moisture conditions (b), snow (c), and fire severity (d). Output data from each scenario were then fit with the exponential equation: $ALD = a * e^{-b*OHT}$ and are summarized in Table 4. Equations were then used to run Fire-C model to evaluate sensitivity of soil carbon to various climate scenarios.
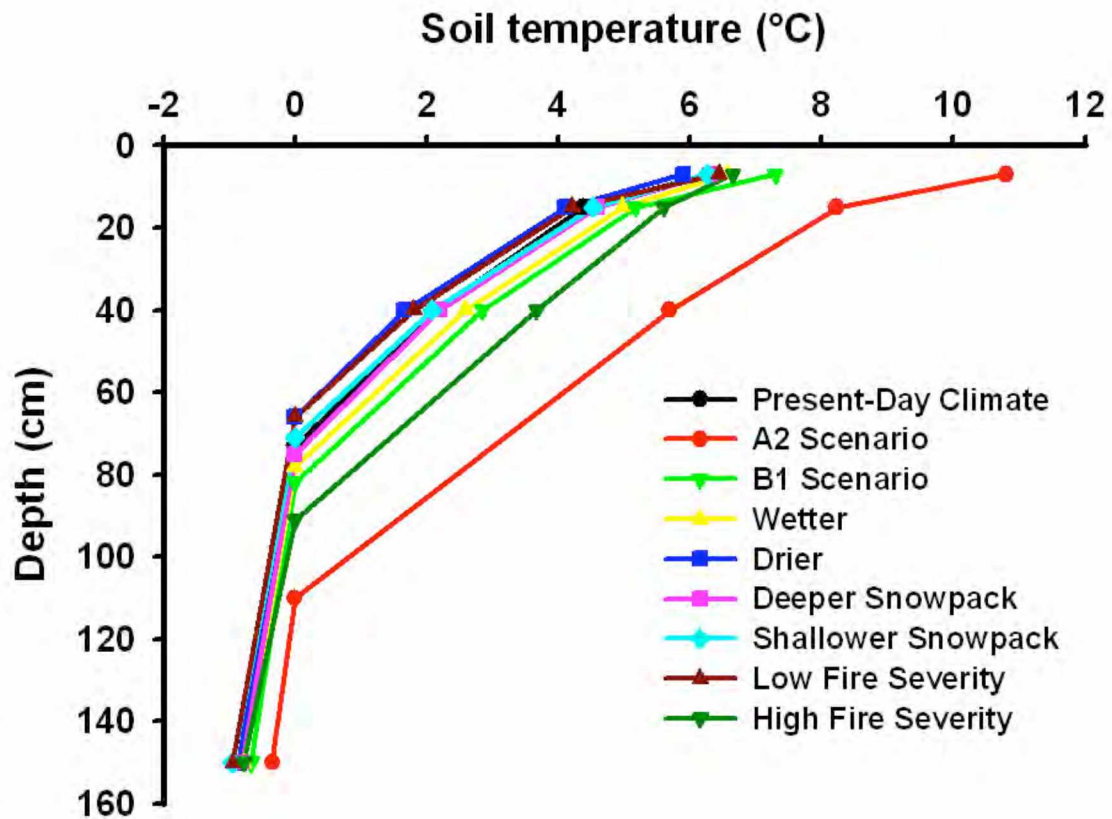
Figure 6. Sensitivity of mean monthly temperature (MMT) in August to a suite of climatic and fire scenarios as modeled from GIPL. The depth of temperature data reflect positioning in shallow organic horizons (< 10 cm), deep organic horizons (15 cm), unfrozen mineral soil in the active layer (40 cm), and permafrost (1.5 m). August MMT were used at each depth were used to drive the temperature sensitivity of organic matter decomposition (Equations 1 and 2) in the Fire-C model across this suite of climate and disturbance scenarios.
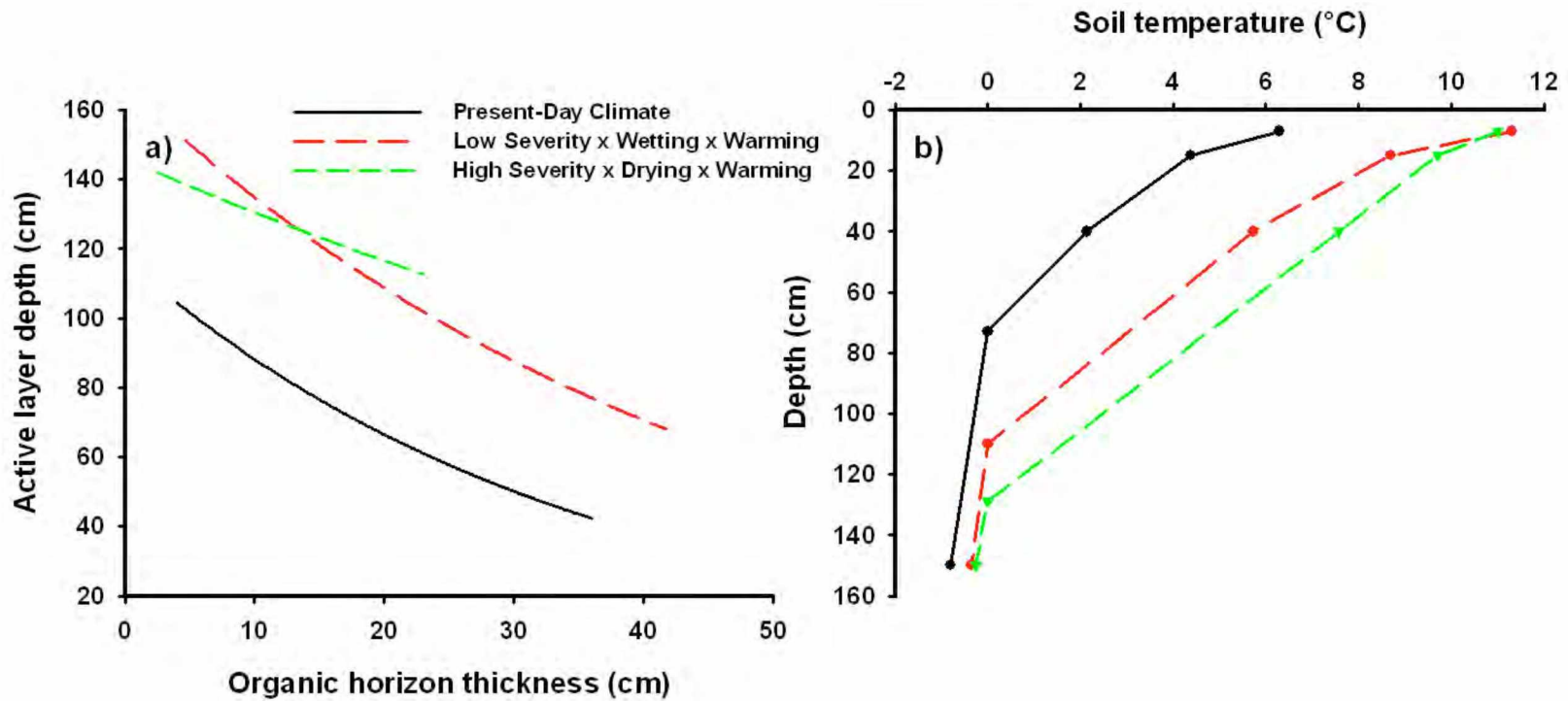
Figure 7. Sensitivity of ALD (a) and mean monthly soil temperature in August (b) to multiple interacting factors. Using the GIPL model, we tested the effects of low fire severity, wetter soil conditions and warmer air temperatures (A2 scenario), high fire severity, drier soil conditions and warmer air temperatures, and changes in snow seasonality (following Euskirchen et al. 2009) associated with future warming (A2 scenario).
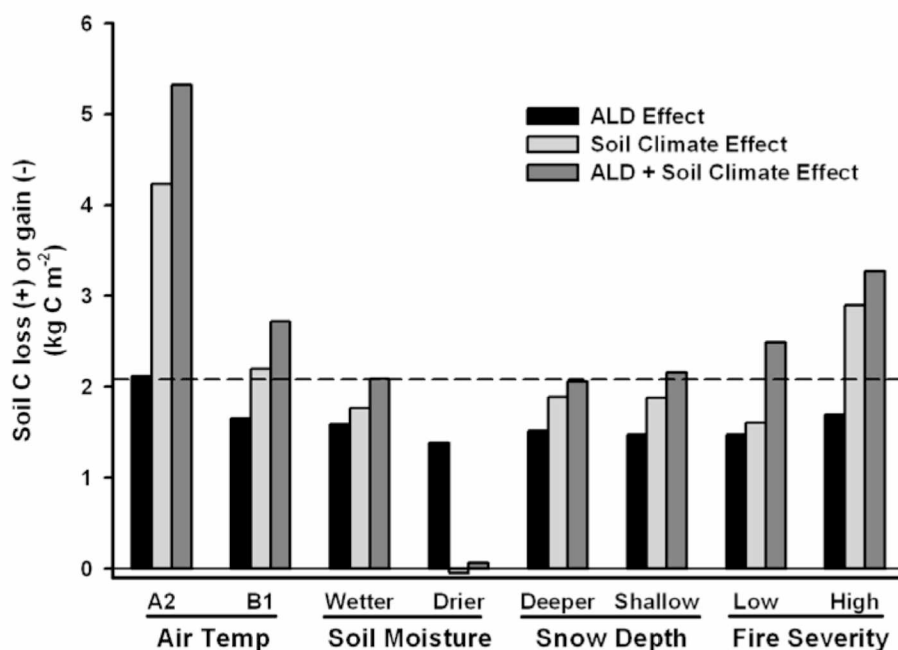
Figure 8. The effect of single climate factors (air temperature, soil moisture, and snow depth) or fire severity on soil C storage. Soil C loss or gain was calculated as the difference in total soil C stocks in top 2 meters of soil between model years 6500 and 7000 years (or approximately 3 fire cycles after step-change in climate/fire). To calculate the active layer depth (ALD) effect, we used only modified the relationship between ALD and organic horizon thickness (from Table 4) for each scenario in the Fire-C model. To calculate the soil climate effect, we modified decomposition constants within the Fire-C model to reflect future changes in soil temperature (Figure 6) and/or soil moisture (Table 1). To calculate the ALD + soil climate effect, we modified both the ALD-OHT relationship and the decomposition constants within the Fire-C model. The dashed black line represents total OC losses (ALD + soil climate) when present-day climate conditions (with no changes in snow, moisture or fire) were run for 3 fire cycles.
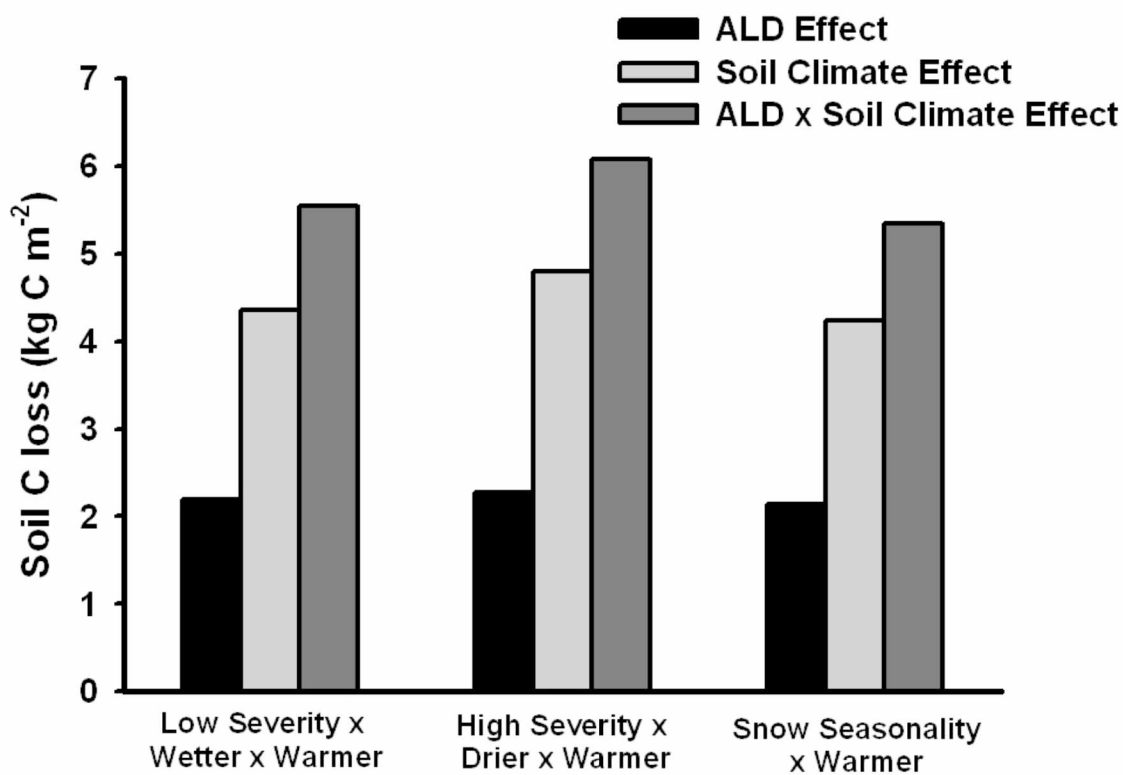
Figure 9. The effects of combined climate/fire factors on soil C storage. The three scenarios reflect reduced fire severity associated with warmer and wetter soil conditions, higher fire severity associated with warmer and drier conditions, and longer snow-free season associated with warmer air temperatures. The ALD and soil climate parameterizations were derived from GIPL output as illustrated in Figure 7.

Supplemental Materials

Field measurements of soil temperature and soil moisture

For the Unburned Mature stand, temperature probes were installed at depths of two, five, 16, 24, 51, and 200 cm. For the 2003 Burn, temperature probes were installed at depths of 3, 8, 13, 81, and 205 cm. For the 1967 stand, temperature probes were installed at depths of 3, 6, 11, 20, and 74 cm.

At the Unburned Mature stand, soil moisture was monitored in the live/dead moss horizon (3 cm), fibric horizon (7 cm), and mesic/humic horizon (22 cm). At the 2003 Burn, soil moisture was monitored in the fibric horizon (6 cm), and mesic/humic horizon (10 cm), and mineral A horizon (18 cm). At the 1967 Burn, soil moisture was only monitored in the mesic/humic horizon (16 cm). Soil moisture probes were calibrated following the methods of O'Donnell et al. (2009a).

Soil thermal dynamics, soil moisture dynamics, and snow depth across fire-thaw chronosequence

Soil temperature patterns varied seasonally across study sites along the fire chronosequence (Supplemental Figure 1a-c). For example, mean winter (December, January, February) temperatures at the ground surface were substantially colder in the Unburned Mature stand (2008 = -9.04 °C; 2009 = -7.74 °C) than in the 2003 Burn (2008 = -2.35 °C; 2009 = -2.18 °C; Figure 2). Mean monthly temperature (MMT) at the ground surface in August, when thaw depth reaches an annual maximum, was similar across

sites, averaging 6.99, 8.23 and 6.18 °C at the Unburned Mature, 1967 Burn, and 2003

Burn, respectively. However, MMT in August at depth was cooler in the Unburned

Mature stand than in the 2003 Burn and 1967 Burn (Supplemental Figure 2).

In general, the 2003 Burn was considerably wetter than the Unburned Mature

stand throughout the organic horizon. At the 2003 Burn, VWC during summer averaged

61.7 ± 13.2 %, 55.5 ± 13.7 %, and 29.7 ± 10.2 % in the fibric, mesic/humic, and A

horizons, respectively, whereas at the Unburned Mature stand, volumetric water content

(VWC) during summer (May – August) averaged 7.8 ± 4.7 %, 17.2 ± 7.0 %, and $30.1 \pm$

13.4 % in the live/dead moss, fibric, and mesic/humic horizons, respectively

(Supplemental Figure 3). Using these VWC values, we then calculated average thermal

conductivity values for each organic soil horizon (Table 2). The higher VWC values in

the 2003 Burn resulted in considerably higher thermal conductivity values ($0.353 - 0.364$

$W\ m^{-1}\ K^{-1}$) than in the Unburned Mature stand ($0.070 - 0.211\ W\ m^{-1}\ K^{-1}$). Using the

GIPL model, we observed good agreement between measured and modeled ALD

(Supplemental Figure 4) at sites across the Hess Creek fire chronosequence.

Supplemental Figures
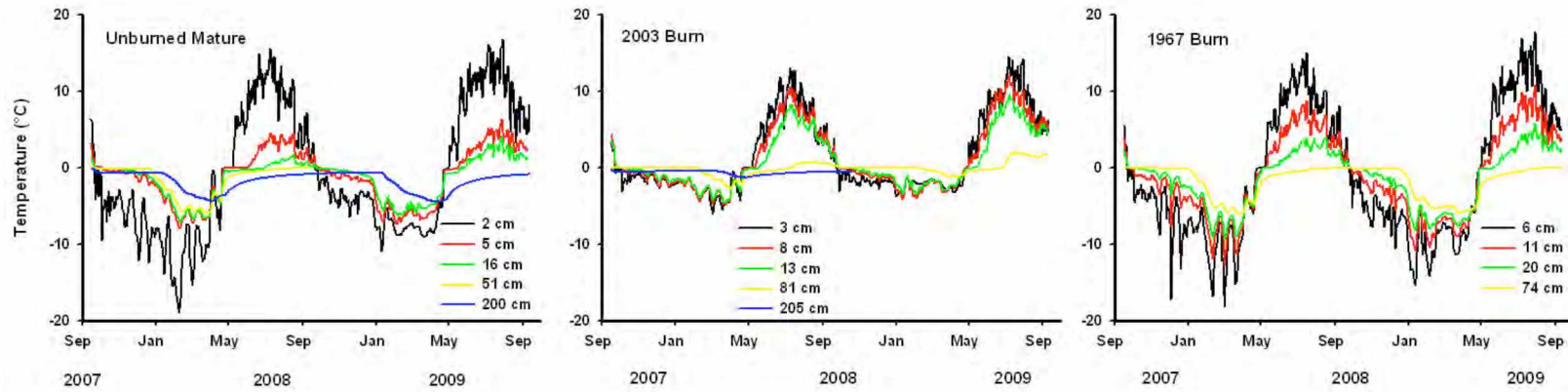
Supplemental Figure 1. Seasonal and interannual variation in soil temperature (°C) at Unburned Mature stand, 2003 Burn, and 1967 Burn.
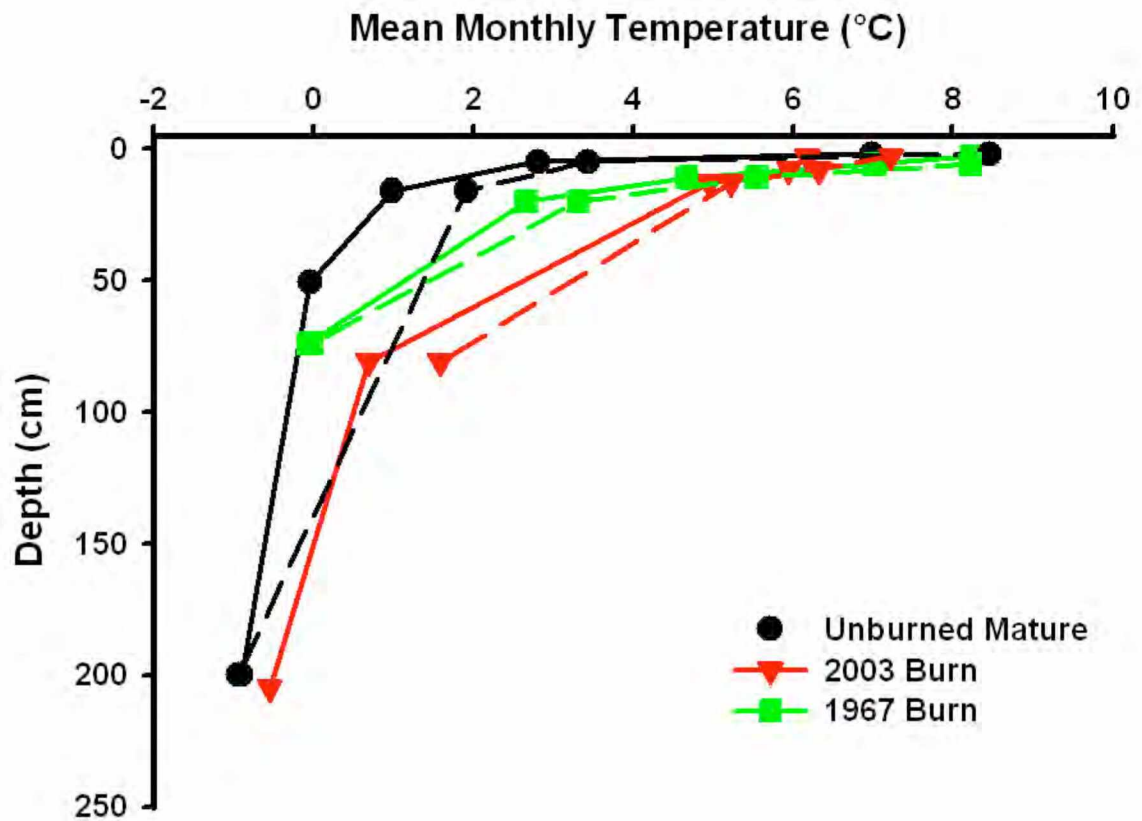
Supplemental Figure 2. Mean monthly temperature profile for August 2008 (solid lines)

and 2009 (dashed lines) at three study sites across the fire chronosequence.
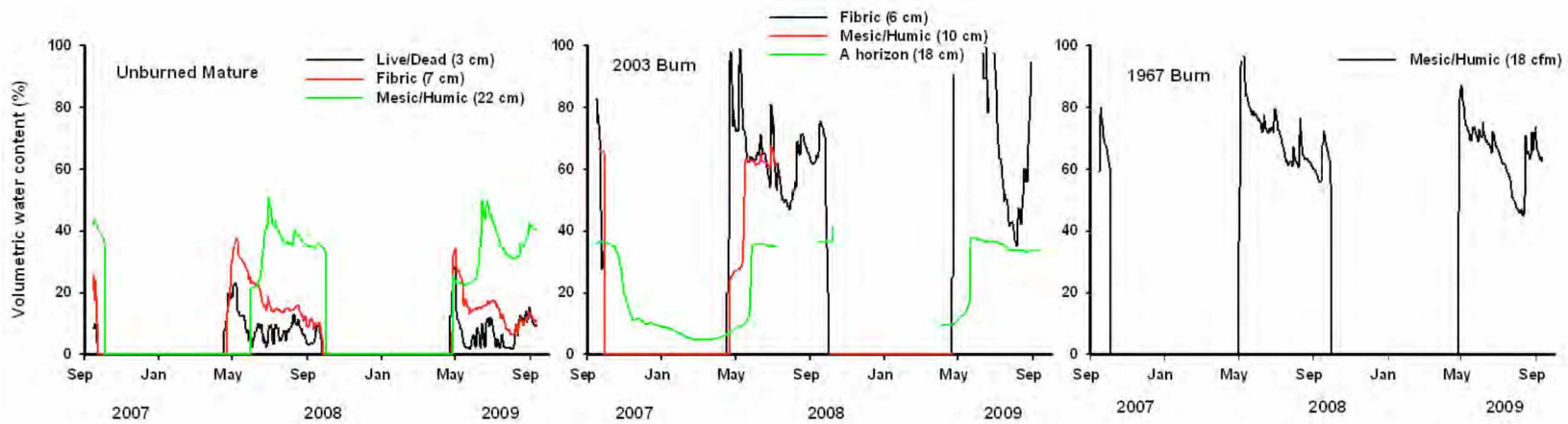
Supplemental Figure 3. Mean daily volumetric water content from September 2007 to September 2009 at three stand ages across fire chronosequence at Hess Creek.
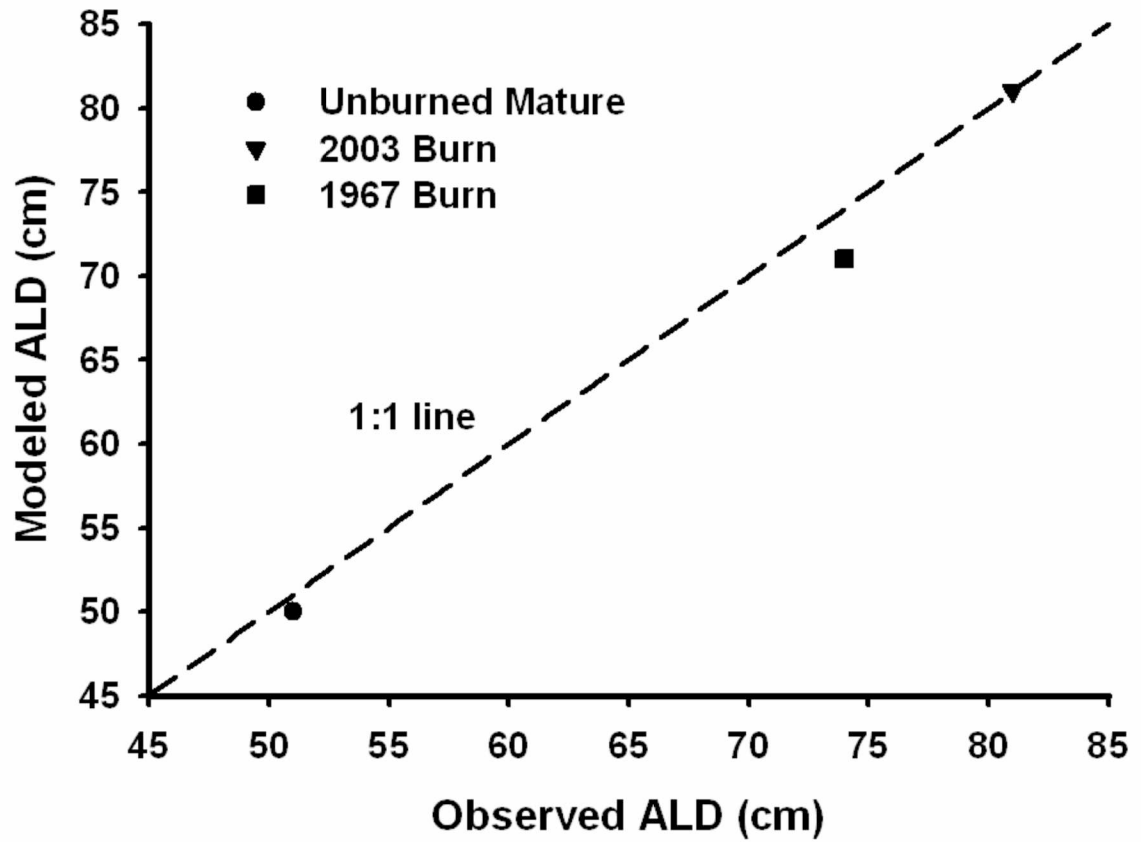
Supplemental Figure 4. Comparison of modeled ALD (from GIPL model) and observed ALD measured in late-August 2008.

Chapter 5: The effects of permafrost thaw on soil hydrologic, thermal and carbon dynamics in an Alaskan peatland[4]

Abstract

Northern peatlands store large quantities of organic carbon (OC) in saturated or frozen peat deposits, accounting for nearly 15% of the global belowground OC pool. Recent warming at high-latitudes has resulted in degradation of permafrost in peatlands, which can have a profound effect on local hydrology and ecosystem OC balance. To assess the impact of permafrost thaw on soil OC dynamics, we measured soil thermal dynamics and soil OC stocks across a collapse-scar bog chronosequence (Permafrost Plateau, Young Bogs, Old Bogs) at Koyukuk Flats National Wildlife Refuge in interior Alaska. Across the chronosequence, we observed dramatic changes in the distribution of soil water associated with thawing of ice-rich frozen peat and lacustrine sediments. The impoundment of relatively warm water in collapse-scar bogs initiated talik formation and the lateral expansion of bogs over time. On average, Permafrost Plateaus stored 137 ± 36 kg C m^{-2}, whereas OC storage in Young Bogs and Old Bogs averaged 87 ± 14 and 60 ± 1 kg C m^{-2}, respectively. Based on our reconstructions using radiocarbon data, immediately following permafrost thaw, OC dynamics in shallow and deep peat horizons began to operate separately, with the accumulation of OC occurring in near-surface bog

peat layers and rapid decomposition and loss of OC from inundated forest peat layers.

Approximately 1000 years following permafrost thaw, OC accumulation in surface bog

peat layers slowed, with little change in OC storage over the subsequent 2000 years. In

the deep forest peat layers that became inundated with unfrozen bog water,

decomposition reduced OC stocks by nearly half after 1000 years, at which point OC

losses also stabilized. Accumulation rates at the surface were not sufficient to balance

deep OC losses, resulting in a net loss of 26 g C m^{-2} y^{-1} from the entire peat column

during the 3000 years following thaw. These findings suggest that permafrost thaw and

the subsequent release of OC from previously frozen peat deposits will likely reduce the

strength of the northern peatlands as a carbon dioxide sink, and consequently, accelerate

rates of atmospheric warming.

Introduction

Peatlands account for approximately 19% of the northern circumpolar permafrost

region, and store 419-455 Pg of organic carbon (OC; Gorham 1991; Apps and others

1993; Tarnocai and others 2009). In the subarctic, nearly 48% of soil OC is stored in

frozen peat deposits (Tarnocai and others 2007). Having developed over several

thousand years since the last glaciation (Harden and others 1992), northern peatlands

have generally functioned as long-term sinks for atmospheric carbon dioxide (CO_2) and

sources of atmospheric methane (CH_4; Blodau 2002; Smith and others 2004), and have

functioned to cool the atmosphere (Frolking and Roulet 2007). However, climate-driven

changes in permafrost extent or wildfire frequency could reduce the sink strength of

northern peatlands (McGuire and others 2010) through the release of OC stored in frozen or saturated peat (Turetsky and others 2002a; Dise 2009; Dorrepaal and others 2009). Permafrost degradation is of particular concern, given the recent acceleration of permafrost thaw in subarctic peatlands (Payette and others 2004; Camill 2005) and future projections of circumpolar permafrost thaw (Euskirchen and others 2006; Delisle 2007; Lawrence and others 2008).

Permafrost governs soil drainage and vegetation composition in peatlands (Camill 1999; Yoshikawa and Hinzman 2003), and consequently influences rates of OC storage and release from soils (Turetsky and others 2007). Permafrost thaw in peatlands typically results in the subsidence of the ground surface (i.e. thermokarst) and increased saturation of surface peat. This post-thaw shift in local hydrology has been shown to drive increased rates of methane emissions (Turetsky and others 2002b; Christensen and others 2004; Wickland and others 2006) and soil OC accumulation (Robinson and Moore 1999, 2000) in thermokarst features relative to undisturbed soils. However, considerable uncertainty remains regarding the effects of permafrost thaw on soil carbon balance (Limpens and others 2008) and the magnitude of carbon cycle feedbacks to the climate system (Schuur and others 2008; McGuire and others 2009). For example, deep C stocks in peatlands may be more sensitive to warming than previously thought (Dorrepaal and others 2009), which suggests that permafrost thaw in peatlands may amplify atmospheric warming. Furthermore, the temperature sensitivity of decomposition in northern peatlands is tightly coupled to changes in peat thickness and water table (Ise and others 2008), which are also likely to change with future warming.

OC accumulation and storage is generally higher in bogs relative to other peatland types in permafrost regions (Robinson and Moore 1999; Tarnocai and others 2007; Hugelius and Kuhry 2009). Collapse-scar bogs are common thermokarst features in peatlands of Alaska and Canada (Thie 1974; Zoltai and Vitt 1990; Halsey and others 1995; Beilman and others 2001; Jorgenson and Osterkamp 2005), and have formed from the thawing of ice-rich, fine-grained mineral soils. These bogs are easily identifiable in peatland landscapes as circular depressions, expanding laterally over time at a rate of 0.1 to 0.5 m y^{-1} (Jorgenson and others 2001). Shifts in vegetation composition have been observed across collapse-scar successional ages (Camill 1999; Jorgenson and others 2001) as has the cyclic aggradation and degradation of permafrost (Zoltai 1993). OC accumulation in collapse-scar bogs is generally higher than in peat plateaus underlain by permafrost (Trumbore and Harden 1997; Robinson and Moore 2000; Myers-Smith and others 2008), due to post-thaw saturation of peat, increased nutrient availability and reduced organic matter decomposition. However, uncertainly exists regarding changes in OC storage and accumulation with time since thaw, given the complex interaction of vegetation, soil thermal and carbon dynamics in northern peatlands (Robinson and Moore 2000).

Here, we examine soil C accumulation and loss following permafrost thaw across a collapse-scar bog chronosequence in peatlands of interior Alaska. Chronosequence studies have effectively characterized decadal to millennial scale effects of fire and deglaciation on soil C dynamics in the boreal region (Harden and others 1992, 1997; Wang and others 2003; O'Neill and others 2003). Our primary objectives were to 1)

assess spatial and temporal variability of soil thermal active layer regimes across a collapse-scar bog chronosequence, and 2) compare soil moisture and water table conditions among sites, and 3) evaluate the effect of permafrost thaw and collapse-scar bog evolution on soil OC accumulation and loss. To our knowledge, no studies have used thaw chronosequences in northern peatlands to assess the effects of permafrost thaw on soil thermal, hydrologic, and carbon dynamics. This approach provides a natural gradient in permafrost degradation, vegetation composition, and soil OC storage. To address the first objective, we measured soil thermal dynamics (temperature, thaw depth, and surface topography) across a collapse-scar bog chronosequence and across lateral transects spanning a gradient of permafrost and soil drainage. To address the second objective, we made one time measurements of water surface elevations and continuously monitored soil moisture. To address the third objective, we compared OC storage among study sites and calculated rates of carbon accumulation and loss using chronosequence and radiocarbon methodologies. We discuss the implications of these findings with respect to future permafrost thaw and carbon cycle feedbacks from northern peatlands to the climate system.

Methods

Study area

We conducted our studies at Koyukuk National Wildlife Refuges (NWR), located in western Interior Alaska (Figure 1). Koyukuk NWR covers 3.5 million acres of wetlands on the abandoned floodplains and drained thaw lake basins adjacent to the

Koyukuk River, and spans from the southern foothills of the Brooks Range to its confluence with the Yukon River near Galena, AK. The Koyukuk Flats study area is located ~ 50 km north of Galena, and was accessed via floatplane. From 1971 through 2000, mean annual temperature in Galena averaged -3.8 °C, with annual maxima occurring in July (20.4 °C) and minima in January (-26.9 °C; Alaska Climate Research Center, http://climate.gi.alaska.edu/). During that same time period, annual precipitation averaged 331 mm, with 40% of the annual precipitation falling in July through September. Snow typically covers the ground between the months of October and April, with an average maximum accumulation of 50 cm.

Permafrost at the Koyukuk Flats study area is characterized by thick deposits of syngenetically frozen peat (Figure 2a), which were underlain by para-syngenetic permafrost, general consisting of ice-rich lacustrine sediments. The presence of inclined ice lenses in para-syngenetic permafrost is thought to reflect the presence of multiple freezing fronts (Figure 2b; French and Shur 2010). No massive ice wedges were observed at this study region, however ground ice content generally varied between 50 and 90% by volume. Permafrost degradation has been widespread in Koyukuk Flats study area, as evident in the abundant thaw lakes and collapse-scar bogs and fens. In this study we focused on collapse-scar bog features, which form following thaw of ice-rich silt, converting forested ecosystems to wetlands (Jorgenson and Osterkamp 2005).

We sampled collapse-scar bogs that varied with respect to time of permafrost thaw and bog initiation. The age of Young Bogs ranged from 31 to 61 y, as determined

by the difference in mean age of mature black spruce trees on Permafrost Plateau sites

(96 ± 13 y) and the age of dead black spruce trees found in collapse-scar bog features.

The age of Old Bogs ranged from 400 to 2824 y, as determined by radiocarbon (^{14}C)

dating of organic matter at the interface of forest-derived and collapse-scar bog-derived

peat (Table 1).

Vegetation composition varied with landscape position and collapse-scar bog age.

Permafrost plateaus were dominated by black spruce (*Picea mariana*) and *Sphagnum*

fuscum. We commonly observed the presence of *Andromeda polifolia*, *Ledum*

decumbens, and *Rubus chamaemorus*. Drying margins of collapse-scar bogs were

dominated by *Cladina* spp. (*C. stellaris*, *C. arbuscula*, *C. rangiferina*, *C. mitis*) and *L.*

decumbens. Young bogs were dominated by *Eriophorum scheuchzeri* and numerous

Sphagnum spp., including *S. jensenii*, *S. riparium*, *S. lindbergii*, and *S. balticum*. In the

old bogs, we primarily observed the mosses *S. balticum* and *S. flexuosum* and shrubs *A.*

polifolia and *Oxycoccus microcarpus*.

Sampling Design

To address our study objectives, we measured soil thermal and OC storage across

a permafrost thaw chronosequence. We measured soil temperature, soil moisture, water

table depth , and thaw depth at sites along the chronosequence to evaluate changes in

hydrologic and thermal conditions across lateral transects spanning collapse-scar bogs,

drying margins of permafrost plateaus, and the wet central portions of permafrost

plateaus. Soil OC and ^{14}C inventories were measured in permafrost plateaus and

collapse-scar bogs to evaluate the effect of permafrost thaw on soil carbon accumulation and loss.

Field sampling

To evaluate changes in local topography, permafrost and soil drainage, we established two linear transects at the Koyukuk Flats study area (522 and 200 m in length; Figure 1). Relative elevations of the ground and water surface were measured along each transect using an auto-level and rod. At selected points along the transects, we measured thaw depths where permafrost was present. In the absence of permafrost, we recorded the maximum observed depth of thawed soil. Along three collapse-scar bog margins, we made more intensive measurements of the permafrost table recording both probing angle and depth to demarcate talik boundaries.

We monitored soil temperature and soil moisture dynamics at the Koyukuk Flats study area to evaluate spatial variability in soil thermal conditions. From August 2008 to August 2009, we monitored soil temperatures every hour using HOBO Pro V2 two-channel dataloggers (Onset Computer Corporation, Pocasset, MA, USA). Temperature was monitored at the Permafrost Plateau (n=1), Drying Margins (n = 3), and at one Young Bog. Here, we report temperature data from the ground surface (~ 3 cm below moss surface) and deeper in the soil profile (20 to 45 cm below moss surface). Volumetric water content (VWC, %) of organic soil horizons was also logged every hour at the Koyukuk Flats study area using ECH_2O Smart Soil Moisture probes routed to a HOBO microstation (Onset Computer Corporation, Pocasset, MA, USA). At the

Permafrost Plateau and Drying Margin sites, we monitored soil moisture at 5 and 25 cm

below the moss surface. At the Young Bog site, we monitored soil moisture in the top 5-

10 cm below the moss surface (above the water table). We also made one-time water

table depth measurements at each site across the chronosequence.

Soil carbon and radiocarbon inventories

We described and sampled soil horizons across collapse-scar bog

chronosequences following USDA-NRCS (Staff, 1998) and Canadian (Committee, 1998)

methodologies. We sampled wet Permafrost Plateaus (n = 3), Drying Margins of

permafrost plateaus (n = 3), Young Bogs (n = 6), and Old Bogs (n = 3). Common terms

used for describing organic horizons included lichen, live moss (L), dead moss (D; more

moss than roots), fibric (F; slightly decomposed, often dominated by decaying mosses

and woody stems), mesic (M; moderately decomposed), and humic (H; highly

decomposed organics). Mineral soil horizons (A, B, C) were characterized for texture

and the presence of buried organic material. We also described and sampled limnic

sediments (La; organic-rich remnants of former lake basins). Frozen samples were

designated with a lowercase "f" preceding the primary horizon code.

We used a range of tools to sample different soil horizons for chemistry, bulk

density, and moisture content. At all sites, organic soil was sampled using a variety of

soil knives, scissors and corers to measure the volume of soil samples. For easily

compressed, low-density samples, soil blocks were cut with scissors or serrated knives

and dimensions were measured with a ruler. For less compressible shallow soils, samples

were obtained with a 35 mm diameter corer rotated with a portable electric drill. For

deeper unfrozen peats we used a 70 mm diameter by 130 cm long tube that was pushed

and rotated into the peat by hand. A rubber cap was tightened over the corer to maintain

a vacuum in the corer during extraction. At permafrost plateau sites, permafrost cores

(up to 5 m) were obtained using a SIPRE (Snow, Ice, and Permafrost Research

Establishment) corer (7.5 cm inside diameter) with a Tanaka power head. Soils typically

were sampled at 2-3 cm increments within the top 30 cm and at 20 cm increments below

30 cm, although sample increments were occasionally adjusted to avoid crossing

stratigraphic horizons. We sampled peat until either a basal mineral or limnic horizon was

encountered to allow calculation of C stocks relative to a standard basal layer across sites.

We analyzed all soil samples for total C and nitrogen (N) using a Carlo Erba NA1500

elemental analyzer. We assumed that total carbon was equal to organic carbon, given the

relatively low pH of soil samples (pH < 6). OC stocks were calculated by horizon type

by multiplying OC concentration (% by mass), bulk density (oven-dry), and horizon

thickness.

We analyzed ^{14}C content on a subset of soil samples to evaluate accumulation

rates and turnover times of organic carbon, to determine the age of Old Bog formation,

and to determine the basal age of peat across study sites. To determine carbon

accumulation rates in Permafrost Plateaus, we analyzed the ^{14}C content of 12 organic

matter samples spanning depths of two to 405 cm below the ground surface (Table 1).

To age collapse-scar bogs, we analyzed ^{14}C content of organic matter at the interface of

forest- and collapse-scar bog-derived peat. When field sampling permitted, we also

analyzed ^{14}C content of the lacustrine sediments (limnic, silt) beneath peat deposits.

Samples were sent to the W.M. Keck C Cycle AMS Laboratory at the University of

California Irvine for analysis as described in Southon *and others* (2004). Organic matter

was combusted at 900 °C in evacuated, sealed quartz tubes in the presence of cupric acid

(CuO) and silver (Ag) wire. Following cryogenic purification, carbon dioxide was

reduced to graphite in a reaction at 500-550 °C using the sealed tube Zn reduction

method (Xu *and others*, 2007). Radiocarbon data are reported as Δ^{14}C, or the per mil

deviation of the ^{14}C/^{12}C ratio in the sample from that of an oxalic standard that has been

decay corrected to 1950 (Stuiver and Polach, 1977). The Δ^{14}C values we report have

been corrected for mass-dependent fractionation using the *in situ* simultaneous AMS δ^{13}C

measurement.

Soil carbon accumulation and loss

　　　　To quantify rates of C accumulation at our study sites, we used both

chronosequence (e.g. Harden and others 1997) and radiocarbon approaches (e.g.

Trumbore and Harden 1997). For both methods, the net change in C storage (*dC/dt*) is

governed by constant annual C inputs (*I*; kg C m^{-2} y^{-1}), the fractional decomposition

constant (*k*; y^{-1}), and OC stocks in a given year (*C(t)*). The carbon balance for any given

year is reflected in the equation

$$dC/dt = I - kC(t) \qquad\qquad (1)$$

Assuming that initial C concentration is zero, solving this equation yields the following

equation:

$$C(t) = (I/k)*(1 - exp^{(-kt)}) \qquad\qquad (2)$$

For the chronosequence approach, we plotted cumulative C in bog peat (i.e. C in *Sphagnum*-derived peat above forested peat) versus bog age (t). Bog age was determined using either the radiocarbon age of organic matter at the bog-forest peat transition or by aging dead trees in the bog relative to mature trees on the adjacent permafrost plateau. The relationship between cumulative bog peat C and t was then fit with equation (2) to derive estimates of I and k post-thaw C accumulation.

To determine net rates of C accumulation prior to permafrost thaw, we used the radiocarbon approach at a permafrost plateau at Koyukuk Flats. For this profile, we calculated C accumulation rates in both shallow soil (i.e. active layer, 0-40 cm) and deep soil (i.e. permafrost, 40-481 cm). For each depth increment, we plotted cumulative C versus radiocarbon age and then fit equation (2) to the relationship to derive estimates of I and k.

We estimated C losses upon thaw and inundation by separately examining the near-surface bog peat and deeper forest peat. One important problem in using methods based on age dating and C accumulation dynamics is that the original C mass in deep forest peat layers is not explicitly known. To address this, we first calculated the initial forest peat C stocks (C_0; kg C m^{-2}) at the time of permafrost thaw using the following equation:

$$C_0 = C(t)-(I/k)*(1-e^{-kt}) \qquad (3)$$

where t is time since permafrost thaw and inundation (i.e. bog age), and I and k the same as for equations 1 and 2. To estimate the initial C stocks for forest peat in the Young Bogs, we derived the parameters I and k from the relationship between cumulative OC

stocks and radiocarbon age for active layer soils at the Permafrost Plateau site. This provides a model for C dynamics that is based on recent rates of C accumulation that are shallow and likely reflect a forested analog for shallow peat. For Old Bogs we derived the parameters I and k from the relationship between cumulative OC stocks and ^{14}C age for deeper permafrost soils at the Permafrost Plateau site, which in turn, provides a model for C dynamics of deep peat. Then, to estimate C loss rates of inundated forest peat for Young and Old Bogs, we calculated the difference between C_0 and present-day C ($C(t)$) stocks, divided by the mean age of Young and Old Bogs, respectively.

Statistical analysis

Water table depth was analyzed using a one-way analysis of variance (ANOVA) with site as the main effect. Soil OC stocks (kg C m^{-2}) were analyzed using a two-way ANOVA with site and peat type as main effects. OC density (g C cm^{-3}), total nitrogen (TN) density (g N cm^{-3}), and C:N ratio were analyzed using a one-way ANOVA with soil type as the main effect. Laboratory incubations were analyzed using a two-way ANOVA with percent of initial soil C respired (%) as the dependent variable, and site and depth as main effects. The two-way ANOVA models also included interactions between main effects. We used Tukey's honestly significant difference (HSD) test for *post hoc* comparisons of means. All statistical analyses were conducted using Statistica software (Statsoft, Inc., Tulsa, Oklahoma, USA). All data are reported as means ± standard error (SE).

Results

Soil temperature dynamics

Thaw depth and water table depth varied spatially across the study area with respect to local variability in relief and permafrost degradation (Figure 3). On Permafrost Plateaus, thaw depth was generally shallow, ranging from 30 to 70 cm. In collapse-scar bog sites (Young and Old Bogs), we generally did not observe the presence of permafrost in the top 3-4 m. However, we did contact permafrost at 251 cm in one Young Bog (YB 6 in Figure 1). We observed sharp boundaries between the presence of permafrost on the drying margins of permafrost plateaus and the absence of permafrost in bogs. By probing for permafrost at varying angles along collapse-scar margins, we were able to demarcate talik boundaries. We detected lateral thawing of permafrost at depths 3-4 m below the ground surface (Figure 4).

Mean annual temperature (MAT) at the ground surface was higher at a Young Bog feature (4.56 °C) than at the Drying Margin (2.27 °C) or the Permafrost Plateau (2.47 °C; Figure 5a). MAT at the base of the active layer (45 cm) of the Permafrost Plateau was 0.11 °C (Figure 5b), resulting in a thermal offset of -2.36 °C between ground surface and permafrost table. MAT at the base of the active layer of the Drying Margin (active layer depth = 44 cm) was -0.73 °C, resulting in a thermal offset of -3.00 °C. MAT at 20 cm in the Young Bog (Figure 5b) was higher than MAT at depth in both the Permafrost Plateau and the Drying Margin.

Soil water dynamics

Water table depth varied across the chronosequence study sites (ANOVA, $df = 3$, $F = 21.54$, $P < 0.0001$). Based on one-time measurements at replicate chronosequence sites, water table depth averaged 35 ± 8 and 51 ± 8 cm below the ground surface at the Drying Margin and Permafrost Plateau sites, respectively. Water table depth was significantly higher at the Young and Old Bogs than at the Permafrost Plateau and Drying Margin sites (Tukey HSD test, $P < 0.05$), collectively averaging 7 ± 1 cm below the ground surface.

On average, shallow VWC (at 5 cm below the moss surface) was lower at the Permafrost Plateau (summer mean = 7.75 ± 0.01 %) than the Drying Margin (summer mean = 22.50 ± 0.09 %) or the Young Bog (summer mean = 44.44 ± 0.23 %; Figure 6a). VWC also varied seasonally within each site. At the Permafrost Plateau, shallow VWC peaked around 45% in late April following snowmelt, and then quickly dropped to below 10% for the remainder of the summer. At the Young Bog, shallow VWC ranged from 45-48% from snowmelt through the summer. At the Drying Margin, shallow VWC peaked near 50% following snowmelt and then sharply decreased to between 20-30% for the rest of the summer. In January, we observed an increase in VWC to around 45%, likely due to melting of snowpack during a mid-winter warming period. On average, deep VWC (25 cm below the moss surface) was lower at the Drying Margin (summer mean = 13.44 ± 0.01%) than at the Permafrost Plateau (summer mean = 44.24 ± 0.23 %). Deep VWC peaked at the Drying Margin (~25%) shortly after snowmelt in late-April,

whereas deep VWC at the Permafrost Plateau (~49%) peaked much later in early June

(Figure 6b). At the permafrost plateau, deep VWC remained relatively high (35-50%)

throughout the summer, whereas deep organic VWC at the Drying Margin decreased as

summer progressed. Since the water table was typically about 10 cm below the moss

surface, we did not monitor deep VWC at the Young Bog.

Soil carbon and radiocarbon inventories

Soil OC stocks varied by a significant interaction (ANOVA; $df = 1$, F = 13.89, P

= 0.003) between site (Permafrost Plateau, Young Bog, Old Bog) and soil type (bog peat

vs forest peat; Figure 7). Soil OC in the forest peat layer of the Permafrost Plateau sites

averaged 136.6 ± 36.5 kg C m^{-2}, which was significantly greater than forest peat stocks at

the Old Bog sites (31.3 ± 4.4 kg C m^{-2}; Tukeys HSD test, P = 0.002) but not significantly

different from the Young Bog sites (111.0 ± 12.0 kg C m^{-2}; P = 0.76; Figure 8). At the

Young Bogs, soil OC stocks were significantly higher in the forest peat layer than in the

bog peat layer (P = 0.0006), whereas in the Old Bogs, we observed no significant

difference between OC stocks in bog and forest peat layers (P = 0.99).

OC density varied with soil type across the collapse-scar bog chronosequence

(ANOVA, $df = 6$, F = 11.563, P < 0.0001). OC density of collapse-scar bog peat was

significantly lower than forest peat from Permafrost Plateau sites (Tukey's HSD test; P =

0.003) and inundated forest peat (P < 0.001; Table 2). Across all soil types, collapse-scar

fen peat and limnic sediments had the highest OC density, averaging 0.072 ± 0.004 and

0.095 ± 0.019 g C cm^{-3}, respectively. Silt and collapse-scar bog peat had the lowest OC

density across soil types, averaging 0.022 ± 0.003 and 0.131 ± 0.001 g cm^{-3}, respectively.

Total nitrogen (TN) density also varied with respect to soil type ($df = 6$, F $= 36.605$, $P <$

0.0001). Across all soil types, TN density of collapse-scar bog peat was the lowest,

averaging 0.0003 ± 0.0000 g cm^{-3} (Table 2). We did not observe a significant difference

in TN density among Permafrost Plateau forest peat, Drying Margin forest peat, and

inundated forest peat ($P > 0.05$). C:N ratio also varied with respect to soil type ($df = 6$, F

$= 15.332$, $P < 0.0001$). Permafrost Plateau forest peat, Drying Margin forest peat, and

collapse-scar bog peat had significantly higher C:N ratios than collapse-scar fen peat,

limnic sediments and silt ($P < 0.05$; Table 2).

We observed positive Δ^{14}C values in surface peat at both a Permafrost Plateau site

and an Old Bog site, reflecting the fixation of bomb-spike ^{14}C-CO$_2$ via moss production

(Table 1). At both sites, Δ^{14}C peaked between 15 and 20 cm below the moss surface.

Δ^{14}C generally declined with depth at the permafrost plateau and at the old bog, reflecting

an increase in the age of organic matter with depth. The radiocarbon age of organic

matter at the Permafrost Plateau site was generally older than in the Old Bog, with the

oldest radiocarbon age (10,435 y BP) occurring around four meters. At the Old Bog, the

radiocarbon age of organic matter was greatest at 310 cm (2,985 y BP).

Soil carbon accumulation and loss

We observed a sharp decline in OC stocks in the inundated forest peat layers,

reflected by the exponential equation $C(t) = 36+97*e^{-0.0039t}$ ($R^2 = 0.77$, $P = 0.02$; Figure

8). Over the same time period, we observed the net accumulation of OC in the surface

bog peat layer (Figure 8). Using equation 2, we estimated OC inputs (I) to the surface

bog peat layer as 82.4 ± 0.9 g C m^{-2} y^{-1}, a decomposition constant (k) as 0.0022 ± 0.0004

y^{-1} (turnover time = 455 y) and a recent OC accumulation rate of 12.4 g C m^{-2} y^{-1} (Table

3). For active layer soil at the Permafrost Plateau, we calculated an I of 107.6 ± 7.8 g C

m^{-2} y^{-1} and a k of 0.0216 ± 0.0083 y^{-1} (Table 3). For the entire soil profile at the

Permafrost Plateau (including active layer and permafrost), we calculated an average I of

23.3 ± 13.1 g C m^{-2} y^{-1} and k of 0.0001 ± 0.0001 y^{-1} (Table 3). Using these parameters

and equation 1, we calculated recent (shallow) and long-term (deep) OC accumulation

rates at the Permafrost Plateau as 12.4 and 3.0 g C m^{-2} y^{-1}, respectively (Table 3). Recent

OC accumulation rate in the collapse-scar bog (66.1 g C m^{-2} y^{-1}) was more than five

times greater than in the Permafrost Plateau, but this increased accumulation at the

surface was offset by the decomposition of deep inundated forest peat. The percentage of

initial forest OC loss declined with time since permafrost thaw (Figure 9a). Given an

average Young Bog age of 47 y, we estimate an OC loss rate from inundated forest peat

layers of 368 g C m^{-2} y^{-1} for young bogs (Figure 9b). Given an average Old Bog age of

1480 y, we estimate an OC loss rate from inundated forest peat layers of 31 g C m^{-2} y^{-1}.

Discussion

Spatial variability of hydrologic and soil thermal dynamics

Collapse-scar bogs at Koyukuk Flats NWR formed in response to thawing of ice-

rich peat deposits and subsequent subsidence of the ground surface. The formation of

these collapse-scar bogs appears to initiate a series of positive feedbacks that accelerate

rates of permafrost thaw (Jorgenson and others 2010). Following ground subsidence, soil water drained laterally from the margins of permafrost plateaus into collapse-scar bogs, where it was impounded. We observed lateral differences in soil temperature between collapse-scar bogs and adjacent permafrost plateaus, a result of water redistribution. One consequence of this spatial difference in soil temperature was the formation of *taliks*, or layers of unfrozen ground that persist year-round, which develop vertically and laterally beneath collapse-scar bog features. Persistent talik development at depth results in further collapse and ground subsidence, and thus lateral expansion of the collapse-scar bog. The spatial variability of near-surface ground temperatures in this study are consistent with the findings of Jorgenson and others (2001), who observed warmer ground temperatures (at 3 m) in collapse-scar bogs and fens than in adjacent lowland black spruce stands. The presence of shallow water bodies can have a profound influence on the ground thermal regime of permafrost regions, as reported in studies of lakes in arctic tundra (Lachenbruch and others 1962; Burn 2005; West and Plug 2008; Jorgenson and others 2010). However, few studies have characterized the effect of soil water on the ground thermal conditions in subarctic peatlands where permafrost is actively degrading (Jorgenson and others 2001).

Our findings document how permafrost thaw results not only in the wetting of surface peat in collapse-scar bogs but also in the drying of soils on permafrost plateaus. Permafrost thaw and lateral redistribution of soil water also created a drying zone along the margins of permafrost plateaus, evident in the reduced soil moisture content at depth relative to the wet central portions of the permafrost plateaus (Figure 6b) and in the

colonization of lichens (*Cladina spp*) on top of *Sphagnum fuscum* along drying margins.

Viewed from a vertical or one-dimensional perspective, it would appear that the

permafrost beneath drying margins is relatively stable, given the large thermal offset

between the permafrost table and the ground surface (Figure 5) and the shallow thaw

depths. However, from a two-dimensional perspective, it becomes clear that permafrost

along the drying margins of permafrost plateaus is vulnerable to thaw from lateral

degradation, as discussed above. Thermal models have begun to address issues of talik

development and freeze-up in association with thaw lake cycles in arctic regions (Ling

and Zhang 2003, 2004; West and Plug 2008). Findings from this study highlight the

need for thermal models that address this two- and three-dimensional complexity of

permafrost degradation in northern peatlands as well.

Effects of permafrost thaw on soil C dynamics in an Alaskan peatland

Permafrost plateaus at the Koyukuk Flats have accumulated large amounts of OC

in thick peat deposits over the past 10,000 years, with OC stocks averaging 136.6 ± 36.5

kg C m^{-2}. These measurements are consistent with other reports of OC storage in frozen

peat deposits of the subarctic (Tarnocai and others 2007), suggesting that permafrost

plateaus are important sinks for atmospheric CO_2 across the North American boreal

region. OC stabilization in soils of permafrost plateaus was likely facilitated by the

vertical aggradation of permafrost that coincided with the vertical accumulation of peat

deposits. This process, referred to as syngenetic permafrost aggradation, was reflected in

the lenticular cryostructures observed in frozen peat deposits. As a result, soil OC at the

base of the active layer was continually incorporated into the permafrost pool, where organic matter decomposition likely ceased due to sub-zero temperatures and minimal unfrozen water content (Rivkina and others 2000; Romanovsky and Osterkamp 2000). Rates of recent OC accumulation are consistent with prior studies at permafrost landforms in boreal peatlands (Robinson and Moore 1999, 2000; Turetsky and others 2007; Myers-Smith and others 2008).

Following permafrost thaw and collapse-scar bog formation, shallow and deep peat horizons begin to operate separately, with the accumulation of OC occurring in near-surface peat layers and loss of OC from deep peat layers. Recent OC accumulation rates in near-surface peat layers of collapse-scar bogs were more than five times greater than recent accumulation rates at the Permafrost Plateau, a pattern observed in previous studies (Robinson and Moore 1999; Turetsky and others 2007; Myers-Smith and others 2008). Our findings suggest that this pattern was likely due to a decrease in organic matter decomposition rate, as reflected in the lower k value in the collapse-scar bog relative to the Permafrost Plateau (Table 3), and not due to changes in moss net primary production (or I). The rapid decline of OC stocks in deep peat layers following permafrost thaw was presumably in response to increased decomposition driven by recently thawed peat deposits. We calculated a long-term loss rate of 31 g C m^{-2} y^{-1} from deep forest peat layers, which is comparable to CH$_4$ loss rates from Siberian thaw lakes (25 g CH$_4$ m^{-2} y^{-1}; Walter and others 2006) and old OC loss from thermokarst features at an Alaskan alpine tundra site (22-63 g C m^{-2} y^{-1}; Schuur and others 2009). Over time,

however, decomposition of the remaining recalcitrant OC slows, with about one-half of the total forest-derived OC persisting over long periods.

The divergence in OC trajectories between shallow and deep peat layers is likely due to the differences in origin and decomposability of organic matter between layers. In shallow layers, "bog peat" (*S. riparium, S. balticum*, etc.) accumulates in response to the impoundment of water in collapse-scar bog features. OC accumulation in the bog peat layer is likely enhanced following the transfer of undecomposed organic matter from the acrotelm (peat above water table) to the catotelm (peat below water table; Clymo 1984). In general, decomposition rates in the catotelm decline with the age and depth of organic matter as a result of the decay that has already occurred (Clymo and others 1998; Frolking and others 2001). However, the deep peat layers in these collapse-scar bogs originate from "forest peat" (*S. fuscum*), which had likely undergone minimal decay prior to incorporation into the permafrost pool (Hugelius and Kuhry 2009; Sannel and Kuhry 2009). As forest peat stocks thawed and became saturated in collapse-scar bogs, decomposition of this relatively old, yet unprocessed organic matter was able to proceed, driving OC loss from deep peat layers.

Vulnerability of soil C in frozen peat deposits

Previous studies have suggested that soil OC in northern peatlands is highly vulnerable to climate warming (Tarnocai 2006; Dorrepaal and others 2009; Kuhry and others 2010), given the large size of this pool and its potential release to the atmosphere (Gruber and others 2004). Our findings support these studies, indicating that soil OC stored in permafrost plateaus is highly vulnerable to thaw, decomposition, and

subsequent release to the atmosphere. This is due, in part, to the high vulnerability of peatland permafrost to the presence of surface water in collapse-scar bog features (Jorgenson and others 2010). Upon thaw and inundation, forest peat was rapidly degraded, with 65% of the initial OC stocks remaining after 100 years and 43% remaining after 1000 years. Over the 3000 year collapse-scar bog chronosequence, surface OC accumulation in bog peat layers was insufficient to balance deep OC losses from forest peat layers, resulting in a net OC loss of 26 g C m^{-2} y^{-1} from collapse-scar bogs to the atmosphere. Given the large pool size of OC in frozen peat deposits in North America alone (Tarnocai and others 2007), soil OC release from thawed peat deposits may function as a strong positive feedback to atmospheric warming. Much of this soil OC will be released to the atmosphere as CH_4, given published gas flux measurements from collapse-scar bogs in the boreal region (Prater and others 2007; Myers-Smith and others 2007).

Uncertainty still exists regarding the magnitude of carbon-cycle-feedbacks from northern peatlands to the atmosphere. For instance, lateral degradation of permafrost in peatlands has not been explicitly considered in land-surface models, perhaps due to the complexity of modeling non-conductive heat transfer processes (Kane and others 2001). Given the apparent vulnerability of soil OC stocks in peatland permafrost landforms, future research should focus on the controls that govern permafrost degradation in northern peatlands and the spatial extent of these processes. Furthermore, while peatlands have historically functioned as carbon sinks, recent evidence suggests that the net C accumulation has slowed due to warming and disturbance (Turetsky and others

2002a; Canadell and others 2007). Based on our findings, thawing of perennially frozen peat deposits in northern peatlands may contribute to this reduction in C sink strength.

Acknowledgements

References

Apps MJ, Kurz WA, Luxmoore RJ, Nilsson LO, Sedjo RA, Schmidt R, Simpson LG, Vinson TS. 1993. Boreal forests and tundra. Water, Air and Soil Pollution 70: 39-53.

Beilman DW, Vitt DH, and Halsey LA. 2001. Localized permafrost peatlands in western Canada: definitions, distribution, and degradation. Arctic, Antarctic, and Alpine Research 33: 70-77.

Blodau C. 2002. Carbon cycling in peatlands – A review of processes and controls. Environmental Reviews 10: 111-134.

Burn CR. 2005. Lake-bottom thermal regimes, western Arctic coast, Canada. Permafrost and Periglacial Processes 16: 355-367.

Camill P. 1999. Patterns of boreal permafrost peatland vegetation across environmental gradients sensitive to climate warming. Candian Journal of Botany 77: 721-733.

Camill P. 2005. Permafrost thaw accelerates in boreal peatlands during late-20th century climate warming. Climatic Change 68: 135-152.

Canadell J, Pataki D, Gifford R, Houghton R, Luo Y, Raupach M, Smith P, Steffen W. 2007. Saturation of the terrestrial carbon sink. Canadell JG, Pataki DE, Pitelka LF, editors. Terrestrial Ecosystems in a Changing World. Berlin: Springer. p59-78.

Christensen TR, Johansson T, Akerman HJ, Mastepanov M, Malmer N, Friborg T, Crill P, Svensson BH. 2004. Thawing of sub-arctic permafrost: effects on vegetation and methane emissions. Geophysical Research Letters 31: doi:10.1029/2003GL018680.

Clymo RS. 1984. The limits to peat bog growth. Philosophical Transactions of the Royal Society of London, Series B 303: 605-654.

Clymo RS, Turunen J, Tolonen K. 1998. Carbon accumulation in peatlands. Oikos 81: 368-388.

Committee CASC. 1998. The Canadian System of Soil Classification. Ontario: NRC

Canada Research Press.

Delisle G. 2007. Near-surface permafrost degradation: How severe during the 21st

century? Geophysical Research Letters 34: doi:10.1029/2007GL029323.

Dise NB. 2009. Peatland response to global change. Science 326: 810-811.

Dorrepaal E, Toet S, van Logtestijn RSP, Swart E, van de Weg MJ, Callahan TV, Aerts

R. 2009. Carbon respiration from subsurface peat accelerated by climate warming

in the subarctic. Nature 460: doi:10.1038/nature08216.

Euskirchen ES, McGuire AD, Kicklighter DW, Zhuang Q, Clein JS, Dargaville RJ, Dye

DG, Kimball JS, McDonald KC, Melillo JM, Romanovsky VE, Smith NV. 2006.

Importance of recent shifts in soil thermal dynamics on growing season length,

productivity and carbon sequestration in terrestrial high-latitude ecosystems.

Global Change Biology 12: 731-750.

French H, Shur Y. 2010. The principles of cryostratigraphy. Earth-Science Reviews 101:

190-206.

Frolking S, Roulet NT, Moore TR, Richard PJH, Lavoie M, Muller SD. 2001. Modeling

northern peatland decomposition and peat accumulation. Ecosystems 4: 479-498.

Frolking S, Roulet NT. 2007. Holocene radiative forcing impact of northern peatland

carbon accumulation and methane emissions. Global Change Biology 13: 1079-

1088.

Gorham E. 1991. Northern peatlands: role in the carbon cycle and probable responses to climatic warming. Ecological Applications 1: 182-195.

Gruber N, Friedlingstein P, Field CB, Valentini R, Heimann M, Richey JE, Lankao PR, Schulze E-D, Chen CTA. 2004. The vulnerability of the carbon cycle in the 21st century: an assessment of carbon-climate-human interactions. Field CB, Raupach MR, MacKenzie SH, editors. The Global Carbon Cycle: Integrating Humans, Climate, and the Natural World. Washington, DC: Island Press. p45-76.

Halsey LA, Vitt DH, Zoltai SC. 1995. Disequilibrium response of permafrost in boreal continental western Canada to climate change. Climatic Change 30: 57-73.

Harden JW, Sundquist ET, Stallard RF, Mark RK. 1992. Dynamics of soil carbon deglaciation of the Laurentide Ice Sheet. Science 258: 1921-1924.

Harden JW, O'Neill KP, Trumbore SE, Veldhuis H, Stocks BJ. 1997. Moss and soil contributions to annual net carbon flux of a maturing boreal forest. Journal of Geophysical Research 102: 28805-28816.

Hugelius G, Kuhry P. 2009. Landscape partitioning and environmental gradient analysis of soil organic carbon in a permafrost environment. Global Biogeochemical Cycles 23: GB3006, doi:10.1029/2008GB003419.

Ise T, Dunn AL, Wofsy SC, Moorcroft PR. 2008. High sensitivity of peat decomposition to climate change through water-table feedback. Nature Geoscience 1: 763-766.

Jorgenson MT, Racine CH, Walters JC, Osterkamp TE. 2001. Permafrost degradation and ecological changes associated with a warming climate in Central Alaska. Climatic Change 48: 551-579.

Jorgenson MT, Osterkamp TE. 2005. Response of boreal ecosystems to varying modes of permafrost degradation. Canadian Journal of Forest Research 35: 2100-2111.

Jorgenson MT, Romanovsky V, Harden J, Shur Y, O'Donnell J, Schuur EAG, Kanevskiy M, Marchenko S. 2010. Resilience and vulnerability of permafrost to climate change. Canadian Journal of Forest Research 40: 1219-1236.

Kane DL, Hinkel KM, Goering DJ, Hinzman LD, Outcalt SI. 2001. Non-conductive heat transfer associated with frozen soils. Global and Planetary Change 29: 275-292.

Kuhry P, Vitt DH. 1996. Fossil carbon/nitrogen ratios as a measure of peat decomposition. Ecology 77: 271-275.

Kuhry P, Dorrepaal E, Hugelius G, Schuur EAG, Tarnocai C. 2010. Potential remobilization of belowground permafrost carbon under future global warming. Permafrost and Periglacial Processes 21: 208-214.

Lachenbruch AH, Brewer MC, Greene GW, Marshall BV. 1962. Temperatures in permafrost. Herzfeld CM, editor. Temperature: Its measurement and control in science and industry, Vol 3, Part 1. New York: Reinhold, p791-803.

Lawrence DM, Slater AG, Romanovsky VE, Nicolsky DJ. 2008. Sensitivity of a model projection of near-surface permafrost degradation to soil column depth and representation of soil organic matter. Journal of Geophysical Research 113: F02011, doi:10.1029/2007JF000883.

Limpens J, Berendse F, Blodau C, Canadell JG, Freeman C, Holden J, Roulet N, Rydin H, Schaepman-Strub G. 2008. Peatlands and the carbon cycle: from local processes to global implications – a synthesis. Biogeosciences 5: 1475-1491.

Ling F, Zhang T. 2003. Numerical simulation of permafrost thermal regime and talik development under shallow lakes on the Alaskan Arctic Coastal Plain. Journal of Geophysical Research 108: doi:10.1029/2002JD003014.

Ling F, Zhang T. 2004. Modeling study of talik freeze-up and permafrost response under drained thaw lakes on the Alaskan Arctic Coastal Plain. Journal of Geophysical Research 109: doi:10/1029/2003JD003886.

McGuire AD, Anderson LG, Christensen TR, Dallimore S, Guo L, Hayes DJ, Heimann M, Lorenson TD, Macdonald RW, Roulet N. 2009. Sensitivity of the carbon cycle in the Arctic to climate change. Ecological Monographs 79: 523-555.

McGuire AD, Hayes DJ, Kicklighter DW, Manizza M, Zhuang Q, Chen M, Follows MJ, Gurney KR, McClelland JW, Melillo JM, Peterson BJ, Prinn R. 2010. An analysis of the carbon balance of the Arctic Basin from 1997 to 2006. Tellus 62B: 455-474.

Myers-Smith IH, McGuire AD, Harden JW, Chapin FS III. 2007. Influence of

   disturbance on carbon exchange in a permafrost collapse and adjacent burned

   forest. Journal of Geophysical Research 112: doi:10.1029/2007JG000423.

Myers-Smith IH, Harden JW, Wilmking M, Fuller CC, McGuire AD, Chapin FS III.

   2008. Wetland succession in a permafrost collapse: interactions between fire and

   thermokarst. Biogeosciences 5: 1273-1286.

O'Neill KP, Kasischke ES, Richter DD. 2003. Seasonal and decadal patterns of soil

   carbon uptake and emission along an age sequence of burned black spruce stands

   in interior Alaska. Journal of Geophysical Research 108:

   doi:10.1029/2001JD000443.

Payette S, Delwaide A, Caccianiga M, Beauchemin M. 2004. Accelerated thawing of

   subarctic peatland permafrost over the last 50 years. Geophysical Research

   Letters 31: doi:10.1029/2004GL020358.

Prater JL, Chanton JP, Whiting GJ. 2007. Variation in methane production pathways

   associated with permafrost decomposition in collapse-scar bogs of Alberta,

   Canada. Global Biogeochemical Cycles 21: doi:10.1029/2006GB002866.

Rivkina E, Friedmann E, McKay C, Gilichinsky D. 2000. Metabolic activity of

   permafrost bacteria below the freezing point. Applied and Environmental

   Microbiology 66: 3230-3233.

Robinson SD, Moore TR. 1999. Carbon and peat accumulation over the past 1200 years in a landscape with discontinuous permafrost, northwest Canada. Global Biogeochemical Cycles 13: 591-601.

Robinson SD, Moore TR. 2000. The influence of permafrost and fire upon carbon accumulation in high boreal peatlands, Northwest Territories, Canada. Arctic, Antarctic, and Alpine Research 32: 155-166.

Romanovsky VE, Osterkamp TE. 2000. Effects of unfrozen water on heat and mass transport processes in the active layer and permafrost. Permafrost and Periglacial Processes 11: 219-239.

Sannel ABK, Kuhry P. 2009. Holocene peat growth and decay dynamics in sub-arctic peat plateaus, west-central Canada. Boreas: doi:10.1111/j.1502-3885.2008.00048.x.

Schuur EAG, Bockheim J, Canadell JG, Euskirchen E, Field CB, Goryachkin SV, Hagemann S, Kuhry P, Lafleur PM, Lee H, Mazhitova G, Nelson FE, Rinke A, Romanovsky VE, Shiklomanov N, Tarnocai C, Venevsky S, Vogel JG, Zimov SA. 2008. Vulnerability of permafrost carbon to climate change: implications for the global carbon cycle. Bioscience 58: 701-714.

Schuur EAG, Vogel JG, Crummer KG, Lee H, Sickman JO, Osterkamp TE. 2009. The effect of permafrost thaw on old carbon release and net carbon exchange from tundra. Nature 459, doi:10.1038/nature08031.

Shur YL, Kanevskiy M, White DM, Connor B. 2010. Geotechnical investigations for the Dalton Highway Innovation Project as a case study of the ice-rich syngenetic permafrost. AUTC assigned project # 207122.

Smith LC, MacDonald GM, Velichko AA, Beilman DW, Borisova OK, Frey KE, Kremenetski KV, Sheng Y. 2004. Siberian peatlands: a net carbon sink and global methane source since the early Holocene. Science 303: doi:10.1126/science.1090553.

Southon J, Santos G, Druffel-Rodriguez K, Druffel E, Trumbore S, Xu X, Griffin S, Ali S, Mazon M. 2004. The Keck Carbon Cycle AMS laboratory, University of California Irvine: initial operation and background surprise. Radiocarbon 46: 41-49.

Staff SS. 1998. Keys to soil taxonomy. Blacksburg (VA): Pocahontas Press, Inc. 599p.

Stuiver M, Polach HA. 1977. Discussion: reporting of ^{14}C data. Radiocarbon 19: 355-363.

Tarnocai C. 2006. The effect of climate change on carbon in Canadian peatlands. Global and Planetary Change 53: 222-232.

Tarnocai, C., Ping C-L, Kimble J. 2007. Carbon Cycles in the Permafrost Region of

North America. King AW, Dilling L, Zimmerman GP, Fairman DM, Houghton

RA, Marland G, Rose AZ, Wilbanks TJ, editors. The First State of the Carbon

Cycle Report (SOCCR): The North American Carbon Budget and Implications

for the Global Carbon Cycle. A Report by the U.S. Climate Change Science

Program and the Subcommittee on Global Change Research. Asheville (NC):

National Oceanic and Atmospheric Administration, National Climatic Data

Center. p. 127-138.

Tarnocai C, Canadell JG, Schuur EAG, Kuhry P, Mazhitova G, Zimov S. 2009. Soil

organic carbon pools in the northern circumpolar permafrost region. Global

Biogeochemical Cycles 23: doi:1029/2008GB003327.

Thie J. 1974. Distribution of thawing permafrost in the southern part of the discontinuous

permafrost zone in Manitoba. Arctic 27: 189-200.

Trumbore SE, Harden JW. 1997. Accumulation and turnover of carbon in organic and

mineral soils of the BOREAS northern study area. Journal of Geophysical

Research 102: 28817-28830.

Turetsky M, Wieder K, Halsey L, Vitt D. 2002a. Current disturbance and the diminishing

peatland carbon sink. Geophysical Research Letters 29:

doi:10.1029/2001GL014000.

Turetsky MR, Wieder RK, Vitt DH. 2002b. Boreal peatland C fluxes under varying permafrost regimes. Soil Biology and Biochemistry 34: 907-912.

Turetsky MR, Wieder RK, Vitt DH, Evans RJ, Scott KD. 2007. The disappearance of relict permafrost in boreal North America: effects of peatland carbon storage and fluxes. Global Change Biology 13: 1922-1934.

Xu X, Trumbore SE, Zheng S, Southon JR, McDuffee KE, Luttgen M, Liu JC. 2007. Modifying a sealed tube zinc reduction method for preparation of AMS graphite targets: Reducing background and attaining high precision. Nuclear Instruments and Methods in Physics Research B 259: 320-329.

Walter KM, Zimov SA, Chanton JP, Verbyla D, Chapin FS III. 2006. Methane bubbling from Siberian thaw lakes as a positive feedback to climate warming. Nature 443: doi:10.1038/nature05040.

Wang C, Bond-Lamberty B, Gower ST. 2003. Carbon distribution of a well- and poorly-drained black spruce chronosequence. Global Change Biology 9: 1066-1079.

West JJ, Plug LJ. 2008. Time-dependent morphology of thaw lakes and taliks in deep and shallow ground ice. Journal of Geophysical Research 113: doi:10.1029/2006JF000696.

Wickland KP, Striegl RG, Neff JC, Sachs T. 2006. Effects of permafrost melting on CO_2 and CH_4 exchange of a poorly drained black spruce lowland. Journal of Geophysical Research 111: doi:10.1029/2005JG000099.

Yoshikawa K, Hinzman LD. 2003. Shrinking thermokarst ponds and groundwater
dynamics in discontinuous permafrost near Council, Alaska. Permafrost and
Periglacial Processes 14: 151-160.

Zoltai SC, Vitt DH. 1990. Holocene climatic change and the distribution of peatlands in
western interior Canada. Quaternary Research 33: 231-240.

Zoltai SC. 1993. Cyclic development of permafrost in the peatlands of Northwestern
Alberta, Canada. Arctic and Alpine Research 25: 240-246.

TABLES

Table 1. Summary of radiocarbon data for soil organic matter at permafrost plateau and old bog sites.

Basal Depth (cm)	Field Horizon Code	Sample Description	$\delta^{13}C$ (‰)	Fraction Modern	$\Delta^{14}C$ (‰)	^{14}C age (y BP)
Permafrost Plateau 1						
185	fA	organic-rich silt with small inclusions of charred plant material	-26.1 ± 0.2	0.3773 ± 0.0007	-625.4 ± 0.7	7830 ± 20
Permafrost Plateau 2						
2	L	live *Sphagnum fuscum*	-27.8 ± 0.2	1.0683 ± 0.0017	60.7 ± 1.7	modern
6	D	dead *Sphagnum* leaves and stems	-27.7 ± 0.2	1.1313 ± 0.0018	123.3 ± 1.8	modern
10	D	dead *Sphagnum* leaves and stems	-27.2 ± 0.2	1.2564 ± 0.0020	247.5 ± 2.0	modern
15	D	dead *Sphagnum* leaves and stems	-27.3 ± 0.2	1.3329 ± 0.0022	323.4 ± 2.2	modern
25	D	dead *Sphagnum* leaves and stems	-26.1 ± 0.2	1.2359 ± 0.0020	227.1 ± 2.0	modern

Table 1 (continued) Summary of radiocarbon data for soil organic matter at permafrost plateau and old bog sites.

31	F	dead *Sphagnum* leaves and stems	-25.7 ± 0.2	0.9849 ± 0.0018	-22.1 ± 1.8	120 ± 15
50	fD	*Chamaedaphne calyculata* leaves, few Sphagnum	-27.8 ± 0.2	0.9828 ± 0.0016	-24.1 ± 1.6	140 ± 15
101	fM	decomposed *Sphagnum* leaves and stems	-26.1 ± 0.2	0.8945 ± 0.0015	-111.9 ± 1.5	895 ± 15
210	fM	decomposed *Sphagnum* leaves and stems	-26.9 ± 0.2	0.5906 ± 0.0010	-413.6 ± 1.0	4230 15
313	fM	sedge roots, *Calliergon* spp. Moss	-27.5 ± 0.2	0.2972 ± 0.0007	-704.9 ± 0.7	9745 ± 20
369	fM	detrital peat fragments	-27.2 ± 0.2	0.4132 ± 0.0008	-589.8 ± 0.8	7100 ± 15
405	fM	fen peat, sedge leaves; Scorpidum scorpioides leaves and stems	-28.4 0.2	0.2728 ± 0.0006	-729.2 ± 0.6	10435 ± 20
Permafrost Plateau 3						
143	fM	dark brown frozen peat	-23.8 ± 0.2	0.4559 ± 0.0008	-547.3 ± 0.8	6310 ± 15
Old Bog 1						
2	L	live *Sphagnum* spp.	-24.6 ± 0.2	1.0707 ± 0.0018	63.1 ± 1.8	Modern
6	L	live *Sphagnum* spp.	-25.4 ± 0.2	1.0709 ± 0.0017	63.3 ± 1.7	Modern

Table 1 (continued) Summary of radiocarbon data for soil organic matter at permafrost plateau and old bog sites.

10	D	dead *Sphagnum* leaves and stems	-24.3 ± 0.2	1.0889 ± 0.0018	81.2 ± 1.8	modern
16	D	dead *Sphagnum* leaves and stems	-23.7 ± 0.2	1.1306 ± 0.0018	122.6 ± 1.8	modern
20	D	dead *Sphagnum* leaves and stems	-24.1 ± 0.2	1.1814 ± 0.0022	173.0 ± 2.2	modern
36	D	dead *Sphagnum* leaves and stems	-25.4 ± 0.2	0.9794 ± 0.0017	-27.6 ± 1.7	165 ± 15
52	D	slightly decomposed *Sphagnum* stems	-25.6 ± 0.2	0.9610 ± 0.0015	-45.9 ± 1.5	320 ± 15
100	D	Sphagnum stems, *Chamaedaphne calyculata* leaves	-22.9 ± 0.2	0.9637 ± 0.0018	-43.2 ± 1.8	295 ± 20
147	D	Sphagnum stems, *Chamaedaphne calyculata* leaves	-24.9 ± 0.2	0.9637 ± 0.0015	-43.1 ± 1.5	295 ± 15
200	D	Sphagnum stems, *Carex limosa*	-23.2 ± 0.2	0.8925 ± 0.0016	-113.8 ± 1.6	915 ± 15
290	F	Sphagnum stems, *Chamaedaphne calyculata* leaves; tiny sedge or woody stems	-24.8 ± 0.2	0.8596 ± 0.0014	-146.5 ± 1.4	1215 ± 15
310	M	Sphagnum fuscum; *Picea mariana* wood fragment, charcoal	-25.5 ± 0.2	0.6897 ± 0.0011	-315.2 ± 1.1	2985 ± 15

Table 1 (continued) Summary of radiocarbon data for soil organic matter at permafrost plateau and old bog sites.

Old Bog 2

60	M	Sphagnum and *Carex limosa* parts	-26.1 ± 0.2	0.9843 ± 0.0016	-22.7 ± 1.6	125 ± 15
140	M	Sphagnum stems and leaves	-24.7 ± 0.2	0.9535 ± 0.0015	-53.3 ± 1.5	385 ± 15
292	La	limnic sediments with sedge leaf fragments	-23.8 ± 0.2	0.6880 ± 0.0014	-316.9 ± 1.4	3005 ± 20

Old Bog 3

95	M	Sphagnum and *Caliergon* spp. and *Menyanthes trifoliata* parts	-24.9 ± 0.2	0.9517 ± 0.0018	-55.1 ± 1.8	400 ± 20
189	M	sedge leaves, woody plant fragments	-25.7 ± 0.2	0.7101 ± 0.0014	-295.0 ± 1.4	2750 ± 20
280	M	sedge leaves, woody plant fragments	-28.6 ± 0.2	0.3934 ± 0.0009	-609.4 ± 0.9	7495 ± 20

Table 2. Summary of organic matter chemistry across different soil types.

Site and Soil Type	n	OC Density gC cm^{-3}	TN Density gC cm^{-3}	C:N
Permafrost Plateau - Forest Peat	89	0.0381 ± 0.0026^a	0.0011 ± 0.0001^{ab}	61 ± 4^a
Drying Margin - Forest Peat	30	0.0700 ± 0.0272^b	0.0010 ± 0.0002^{ab}	69 ± 6^a
Collapse-Scar Bog Peat	113	0.0131 ± 0.0009^c	0.0003 ± 0.0000^c	59 ± 2^a
Collapse-Scar Fen Peat	7	0.0724 ± 0.0038^{ab}	0.0038 ± 0.0001^d	21 ± 3^b
Inundated Forest Peat	115	0.0351 ± 0.0020^a	0.0008 ± 0.0001^b	58 ± 2^{ab}
Limnic Sediments	12	0.0954 ± 0.0192^b	0.0036 ± 0.0009^d	37 ± 7^b
Silt	19	0.0218 ± 0.0026^{ac}	0.0017 ± 0.0002^a	12 ± 0^b

Note: Different letters denote statistically significant differences between means, as determined by Tukey's HSD test.

Table 3. Summary of soil C inputs, decomposition constants, and net accumulation rates at Koyukuk Flats.

Site Description	Horizon Description	C	I	k	dC/dt
		kg C m^{-2}	g C m^{-2} yr^{-1}	(yr^{-1})	g C m^{-2} yr^{-1}
Recent accumulation (last 100 years)					
Permafrost Plateau	Active Layer	4.41	107.6 ± 7.8	0.0216 ± 0.0083	12.4
Collapse-Scar Bog	Near-surface bog peat[a]	7.39	82.4 ± 0.9	0.0022 ± 0.0004	66.1
Holocene accumulation in frozen peat					
Permafrost Plateau	Frozen Peat	203.5	23.3 ± 13.1	0.0001 ± 0.0001	3.0
Post-thaw accumulation and loss					
Collapse-Scar Bog	Surface Bog Peat[a]	35.31	82.4 ± 0.9	0.0022 ± 0.0004	4.7
Collapse-Scar Bog	Inundated Forest Peat[b]	105.51	n.d.	n.d	-31.2

[a]From Figure 8

[b]From Figure 9

Figures

Figure 1. Map of Koyukuk Flats study region. Open circles represent the Permafrost Plateau (PP), Young Bog (YB) and Old Bog (OB) study sites. The map insert shows the location of Koyukuk Flats National Wildlife Refuge in the state of Alaska.
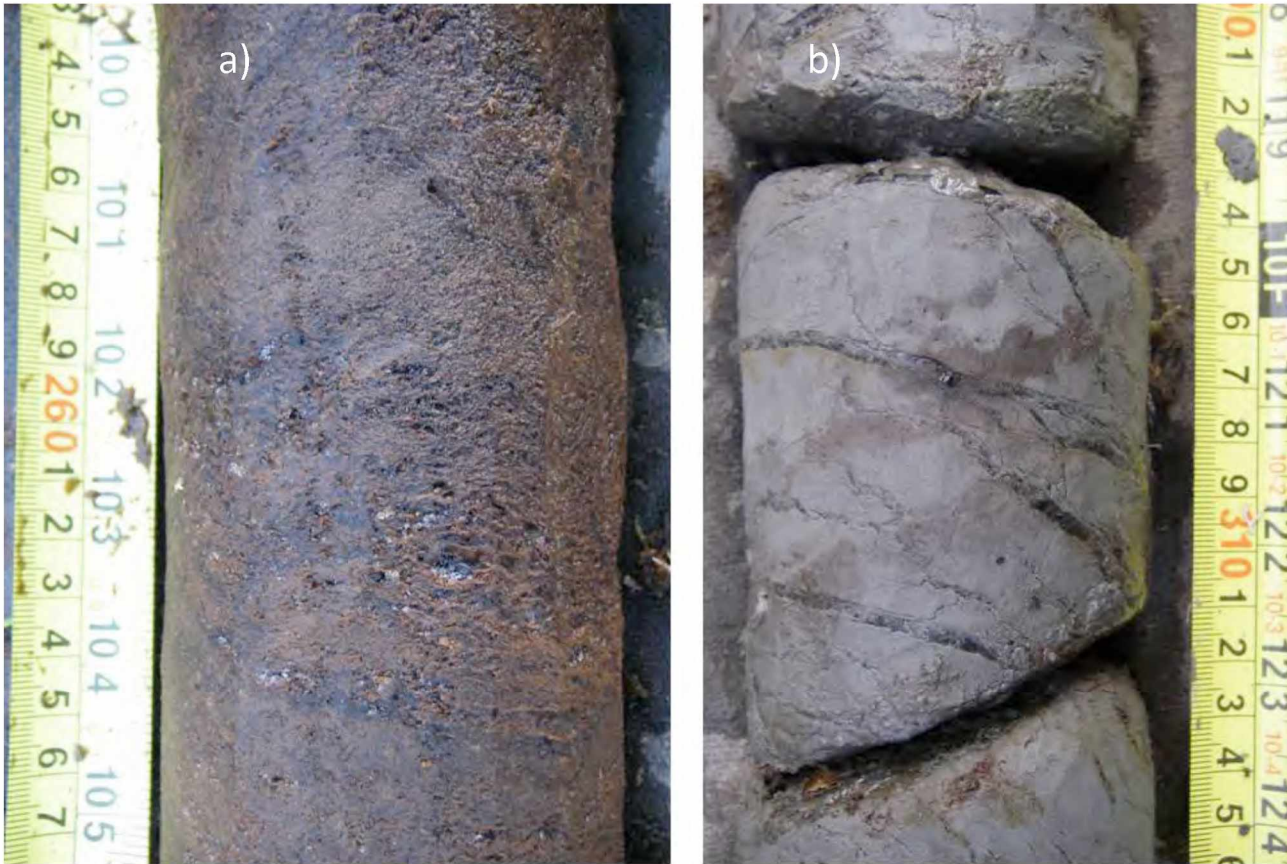
Figure 2. Permafrost cores showing typical cryostructures observed in syngenetically frozen peat (a) and para-syngenetically frozen lacustrine sediments (b).
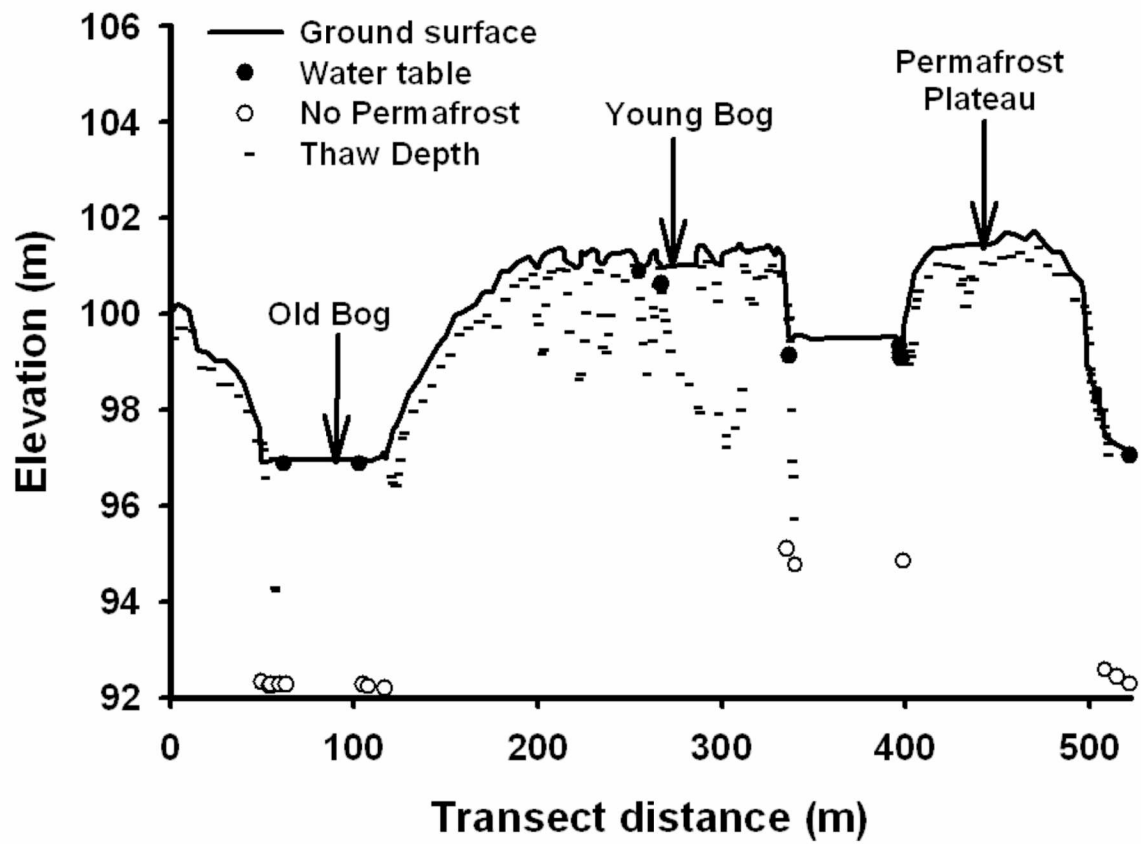
Figure 3. Variation in ground surface relief, thaw depth, and water table depth across a linear transect at the Koyukuk Flats study region.
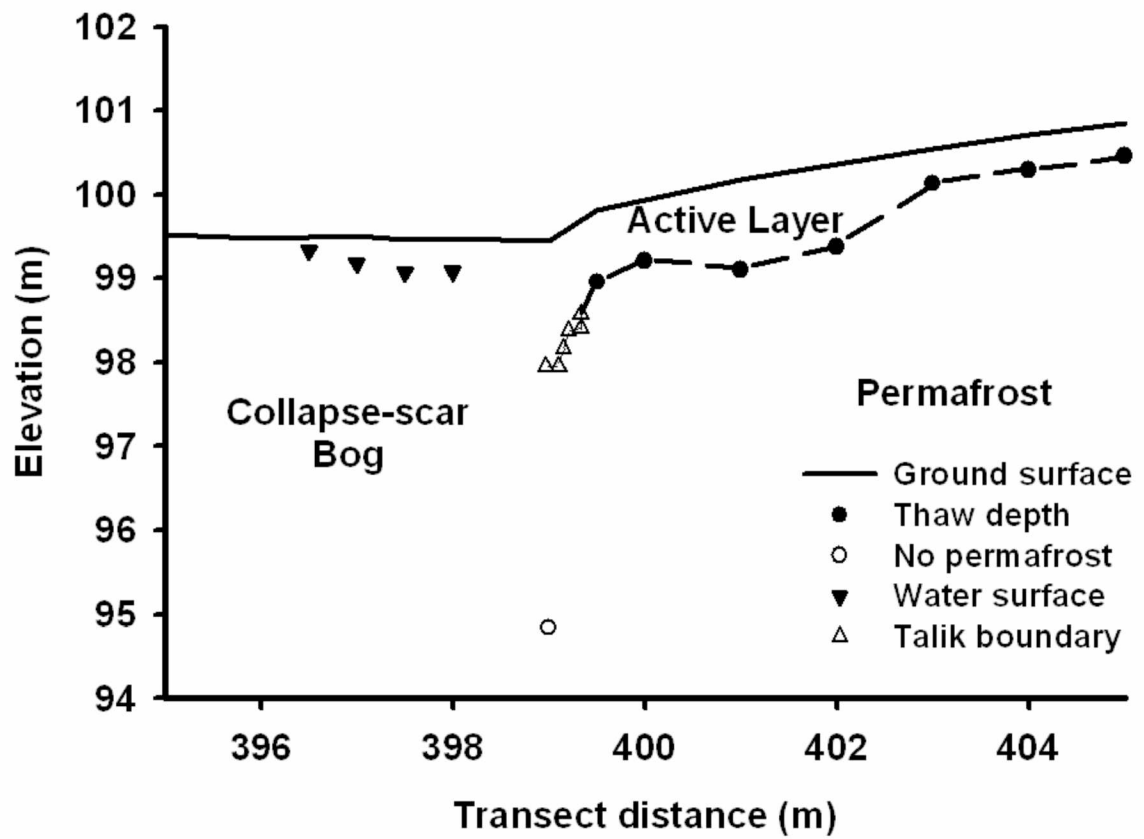
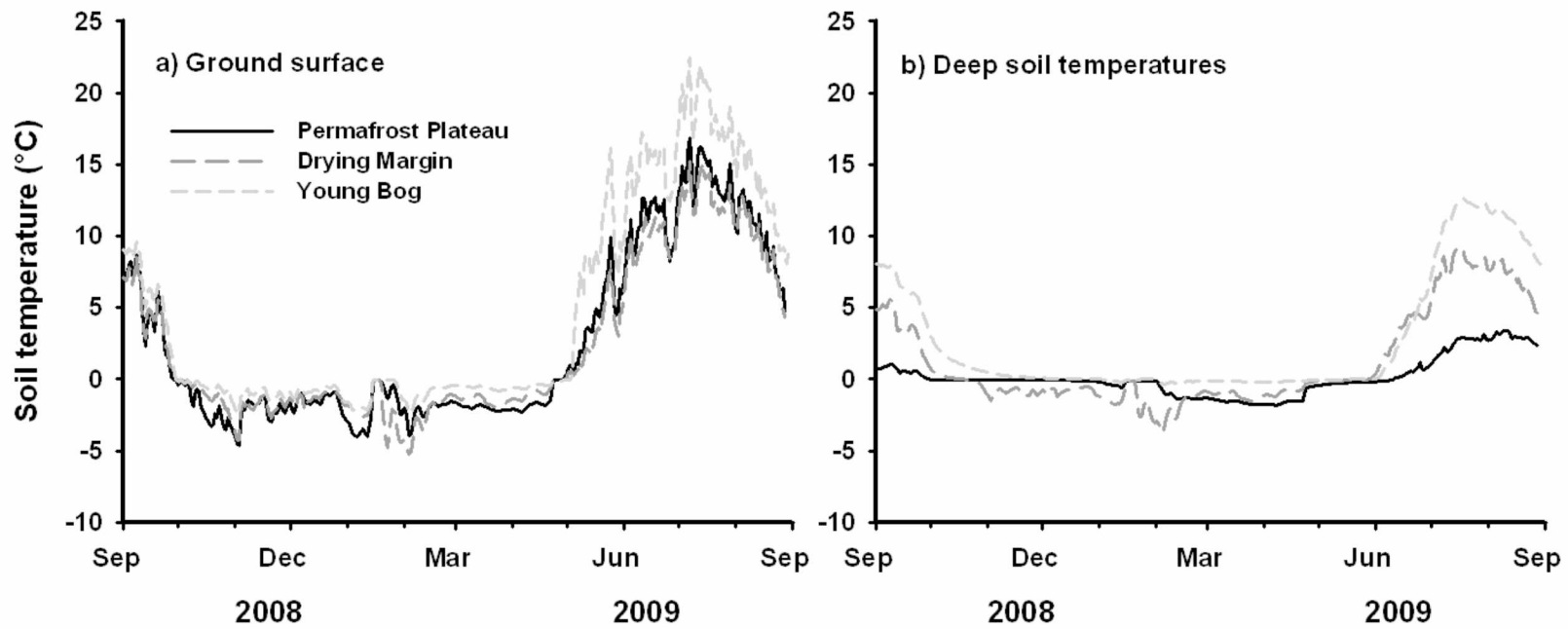**Figure 4.** Talik development along collapse-scar bog margin at Koyukuk Flats study region.

Figure 5. Seasonal variation soil temperature at the ground surface (a) and deeper in the soil profile (b). Deep soil temperatures were measured at 45 cm for the permafrost plateau, 45 cm for the drying margin, and 20 cm for the collapse-scar bog.
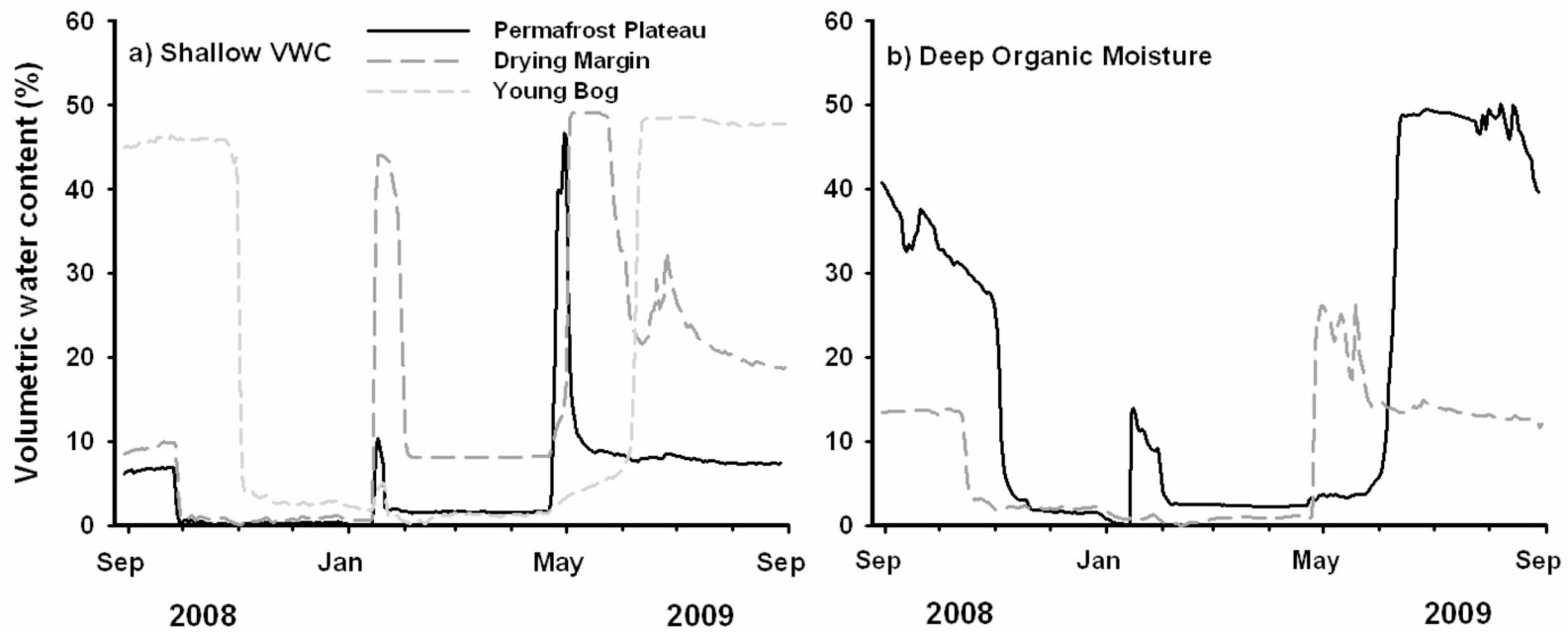
Figure 6. Seasonal variation in volumetric water content of shallow (a) of deep organic soil horizons (b) at a permafrost plateau and the drying margin of two bogs at the Koyukuk Flats study region.
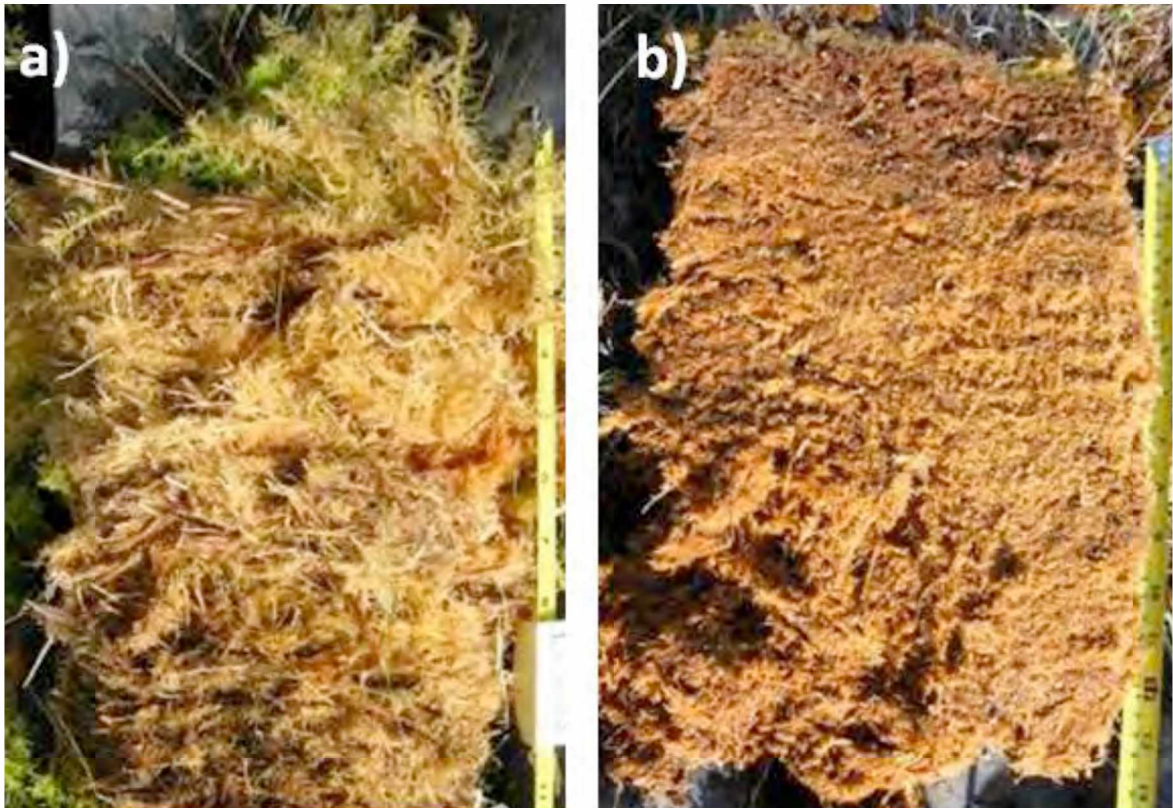
Figure 7. Comparison of bog peat (a) and forest peat (b). Bog peat colonizes collapse-scar bog features following ground subsidence and water impoundment, and is primarily composed of *Sphagnum riparium, S. balticum,* and *S. flexuosum*, with abundant live white roots of *Eriophorum scheuchzeri*. Forest peat accumulates on permafrost plateaus and then becomes inundated in collapse-scar bogs following permafrost thaw. Forest peat is composed primarily of *S. fuscum*, with abundant woody stems.

Figure 8. Comparison of forest and bog peat stocks over time since permafrost thaw at Koyukuk Flats study region. Bog peat, which accumulates following thaw in collaps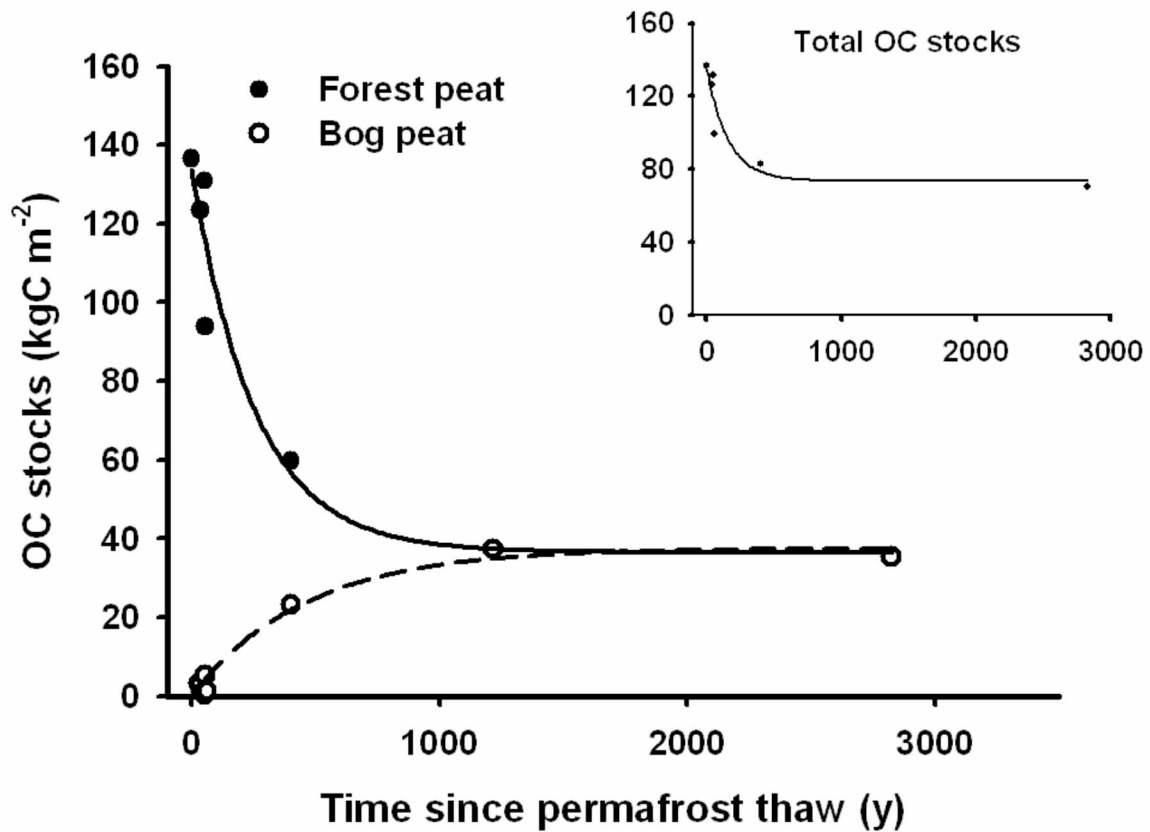e-scar bog features, is composed primarily of *Sphagnum riparium* and *S. balticum*. The inundated forest peat layer refers to the organic matter originally accumulated and stored in soils of permafrost plateaus, which ultimately becomes saturated and buried following permafrost thaw. Forest peat is derived primarily from *S. fuscum*. Points at t = 0 reflect OC stocks from permafrost plateau profiles (n = 3). Where t > 0, points reflect collapse-scar bog age as determined via tree-ring or radiocarbon methodologies. Accumulation of OC in bog peat was determined using equation 2: $C = 37*(1-e^{-0.0022t})$ (R^2 = 0.97; P < 0.0001). Loss of OC from forest peat is reflected by exponential decay equation $C = 36 + 97*e^{-0.0039t}$ (R^2 = 0.77, P = 0.02). The figure insert documents that change in total OC stocks (bog + forest peat layers) across the chronosequence, and is reflected by the equation $73 + 62*e^{-0.0063t}$ (R^2 = 0.85; P = 0.06).
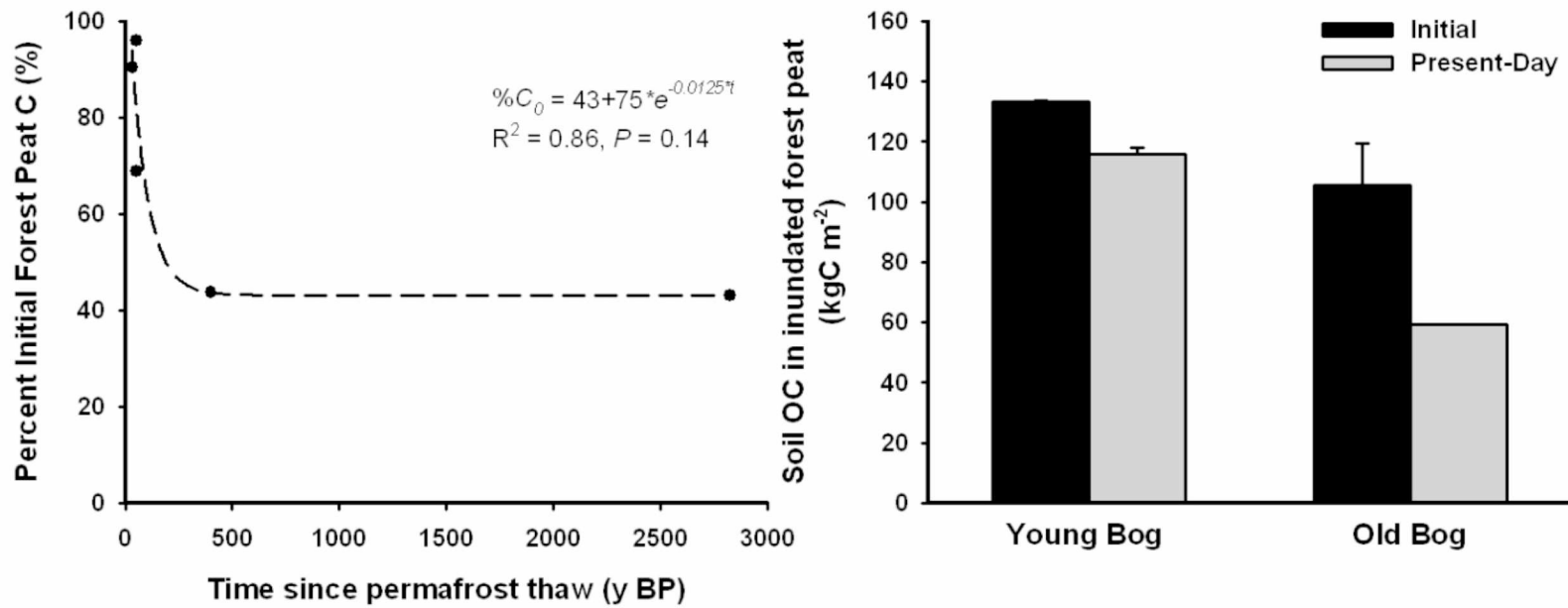
Figure 9. (a) The relationship between the percentage of initial forest peat C (C_0) and time since permafrost thaw (t). (b) Comparison of average OC stocks in initial and present-day forest peat layers inundated in collapse-scar bogs. Initial soil OC stocks (C_0) were calculated using equation 3.

Chapter 6: Conclusions

Overview

Soils of the northern permafrost region store 1672 Pg of organic carbon (C), and approximately 88% of that C is stored in perennially frozen ground (Tarnocai et al. 2009). Climate warming over the next century will likely result in the widespread thawing and loss of near-surface permafrost (Euskirchen et al. 2006; Lawrence et al. 2008), which may release large amounts of soil C to the atmosphere (Walter et al. 2006; Schuur et al. 2009). However, the sensitivity of soil C to future warming and permafrost thaw remains a critical uncertainty in many land-surface and global climate models (Gruber et al. 2004; McGuire et al. 2009). In this dissertation, I examined the effects of permafrost thaw on soil C dynamics in Alaska's boreal region. The primary aim of this research was to refine our understanding of the processes governing soil C accumulation and loss in response to climate-driven degradation of permafrost. Findings from this research, in turn, could inform model projections of carbon cycle feedbacks from the northern permafrost region to the climate system. Herein, I will discuss the primary findings and contributions from this research, their implications, current uncertainties, and future research directions.

Primary findings

Findings from Chapters 2 and 5 highlight the importance of permafrost as a large reservoir for organic C, and contribute to the growing body of literature on soil C pools in the northern permafrost region (e.g. Tarnocai et al. 2009). In Chapter 2, I report stocks of

organic C and inorganic C in Pleistocene loess deposits, commonly referred to as

yedoma. Tarnocai et al. (2009) estimate that yedoma deposits in Siberia and Alaska store

409 Pg of organic C, based on an average loess thickness of 25 m. However, at Hess

Creek, I observed considerable spatial variability in loess thickness (1 to 26 m across 62

boreholes), ground ice content, and soil organic C stocks (162-333 kg C m^{-2}). Given our

limited knowledge of loess thickness and ground ice distribution in the northern

permafrost region (Jorgenson et al. 2010), this finding highlights the difficulties in

estimating yedoma C stocks at the regional or global scale. In Chapter 5, I report organic

C stocks in frozen peat deposits that have accumulated over much of the Holocene. For

loess and peat deposits, organic C accumulated in conjunction with the vertical rise of the

permafrost table during periods of sedimentation/deposition. As a result, organic C at

the base of the active layer was quickly incorporated into the permafrost pool during cold

climatic periods, where decomposition essentially stopped and organic C was stored for

millennia. Today, with warmer climate conditions, permafrost C in both yedoma and

frozen peat is vulnerable to thaw and decomposition.

While many studies have investigated the effect of fire on soil C storage in upland

boreal forests (Harden et al. 2000; Carrasco et al. 2006; Fan et al. 2008), fewer have

examined the effects of fire on deep C pools in frozen mineral soils. To address some of

these uncertainties, I conducted studies to understand the interactive effects of fire and

permafrost on soil C storage. In Chapter 2, I document how wildfire-permafrost

interactions govern soil C accumulation and loss through the fluctuation of active layer

depth across fire cycles. Active layer depth determines the proportion of mineral soil in a

seasonally-thawed (i.e. active layer) or perennially-frozen (i.e. permafrost) state, and in turn, governs the susceptibility of C to decomposition. Under present-day climate conditions and fire severity, my findings suggest that the presence of near-surface permafrost aids OC stabilization through the upward movement of the permafrost table between fire cycles, with changes in active layer depth being driven by ecosystem recovery and moss re-growth. Using a simple model (Fire-C model), I show that permafrost thaw in response to increasing fire severity and frequency caused a net C loss from deep mineral soils, highlighting the vulnerability of soil C to both wildfire and permafrost thaw.

In Chapter 4, I build upon these findings from Chapter 2 by exploring the sensitivity of permafrost and soil C at Hess Creek to future climate factors (air temperature, soil moisture, and snow dynamics) and fire severity. To conduct this study, I coupled field measurements of soil temperature and moisture, laboratory measurements of thermal conductivity (Chapter 3), and a numerical thermal model with the simple process-based C model used in Chapter 2. Findings here suggest that future warming and increases in fire severity will increase the vulnerability of soil C to loss, whereas changes in snow depth and moisture will either decrease or have minimal effect on soil C vulnerability. In general, a large proportion of soil C losses was due to strong response of decomposition rates to warmer temperatures and changing moisture conditions. However, fluctuations in active layer depth across fire cycles also contributed to C loss from mineral soil by governing the amount of C in the frozen or unfrozen phase. Findings also highlight the complexity of interactive climate-disturbance effects (e.g.

changes in fire severity associated with changes in soil moisture), and underscore the need for models that consider the combined effects of climate, fire disturbance, soil hydrology and permafrost thaw.

In Chapter 5, I examined the effect of permafrost thaw on soil hydrologic, soil thermal, and soil C dynamics at a peatland site in the Koyukuk Flats National Wildlife Refuge. Findings from this study describe the redistribution of water across the landscape in response to thermokarst, which in turn, initiates a series of feedbacks that modify local thermal dynamics and rates of C accumulation and loss. In particular, I provide evidence for the development of unfrozen soil layers known as *taliks*, which initiate lateral expansion of collapse-scar bogs. Permafrost thaw enhanced OC accumulation rates in shallow peat layers, while driving rapid loss of OC from deep peat layers. The net effect of permafrost thaw on soil OC balance was a net loss of approximately 31 g C m^{-2} y^{-1} over 3000 years, suggesting the thawing of frozen peat deposits in the boreal region may function as a positive feedback to atmospheric warming.

Implications and uncertainties

In general, the findings from my dissertation suggest that permafrost thaw will likely trigger the loss of deep soil C from soils of Alaska's boreal region, resulting in a strong positive feedback to the climate system. However, the rate and magnitude of C loss from soils to the atmosphere will likely vary across the landscape. In uplands, soil C storage is sensitive to post-fire thawing of permafrost. Future projections (from Chapter

4) suggest that the combined effects of climate warming and wildfire will likely accelerate rates of permafrost thaw and soil C loss from upland forests. In peatlands, soil C storage is highly sensitive to thermokarst development and in particular, the impoundment of surface-water in collapse-scar bogs. Continued climate warming will likely increase the rate of permafrost thaw and the abundance of collapse-scar features across northern peatland landscapes. Based on my observations, the loss of frozen peat deposits from permafrost plateaus will greatly reduce C storage in Alaska's boreal region.

The vulnerability of soil C to permafrost thaw may also vary with soil type and permafrost origin. For instance, yedoma may be more resilient to climate warming and wildfire than other permafrost/soil types due to the high latent heat content and fine grain-size of its ice-rich silts (Shur et al. 2005; Jorgenson et al. 2010). I commonly observed the presence of an ice-rich intermediate layer in near-surface permafrost, which protected deep yedoma C from thawing and mobilization. In contrast, frozen peat deposits are highly vulnerable to the presence of surface water (Jorgenson et al. 2010), and as a result, soil C stored in frozen peat also appears to be vulnerable to thaw and release (Chapter 5). While prior studies have documented the cyclic degradation and aggradation of permafrost (Zolati 1993; Robinson & Moore 2000), it is unclear if future climate conditions or ecosystem adaptations in the near future will be conducive for the recovery of permafrost in northern peatlands.

Feedbacks associated with permafrost thaw, soil C release, and the climate system will likely depend upon the mode of C loss from the ecosystem. The mode of C loss is

intimately tied to post-thaw hydrologic changes in soils. In general, permafrost thaw in upland forests should enhance soil drainage and aerobic decomposition driving the release of CO_2 from soils. In contrast, permafrost thaw in lowlands should promote saturation of peat, anoxic conditions, and CH_4 release from soils. While this paradigm is generally useful for predicting carbon-cycle-feedbacks to the climate system, questions still remain regarding the mechanisms underlying CO_2 or CH_4 release following permafrost thaw. Some questions include (1) What are the constraints on trace gas diffusion through deep thawed yedoma?, (2) What is the role of CH_4 ebullition in northern peatlands? and (3) Will increased fire severity and frequency alter organic matter quality and rates of decomposition?

Uncertainty also exists regarding the response of net primary productivity (NPP) in the boreal region to future warming and permafrost thaw. Increased NPP has the potential to partially offset or balance soil C losses from heterotrophic respiration. Several recent studies have provided evidence for post-thaw increases in soil N (Schuur et al. 2007), which typically limits NPP in the boreal forest. However, other studies have shown that N fertilization can result in the net loss of soil C (Mack et al. 2004). Moreover, enhance production from the release of deep N stores will only be realized if rooting depth increases in conjunction with permafrost thaw. Modeling studies have also illustrated that the response of soil carbon in boreal forest ecosystems depends on the sensitivity of plant production to increasing atmospheric CO_2 (e.g. Balshi et al. 2009), a response that is highly uncertain. Changes in successional trajectories, such as the conversion of black spruce ecosystems to deciduous stands following severe fires

(Johnstone et al. 2010), may also result in increased aboveground NPP. However, severe stand-replacing fires would likely cause loss of permafrost and soil C stocks, as documented in Chapter 2. Clearly, the response of NPP to future climate and disturbance will govern ecosystem C balance and C feedbacks to the climate system.

Future directions

Based on the findings from my dissertation, I recommend three new directions for future research to advance our understanding of soil C responses to permafrost thaw. First, novel findings from this research should be integrated into established process-based modeling frameworks (e.g. the Terrestrial Ecosystem Model, or TEM). Development of terrestrial process-based models will enhance our ability to predict the response of high-latitude ecosystems to continued warming and increased disturbance frequency. While recent advances in model development have begun to address the interactive effects of fire and permafrost on soil C dynamics (Yi et al. 2010), a need exists for new parameterizations that incorporate the effects of permafrost thaw on ground subsidence, erosion, and hydrologic reorganization.

Second, future research should quantify the spatial extent of permafrost thaw in northern peatlands and categorize different modes of thermokarst with respect to soil C dynamics. Permafrost thaw in ice-rich lowlands can transform forested ecosystems into thaw lakes, collapse-scar bogs, or collapse-scar fens (Jorgenson & Osterkamp 2005), each of which operate differently with respect to C dynamics (Walter et al. 2006; Myers-Smith et al. 2007; Turetsky et al. 2008). The application of remote sensing techniques

should improve detection and characterization of permafrost-related landforms and processes (Kaab 2008). Future field campaigns should also test the generalizability of findings from these studies and others in order to improve scaling of plot-based measurements to the regional or global scale.

Finally, future research should also evaluate the physical and biogeochemical feedbacks associated with permafrost thaw and soil C dynamics that foster resilience. Much of the research from my dissertation has focused on the vulnerability of soil C to permafrost thaw; however boreal ecosystems have generally been quite resilient to climate warming and changes to the disturbance regime (Chapin et al. 2010). For instance, permafrost in upland black spruce forests has largely been resilient to fire, due to the stabilizing effects of thick organic horizons and high ground ice content (Jorgenson et al. 2010). Moreover, the persistence of boreal soils as large C reservoirs has likely been due to both this resilience of permafrost (Jorgenson et al. 2010) and the maintenance of current successional trajectories associated with fire (Johnstone et al. 2010). While continued warming will likely drive C loss from boreal soils, more research is need to address potential negative feedbacks that might function to stabilize soil C losses in the future.

References

Balshi MS, McGuire AD, Duffy P, Flannigan M, Kicklighter DW, Melillo J. 2009.
    Vulnerability of carbon storage in North American boreal forests to wildfires

during the 21st century. Global Change Biology: doi:10.1111/j.1365-2486.2009.01877.x.

Carrasco JJ, Neff JC, Harden JW. 2006. Modeling physical and biogeochemical controls over carbon accumulation in a boreal forest soil. Journal of Geophysical Research-Biogeosciences 111: G02004, doi:10.1029/2005JG000087.

Chapin FS III, McGuire AD, Ruess RW, Hollingsworth TN, Mack MC, Johnstone JF, Kasischke ES, Euskirchen ES, Jones JB, Jorgenson T, Kielland K, Kofinas GP, Turetsky MR, Yarie J, Lloyd AH, Taylor DL. 2010. Resilience of Alaska's boreal forest to climatic change. Canadian Journal of Forest Research 40: 1360-1370.

Euskirchen ES, McGuire AD, Kicklighter DW, Zhuang Q, Clein JS, Dargaville RJ, Dye DG, Kimball JS, McDonald KC, Melillo JM, Romanovsky VE, Smith NV. 2006. Importance of recent shifts in soil thermal dynamics on growing season length, productivity and carbon sequestration in terrestrial high-latitude ecosystems. Global Change Biology 12: 731-750.

Fan Z, Neff JC, Harden JW, Wickland KP. 2008. Boreal soil carbon dynamics under a changing climate: A model inversion approach. Journal of Geophysical Research-Biogeosciences 113: G04016, doi:10.1029/2008JG000723.

Gruber N, Friedlingstein P, Field CB, Valentini R, Heimann M, Richey JE, Lankao PR, Schulze E-D, Chen CTA. 2004. The vulnerability of the carbon cycle in the 21st century: an assessment of carbon-climate-human interactions. In: The Global

Carbon Cycle: Integrating Humans, Climate, and the Natural World. CB Field and MR Raupach, editors. Island Press, Washington, DC, USA.

Harden JW, Trumbore SE, Stocks BJ, Hirsch A, Gower ST, O'Neill KP, Kasischke ES. 2000.The role of fire in the boreal carbon budget. Global Change Biology 6 (Suppl. 1): 174-184.

Johnstone JF, Chapin FS III, Hollingsworth TN, Mack MC, Romanovsky V, Turetsky M. 2010. Fire, climate change, and forest resilience in interior Alaska, Canadian Journal of Forest Research 40: 1302-1312.

Jorgenson MT, Osterkamp TE. 2005. Response of boreal ecosystems to varying modes of permafrost degradation. Canadian Journal of Forest Research 35: 2100-2111.

Jorgenson MT, Romanovsky V, Harden J, Shur Y, O'Donnell J, Schuur EAG, Kanevskiy M, Marchenko S. 2010. Resilience and vulnerability of permafrost to climate change. Canadian Journal of Forest Research 40: 1219-1236.

Kaab A. 2008. Remote sensing of permafrost-related problems and hazards. Permafrost and Periglacial Processes 19: 107-136.

Mack MC, Schuur EAG, Bret-Harte MS, Shaver GR, Chapin FS III. 2004. Ecosystem carbon storage in arctic tundra reduced by long-term nutrient fertilization. Nature 431: 440-443.

McGuire AD, Anderson LG, Christensen TR, Dallimore S, Guo L, Hayes DJ, Heimann M, Lorenson TD, Macdonald RW, Roulet N. 2009. Sensitivity of the carbon cycle in the Arctic to climate change. Ecological Monographs 79: 523-555.

Myers-Smith IH, McGuire AD, Harden JW, Chapin FS III. 2007. Influence of
disturbance on carbon exchange in a permafrost collapse and adjacent burned
forest. Journal of Geophysical Research 112: doi:10.1029/2007JG000423.

Lawrence DM, Slater AG, Romanovsky VE, Nicolsky DJ. 2008. Sensitivity of a model
projection of near-surface permafrost degradation to soil column depth and
representation of soil organic matter. Journal of Geophysical Research 113:
F02011, doi:10.1029/2007JF000883.

O'Donnell JA, Harden JW, McGuire AD, Kanevskiy MZ, Jorgenson MT, Xu X. 2010.
The effect of fire and permafrost interactions on soil carbon accumulation in an
upland black spruce ecosystem of interior Alaska: implications for post-thaw
carbon loss, Global Change Biology: In press.

Robinson SD, Moore TR. 2000. The influence of permafrost and fire upon carbon
accumulation in high boreal peatlands, Northwest Territories, Canada. Arctic,
Antarctic, and Alpine Research 32: 155-166.

Schuur EAG, Crummer KG, Vogel JG, Mack MC. 2007. Plant species composition and
productivity following permafrost thaw and thermokarst in Alaskan tundra.
Ecosystems 10: 280-292.

Schuur EAG, Vogel JG, Crummer KG, Lee H, Sickman JO, Osterkamp TE. 2009. The
effect of permafrost thaw on old carbon release and net carbon exchange from
tundra. Nature 459: doi:10.1038/nature08031.

Shur Y, Hinkel KM, Nelson FE. 2005. The transient layer: implications for geocryology and climate-change science. Permafrost and Periglacial Processes 16: 5-17.

Tarnocai C, Canadell JG, Schuur EAG, Kuhry P, Mazhitova G, Zimov S. 2009. Soil organic carbon pools in the northern circumpolar permafrost region. Global Biogeochemical Cycles 23: doi:1029/2008GB003327.

Turetsky MR, Treat CC, Waldrop MP, Waddington JM, Harden JW, McGuire AD. 2008. Short-term response of methane fluxes and methanogen activity to water table and soil warming manipulations in an Alaskan peatland. Journal of Geophysical Research 113: doi:10.1029/2007JG000496.

Walter KM, Zimov SA, Chanton JP, Verbyla D, Chapin FS III. 2006. Methane bubbling from Siberian thaw lakes as a positive feedback to climate warming. Nature 443: doi:10.1038/nature05040.

Yi S, McGuire AD, Kasischke E, Harden JW, Manies KL, Mack M, Turetsky MR. 2010. A dynamic organic soil biogeochemical model for simulating the effects of wildfire on soil environmental conditions and carbon dynamics of black spruce forests, Journal of Geophysical Research-Biogeosciences: In press.

Zoltai SC. 1993. Cyclic development of permafrost in the peatlands of Northwestern Alberta, Canada. Arctic and Alpine Research 25: 240-246.